

Community detection in networks: A user guide

Santo Fortunato*

Center for Complex Networks and Systems Research, School of Informatics and Computing and Indiana University Network Science Institute (IUNI), Indiana University, Bloomington, USA and
Department of Computer Science, Aalto University School of Science, P.O. Box 15400, FI-00076

Darko Hric

Department of Computer Science, Aalto University School of Science, P.O. Box 15400, FI-00076

(Dated: November 4, 2016)

Community detection in networks is one of the most popular topics of modern network science. Communities, or clusters, are usually groups of vertices having higher probability of being connected to each other than to members of other groups, though other patterns are possible. Identifying communities is an ill-defined problem. There are no universal protocols on the fundamental ingredients, like the definition of community itself, nor on other crucial issues, like the validation of algorithms and the comparison of their performances. This has generated a number of confusions and misconceptions, which undermine the progress in the field. We offer a guided tour through the main aspects of the problem. We also point out strengths and weaknesses of popular methods, and give directions to their use.

PACS numbers: 89.75.Fb, 89.75.Hc

Contents

I. Introduction	1
II. What are communities?	3
A. Variables	3
B. Classic view	5
C. Modern view	7
III. Validation	9
A. Artificial benchmarks	9
B. Partition similarity measures	12
C. Detectability	15
D. Structure versus metadata	17
E. Community structure in real networks	19
IV. Methods	22
A. How many clusters?	22
B. Consensus clustering	24
C. Spectral methods	25
D. Overlapping communities: Vertex or Edge clustering?	25
E. Methods based on statistical inference	27
F. Methods based on optimisation	27
G. Methods based on dynamics	31
H. Dynamic clustering	34
I. Significance	35
J. Which method then?	37
V. Software	38
VI. Outlook	39
Acknowledgments	40
References	40

I. INTRODUCTION

The science of networks is a modern discipline spanning the natural, social and computer sciences, as well as engineering (Barrat *et al.*, 2008; Caldarelli, 2007; Cohen and Havlin, 2010; Dorogovtsev and Mendes, 2013; Estrada, 2011; Estrada and Knight, 2015; Newman, 2010). Networks, or graphs, consist of *vertices* and *edges*. An edge typically connects a pair of vertices¹. Networks occur in an huge variety of contexts. Facebook, for instance, is a large social network, where more than one billion people are connected via virtual acquaintanceships. Another famous example is the Internet, the physical network of computers, routers and modems which are linked via cables or wireless signals (Fig. 1). Many other examples come from biology, physics, economics, engineering, computer science, ecology, marketing, social and political sciences, etc..

Most networks of interest display *community structure*, i. e., their vertices are organised into groups, called *communities*, *clusters* or *modules*. In Fig. 2 we show a collaboration network of scientists working at the Santa Fe Institute (SFI) in Santa Fe, New Mexico. Vertices are scientists, edges join coauthors. Edges are concentrated within groups of vertices representing scientists working on the same research topic, where collaborations are more natural. Likewise, communities could represent proteins with similar function in protein-protein interaction networks, groups of friends in social networks, websites on

*Electronic address: santo@indiana.edu

¹ There may be connections between three vertices or more. In this case one speaks of *hyperedges* and the network is a *hypergraph*.

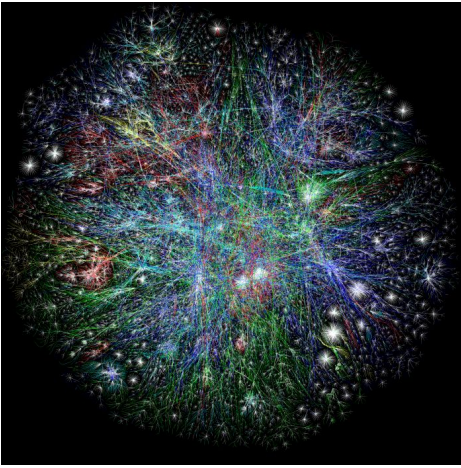


FIG. 1 Internet network. Reprinted figure with permission from www.opte.org.

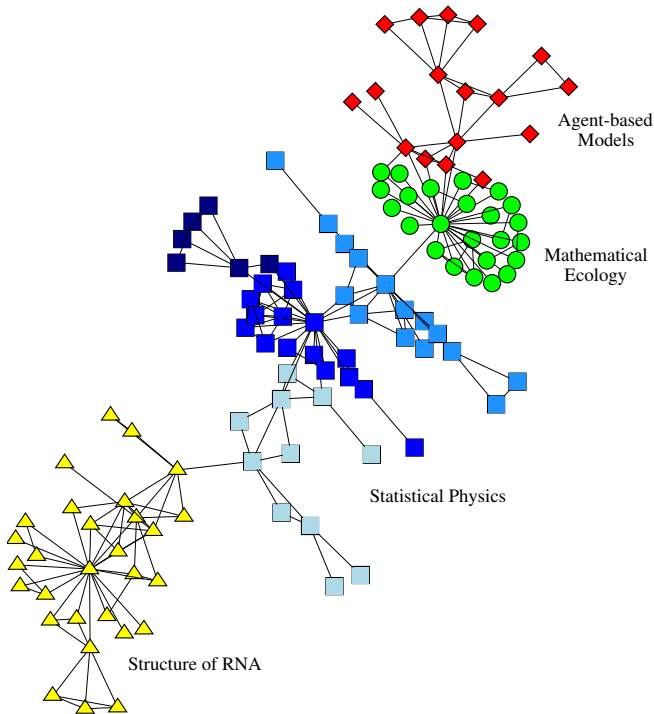


FIG. 2 Collaboration network of scientists working at the Santa Fe Institute (SFI). Edges connect scientists that have coauthored at least one paper. Symbols indicate the research areas of the scientists. Naturally, there are more edges between scholars working on the same area than between scholars working in different areas. Reprinted figure with permission from (Girvan and Newman, 2002). © 2002, by the National Academy of Sciences, USA.

similar topics on the Web graph, and so on.

Identifying communities may offer insight on how the network is organised. It allows us to focus on regions having some degree of autonomy within the graph. It helps to classify the vertices, based on their role with respect to

the communities they belong to. For instance we can distinguish vertices totally embedded within their clusters from vertices at the boundary of the clusters, which may act as brokers between the modules and, in that case, could play a major role both in holding the modules together and in the dynamics of spreading processes across the network.

Community detection in networks, also called *graph* or *network clustering*, is an ill-defined problem though. There is no universal definition of the objects that one should be looking for. Consequently, there are no clear-cut guidelines on how to assess the performance of different algorithms and how to compare them with each other. On the one hand, such ambiguity leaves a lot of freedom to propose diverse approaches to the problem, which often depend on the specific research question and (or) the particular system at study. On the other hand, it has introduced a lot of noise into the field, slowing down progress. In particular, it has favoured the diffusion of questionable concepts and convictions, on which a large number of methods are based.

This work presents a critical analysis of the problem of community detection, intended to practitioners but accessible to readers with basic notions of network science. It is not meant to be an exhaustive survey. The focus is on the general aspects of the problem, especially in the light of recent findings. Also, we discuss some popular classes of algorithms and give advice on their usage. More info on network clustering can be found in several review articles (Chakraborty *et al.*, 2016; Coscia *et al.*, 2011; Fortunato, 2010; Malliaros and Vazirgiannis, 2013; Newman, 2012; Parthasarathy *et al.*, 2011; Porter *et al.*, 2009; Schaeffer, 2007; Xie *et al.*, 2013).

The contents are organised in three main sections. Section II deals with the concept of community, describing its evolution from the classic subgraph-based notions to the modern statistical interpretation. Next we discuss the critical issue of validation (Section III), emphasising the role of artificial benchmarks, the importance of the choice of partition similarity scores, the conditions under which clusters are detectable, the usefulness of metadata and the structural peculiarities of communities in real networks. Section IV hosts a critical discussion of some popular clustering approaches. It also tackles important general methodological aspects, such as the determination of the number of clusters, which is a necessary input for several techniques, the possibility to generate robust solutions by combining multiple partitions, the main approaches to discover dynamic communities, as well as the assessment of the significance of clusterings. In Section V we indicate where to find useful software. The concluding remarks of Section VI close the work.

II. WHAT ARE COMMUNITIES?

A. Variables

We start with a subgraph C of a graph G . The number of vertices and edges are n, m for G and n_C, m_C for C , respectively. The adjacency matrix of G is A , its element A_{ij} equals 1 if vertices i and j are neighbours, otherwise it equals 0. We assume that the subgraph is connected because communities usually are². Other types of group structures do not require connectedness (Section II.C).

The subgraph is schematically illustrated in Fig. 3. Its

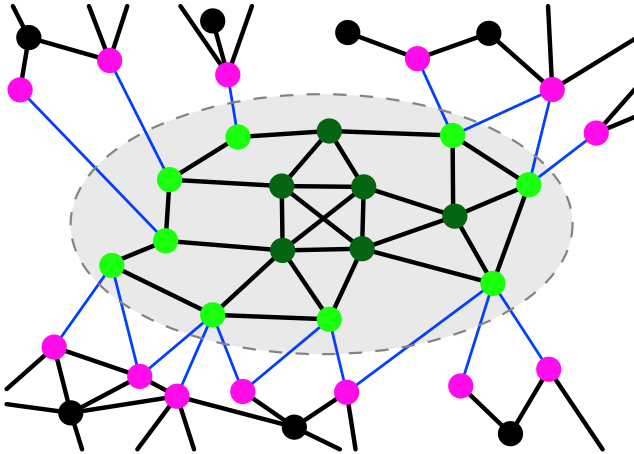


FIG. 3 Schematic picture of a connected subgraph.

vertices are enclosed by the dashed contour. The magenta dots are the external vertices connected to the subgraph, while the black ones are the remaining vertices of the network. The blue lines indicate the edges connecting the subgraph to the rest of the network.

The *internal* and *external* degree k_i^{int} and k_i^{ext} of a vertex i of the network with respect to subgraph C are the number of edges connecting i to vertices of C and to the rest of the graph, respectively. Both definitions can be expressed in compact form via the adjacency matrix A : $k_i^{int} = \sum_{j \in C} A_{ij}$ and $k_i^{ext} = \sum_{j \notin C} A_{ij}$, where the sums run over all vertices j inside and outside C , respectively. Naturally, the degree k_i of i is the sum of k_i^{int} and k_i^{ext} : $k_i = \sum_j A_{ij}$. If $k_i^{ext} = 0$ and $k_i^{int} > 0$ i has neighbours only within C and is an *internal vertex* of C (dark green dots in the figure). If $k_i^{ext} > 0$ and $k_i^{int} > 0$ i has neighbours outside C and is a *boundary vertex* of C (bright green dots in the figure). If $k_i^{int} = 0$, instead, the vertex is disjoint from C . The *embeddedness* ξ_i is the ratio between the internal degree and the degree of vertex i : $\xi_i = k_i^{int}/k_i$. The larger ξ_i , the stronger

the relationship between the vertex and its community. The *mixing parameter* μ_i is the ratio between the external degree and the degree of vertex i : $\mu_i = k_i^{ext}/k_i$. By definition, $\mu_i = 1 - \xi_i$.

Now we present a number of variables related to the subgraph as a whole. We distinguish them in three classes.

The first class comprises measures based on internal connectedness, i. e., on how cohesive the subgraph is. The main variables are:

- *Internal degree* k_C^{int} . The sum of the internal degrees of the vertices of C . It equals twice the number m_C of internal edges, as each edge contributes two units of degree. In matrix form, $k_C^{int} = \sum_{i,j \in C} A_{ij}$.
- *Average internal degree* $k_C^{avg-int}$. Average degree of vertices of C , considering only internal edges: $k_C^{avg-int} = k_C^{int}/n_C$.
- *Internal edge density* δ_C^{int} . The ratio between the number of internal edges of C and the number of all possible internal edges:

$$\delta_C^{int} = \frac{k_C^{int}}{n_C(n_C - 1)}. \quad (1)$$

We remark that $n_C(n_C - 1)/2$ is the maximum number of internal edges that a simple graph with n_C vertices may have³.

The second class includes measures based on external connectedness, i. e., on how embedded the subgraph is in the network or, equivalently, how separated the subgraph is from it. The main variables are:

- *External degree, or cut*, k_C^{ext} . The sum of the external degrees of the vertices of C . It gives the number of external edges of the subgraph (blue lines in Fig. 3). In matrix form, $k_C^{ext} = \sum_{i \in C, j \notin C} A_{ij}$.
- *Average external degree, or expansion*, $k_C^{avg-ext}$. Average degree of vertices of C , considering only external edges: $k_C^{avg-ext} = k_C^{ext}/n_C$.
- *External edge density, or cut ratio*, δ_C^{ext} . The ratio between the number of external edges of C and the number of all possible external edges:

$$\delta_C^{ext} = \frac{k_C^{ext}}{n_C(n - n_C)}. \quad (2)$$

Finally, we have hybrid measures, combining internal and external connectedness. Notable examples are:

² The variables defined in this section hold for any subgraph, connected or not.

³ A simple graph has at most one edge running between any pair of vertices and no self-loops, i. e., no edges connecting a vertex to itself.

Unweighted networks **Weighted networks**

Name	Symbol	Definition	Name	Symbol	Definition
Internal degree	k_i^{int}	$\sum_{j \in C} A_{ij}$	Internal strength	w_i^{int}	$\sum_{j \in C} W_{ij}$
External degree	k_i^{ext}	$\sum_{j \notin C} A_{ij}$	External strength	w_i^{ext}	$\sum_{j \notin C} W_{ij}$
Degree	k_i	$\sum_j A_{ij}$	Strength	w_i	$\sum_j W_{ij}$
Embeddedness	ξ_i	$\frac{k_i^{int}}{k_i}$	Weighted embeddedness	ξ_i^w	$\frac{w_i^{int}}{w_i}$
Mixing parameter	μ_i	$\frac{k_i^{ext}}{k_i}$	Weighted mixing parameter	μ_i^w	$\frac{w_i^{ext}}{w_i}$

TABLE I Basic vertex community variables, for unweighted and weighted networks. A and W are the adjacency and the weight matrix, respectively.

Unweighted networks **Weighted networks**

Name	Symbol	Definition	Name	Symbol	Definition
Internal degree	k_C^{int}	$\sum_{i,j \in C} A_{ij}$	Internal strength	w_C^{int}	$\sum_{i,j \in C} W_{ij}$
Average internal degree	k_C^{av-int}	$\frac{k_C^{int}}{n_C}$	Average internal strength	w_C^{av-int}	$\frac{w_C^{int}}{n_C}$
Internal edge density	δ_C^{int}	$\frac{k_C^{int}}{n_C(n_C-1)}$	Internal weight density	$\delta_{w,C}^{int}$	$\frac{w_C^{int}}{\bar{w}n_C(n_C-1)}$
External degree	k_C^{ext}	$\sum_{i \in C, j \notin C} A_{ij}$	External strength	w_C^{ext}	$\sum_{i \in C, j \notin C} W_{ij}$
Average external degree	k_C^{av-ext}	$\frac{k_C^{ext}}{n_C}$	Average external strength	w_C^{av-ext}	$\frac{w_C^{ext}}{n_C}$
External edge density	δ_C^{ext}	$\frac{k_C^{ext}}{n_C(n-n_C)}$	External weight density	$\delta_{w,C}^{ext}$	$\frac{w_C^{ext}}{\bar{w}n_C(n-n_C)}$
Total degree	k_C	$\sum_{i \in C, j} A_{ij}$	Total strength	w_C	$\sum_{i \in C, j} W_{ij}$
Average degree	k_C^{av}	$\frac{k_C}{n_C}$	Average strength	w_C^{av}	$\frac{w_C}{n_C}$
Conductance	C_C	$\frac{k_C^{ext}}{k_C}$	Weighted conductance	$C_{w,C}$	$\frac{w_C^{ext}}{w_C}$

TABLE II Basic community variables, for unweighted and weighted networks. A and W are the adjacency and the weight matrix, respectively, n_C the number of vertices of the community, n the total number of vertices of the graph, \bar{w} the average weight of the network edges.

- *Total degree*, or *volume*, k_C . The sum of the degrees of the vertices of C . Naturally, $k_C = k_C^{int} + k_C^{ext}$. In matrix form, $k_C = \sum_{i \in C, j} A_{ij}$.
- *Average degree* k_C^{avg} . Average degree of vertices of C : $k_C^{avg} = k_C/n_C$.
- *Conductance* C_C . The ratio between the external degree and the total degree of C :

$$C_C = \frac{k_C^{ext}}{k_C}. \quad (3)$$

All definitions we have given hold for the case of undirected and unweighted networks. The extension to weighted graphs is straightforward, as it suffices to replace the “number of edges” with the sum of the weights carried by every edge. For instance, the internal degree k_v^{int} of a vertex v becomes the *internal strength* w_v^{int} , which is the sum of the weights of the edges joining v with the vertices of subgraph C . For the internal and external edge densities of Eqs. (1) and (2) one would have to replace the numerators with their weighted counterparts and multiply the denominators by the average edge weight $\bar{w} = \sum_{ij} W_{ij}/2m$, where W_{ij} is the element of the *weight matrix*, indicating the weight of the edge joining vertices i and j ($W_{ij} = 0$ if i and j are disconnected) and m the total number of graph edges. In Tables I and II we list all variables we have presented along with their extensions to the case of weighted networks. In directed networks one would have to distinguish between incoming and outgoing edges. Extensions of the metrics are fairly simple to implement, though their usefulness is unclear.

B. Classic view

Figure 4 shows how scholars usually envision community structure. The network has three clusters and in each cluster the density of edges is comparatively higher than the density of edges between the clusters. This can be summarised by saying that communities are dense subgraphs which are well separated from each other. This view has been challenged, recently (Jeub *et al.*, 2015; Leskovec *et al.*, 2009), as we shall see in Section III.E. Communities may overlap as well, sharing some of the vertices. For instance, in social networks individuals can belong to different circles at the same time, like family, friends, work colleagues. Figure 5 shows an example of a network with overlapping communities. Communities are typically supposed to be overlapping at their boundaries, as in the figure. Recent results reveal a different picture, though (Yang and Leskovec, 2014) (Section III.E). A subdivision of a network into overlapping communities is called *cover* and one speaks of *soft clustering*, as opposed to *hard clustering*, which deals with divisions into non-overlapping groups, called *partitions*. The generic term *clustering* can be used to indicate both types of subdivisions. Covers can be *crisp*, when shared

vertices belong to their communities with equal strength, or *fuzzy*, when the strength of their membership can be different in different clusters⁴.

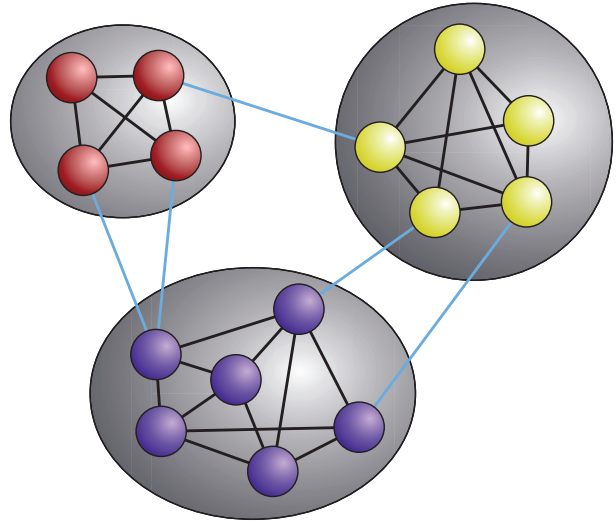


FIG. 4 Classic view of community structure. Schematic picture of a network with three communities.

The oldest definitions of community-like objects were proposed by social network analysts and focused on the internal cohesion among vertices of a subgraph (Moody and White, 2003; Scott, 2000; Wasserman and Faust,

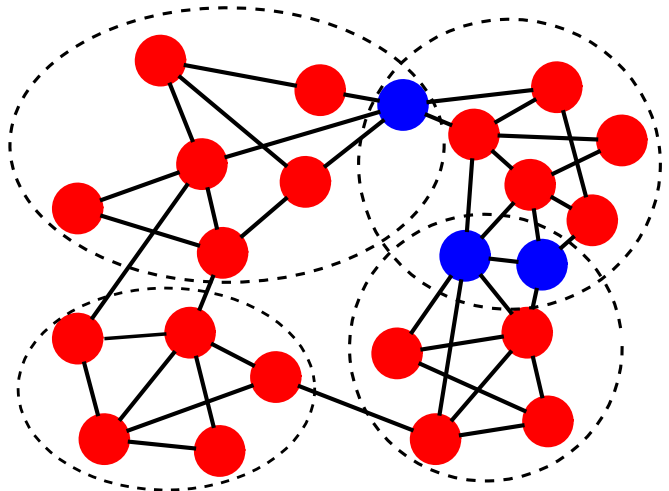


FIG. 5 Overlapping communities. A network is divided in four communities, enclosed by the dashed contours. Three of them share boundary vertices, indicated by the blue dots.

⁴ In the literature the word fuzzy is often used to describe both situations.

1994). The most popular concept is that of *clique* (Luce and Perry, 1949). A clique is a *complete graph*, that is, a subgraph such that each of its vertices is connected to all the others. It is also a maximal subgraph, meaning that it is not included in a larger complete subgraph. In modern network science it is common to call clique any complete graph, not necessarily maximal. Triangles are the simplest cliques. Finding cliques is an **NP**-complete problem (Bomze *et al.*, 1999); a popular technique is the Bron–Kerbosch method (Bron and Kerbosch, 1973).

The notion of cliques, albeit useful, cannot be considered a good candidate for a community definition. While a clique has the largest possible internal edge density, as all internal edges are present, communities are not complete graphs, in general. Moreover, all vertices have identical role in a clique, while in real network communities some vertices are more important than others, due to their heterogeneous linking patterns. Therefore, in social network analysis the notion has been relaxed, generating the related concepts of *n-cliques* (Alba, 1973; Luce, 1950), *n-clans* and *n-clubs* (Mokken, 1979). Other definitions are based on the idea that a vertex must be adjacent to some minimum number of other vertices in the subgraph. A *k-plex* is a maximal subgraph in which each vertex is adjacent to all other vertices of the subgraph except at most *k* of them (Seidman and Foster, 1978). Details on the above definitions can be found in specialised books (Scott, 2000; Wasserman and Faust, 1994).

For a proper community definition, one should take into account both the internal cohesion of the candidate subgraph and its separation from the rest of the network. A simple idea that has received a great popularity is that a community is a subgraph such that “the number of internal edges is larger than the number of external edges”⁵. This idea has inspired the following definitions. An *LS-set* (Luccio and Sami, 1969), or *strong community* (Radicchi *et al.*, 2004), is a subgraph such that the internal degree of each vertex is greater than its external degree. A relaxed condition is that the internal degree of the subgraph exceeds its external degree [*weak community* (Radicchi *et al.*, 2004)]⁶. A strong community is also a weak community, while the converse is not generally true.

A drawback of these definitions is that one separates the subgraph at study from the rest of the network, which is taken as a single object. But the latter can be in turn divided into communities. If a subgraph *C* is a proper community, it makes sense that each of its vertices is

more strongly attached to the vertices of *C* than to the vertices of any other subgraph. This concept, proposed by Hu *et al.* (Hu *et al.*, 2008), is more in line (though not entirely) with the modern idea of community that we discuss in the following section. It has generated two alternative definitions of strong and weak community. A subgraph *C* is a strong community if the internal degree of any vertex within *C* exceeds the internal degree of the vertex within any other subgraph, i. e., the number of edges joining the vertex to those of the subgraph; likewise, a community is weak if its internal degree exceeds the (total) internal degree of its vertices within every other community. A strong (weak) community à la Radicchi *et al.* is a strong (weak) community also in the sense of Hu *et al.*. The opposite is not true, in general (Fig. 6). In particular, a subgraph can be a strong community in the sense of Hu *et al.* even though all of its vertices have internal degree smaller than their respective external degree.

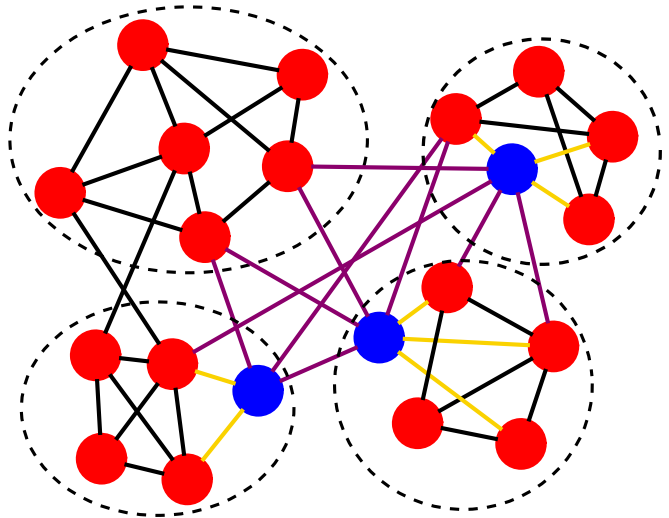


FIG. 6 Strong and weak communities. The four subgraphs enclosed in the contours are weak communities according to the definitions of Radicchi *et al.* (Radicchi *et al.*, 2004) and Hu *et al.* (Hu *et al.*, 2008). They are also strong communities according to Hu *et al.*, as the internal degree of each vertex exceeds the number of edges joining the vertex with the vertices of every other subgraph. However, three of the subgraphs are not strong communities according to Radicchi *et al.*, as some vertices (indicated in blue) have external degree larger than their internal degree (the internal and external edges of these vertices are coloured in yellow and magenta, respectively).

The above definitions of communities use *extensive* variables: their value tends to be the larger, the bigger the community (e. g., the internal and external degrees). But there are also variables discounting community size. An example is the internal cluster density $\delta_{int}(C)$ of Eq. (1). One could assume that a subgraph *C* with *k* vertices is a cluster if $\delta_{int}(C)$ is larger than a threshold ξ . Setting the size of the subgraph is necessary because otherwise any clique would be among the best possible

⁵ Here we focus on the case of unweighted graphs, extensions of all definitions to the weighted case are immediate.

⁶ The definition of weak community is the natural implementation of the naïve expectation that there must be more edges inside than outside. However, for a subgraph *C* to be a weak community it is not necessary that the number of internal edges m_C exceeds that of external edges k_C^{ext} . Since the internal degree $k_C^{int} = 2m_C$ (Section II.A) the actual condition is $2m_C > k_C^{ext}$.

communities, including trivial two-cliques (simple edges) or triangles.

C. Modern view

As we have seen in the previous section, traditional definitions of community rely on counting edges (internal, external), in various ways. But what one should be really focusing on is the *probability* that vertices share edges with a subgraph. The existence of communities implies that vertices interact more strongly with the other members of their community than they do with vertices of the other communities. Consequently, there is a preferential linking pattern between vertices of the same group. This is the reason why edge densities end up being higher within communities than between them. We can formulate that by saying that vertices of the same community have a higher probability to form edges with their partners than with the other vertices.

Let us suppose that we estimated the edge probabilities between all pairs of vertices, somehow. We can define the groups by means of those probabilities. It is a scenario similar to the classic one we have seen in Section II.B, where we add and compare probabilities, instead of edges. Natural definitions of strong and weak community are:

- A *strong community* is a subgraph each of whose vertices has a higher probability to be linked to every vertex of the subgraph than to any other vertex of the graph.
- A *weak community* is a subgraph such that the average edge probability of each vertex with the other members of the group exceeds the average edge probability of the vertex with the vertices of any other group⁷.

The difference between the two definitions is that, in the concept of strong community, the inequality between edge probabilities holds at the level of every pair of vertices, while in the concept of weak community the inequality holds only for averages over groups. Therefore, a strong community is also a weak community, but the opposite is not true, in general.

Now we can see why the former definitions of strong and weak community (Hu *et al.*, 2008; Radicchi *et al.*, 2004) are not satisfactory. Suppose to have a network with two subgraphs A and B of very different sizes, say with n_A and $n_B \gg n_A$ vertices (Fig. 7). The network is generated by a model where the edge probability is

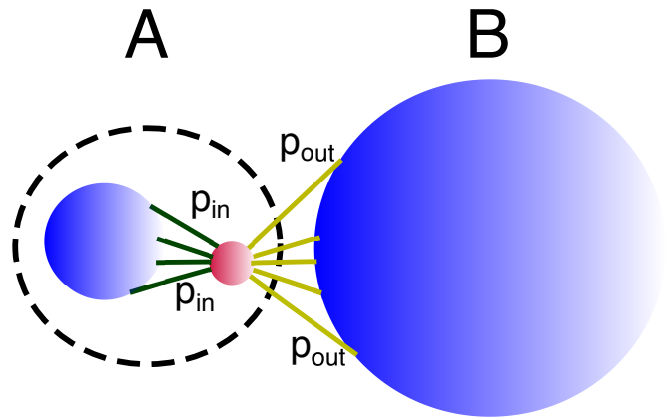


FIG. 7 Problems of the classic notions of strong and weak communities. A network is generated by the illustrated model, with two subgraphs A and B and edge probabilities p_{in} between vertices of the subgraphs and $p_{out} < p_{in}$ between vertices of A and B . The red circle is a representative vertex of subgraph A , the smaller blue circle represents the rest of the vertices of A . The subgraphs are both strong and weak communities in the probabilistic sense, but they may be neither strong nor weak communities according to the classic definitions by Radicchi *et al.* (Radicchi *et al.*, 2004) and Hu *et al.* (Hu *et al.*, 2008), if B is sufficiently larger than A .

p_{in} between vertices of the same group and $p_{out} < p_{in}$ for vertices of different groups. The two subgraphs are communities both in the strong and in the weak sense, according to the probability-based definitions above. The expected internal degree of a vertex of A is $k_A^{int} = p_{in}n_A$: since there are n_A possible internal neighbours⁸. Likewise, the expected external degree of a vertex of A is $k_A^{ext} = p_{out}n_B$. The expected internal and external degrees of A are $K_A^{int} = p_{in}n_A^2$ and $K_A^{ext} = p_{out}n_An_B$. For any two values of p_{in} and $p_{out} < p_{in}$ one can always choose n_B sufficiently larger than n_A that $k_A^{int} < k_A^{ext}$, which also implies that $K_A^{int} < K_A^{ext}$. In this setting the subgraphs are neither strong nor weak communities, according to the definitions proposed by Radicchi *et al.* and Hu *et al.*

How can we compute the edge probabilities between vertices? This is still an ill-defined problem, unless one has a model stating how edges are formed. One can make many hypotheses on the process of edge formation. For instance, if we take social networks, we can assume that the probability that two individuals know each other is a decreasing function of their geographical distance, on average (Liben-Nowell *et al.*, 2005). Each set of assump-

⁷ Since we are comparing average probabilities, which come with a standard error, the definition of weak community should not rely on the simple numeric inequality between the averages, but on the statistical significance of their difference. Significance will be discussed in Section IV.I.

⁸ The number of possible community neighbours should actually be $n_A - 1$, but for simplicity one allows for the formation of self-edges, from a vertex to itself. Results obtained with and without self-edges are basically undistinguishable, when community sizes are much larger than one. We shall stick to this setup throughout the paper.

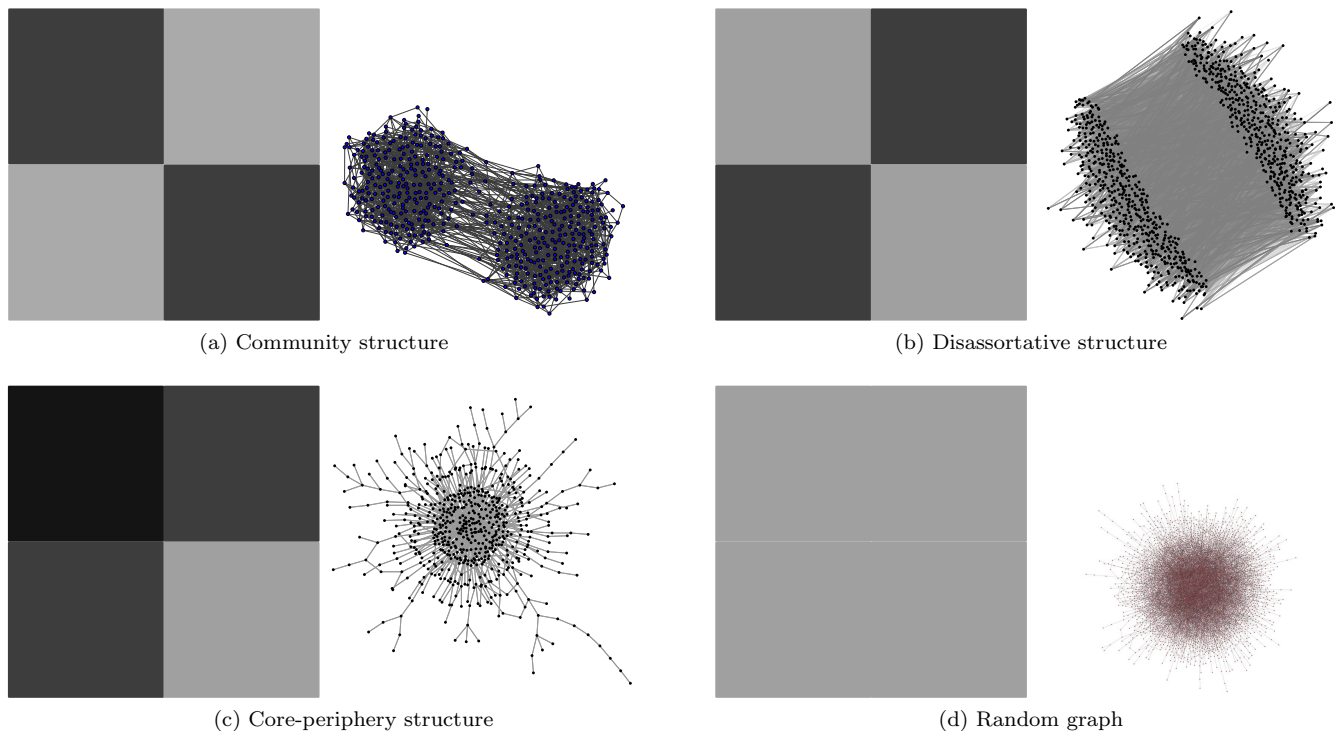


FIG. 8 Stochastic block model. We show the schematic adjacency matrices of network realisations produced by the model for special choices of the edge probabilities, along with one representative realisation for each case. For simplicity we show the case of two blocks of equal size. Darker blocks indicate higher edge probabilities and consequently a larger density of edges inside the block. Figure 8a illustrates community (or assortative) structure: the probabilities (link densities) are much higher inside the diagonal blocks than elsewhere. Figure 8b shows the opposite situation (disassortative structure). Figure 8c illustrates a core-periphery structure. Figure 8d shows a random graph à la Erdős and Rényi: all edge probabilities are identical, inside and between the blocks, so there are no actual groups. Adapted figure with permission from (Jeub *et al.*, 2015). © 2015, by the American Physical Society.

tions defines a model. For our purposes, eligible models should take into account the possible presence of groups of vertices, that behave similarly.

The most famous model of networks with group structure is the *stochastic block model* (SBM) (Fienberg and Wasserman, 1981; Holland *et al.*, 1983; Snijders and Nowicki, 1997). Suppose we have a network with n vertices, divided in q groups. The group of vertex i is indicated with the integer label $g_i = 1, 2, \dots, q$. The idea of the model is very simple: the probability $P(i \leftrightarrow j)$ that vertices i and j are connected depends exclusively on their group memberships: $P(i \leftrightarrow j) = p_{g_i g_j}$. Therefore, it is identical for any i and j in the same groups. The probabilities $p_{g_i g_j}$ form a $q \times q$ symmetric matrix⁹, called the *stochastic block matrix*. The diagonal elements p_{kk} ($k = 1, 2, \dots, q$) of the stochastic block matrix are the probabilities that vertices of block k are neighbours,

whereas the off-diagonal elements give the edge probabilities between different blocks¹⁰.

For $p_{kk} > p_{lm}, \forall k, l, m = 1, 2, \dots, q$, with $l \neq m$, we recover community structure, as the probabilities that vertices of the same group are connected exceed the probabilities that vertices of different groups are joined (Fig. 8a). It is also called *assortative structure*, as it privileges bonds between vertices of the same group. The model is very versatile, though, and can generate various types of group structure. For $p_{kk} < p_{lm}, \forall k, l, m = 1, 2, \dots, q$, with $l \neq m$, we have *disassortative structure*, as edges are more likely between the blocks than inside them (Fig. 8b). In the special case in which $p_{kk} = 0, \forall k = 1, 2, \dots, q$ we recover *multipartite struc-*

⁹ For directed graphs, the matrix is in general asymmetric. The extension of the stochastic block model to directed graphs is straightforward. Here we focus on undirected graphs.

¹⁰ In another definition of SBM the number of edges e_{rs} between blocks r and s is fixed ($r, s = 1, 2, \dots, q$), instead of the edge probabilities. If $e_{rs} \gg 1, \forall r, s = 1, 2, \dots, q$ the two models are fully equivalent if the edge probabilities p_{rs} are chosen such that the expected number of edges running between r and s coincides with e_{rs} .

ture, as there are edges only between the blocks. If $q = 2$, $p_{11} \gg p_{12} \gg p_{22}$, we have *core-periphery structure*: the vertices of the first block (core) are relatively well-connected amongst themselves as well as to a peripheral set of vertices that interact very little amongst themselves (Fig. 8c). If all probabilities are equal, $p_{ij} = p$, $\forall i, j$, we recover the classic random graph à la Erdős and Rényi (Erdős and Rényi, 1959; Erdős and Rényi, 1960) (Fig. 8d). Here any two vertices have identical probability of being connected, hence there is no group structure. This has become a fundamental axiom in community detection, and has inspired some popular techniques like, e. g., modularity optimisation (Newman, 2004b; Newman and Girvan, 2004) (Section IV.F). Random graphs of this type are also useful in the validation of clustering algorithms (Section III.A).

Alternative community definitions are based on the interplay between network topology and dynamics. Diffusion is the most used dynamics. Random walks are the simplest diffusion processes. A simple random walk is a path such that the vertex reached at step t is a random neighbour of the vertex reached at step $t - 1$. A random walker would be spending a long time within communities, due to the supposedly low number of routes taking out of them (Delvenne *et al.*, 2010; Rosvall and Bergstrom, 2008; Rosvall *et al.*, 2014). The evolution of random walks does not depend solely on the number or density of edges, in general, but also on the structure and distribution of paths formed by consecutive edges, as paths are the routes that walkers can follow. This means that random walk dynamics relies on *higher-order structures* than simple edges, in general. Such relationship is even more pronounced when one considers Markov dynamics of second order or higher, in which the probability of reaching a vertex at step $t + 1$ of the walk does not depend only on where the walker sits at step t , but also on where it was at step $t - 1$ and possibly earlier (Persson *et al.*, 2016; Rosvall *et al.*, 2014). Indeed, one could formulate the network clustering problem by focusing on higher order structures, like *motifs* (e. g., triangles) (Arenas *et al.*, 2008a; Benson *et al.*, 2016; Serroux *et al.*, 2011). The advantage is that one can preserve more complex features of the network and its communities, which typically get lost when one uses network models solely based on edge probabilities, like SBMs¹¹. The drawback is that calculations become more involved and lengthy.

Is a definition of community really necessary? Actually not, most techniques to detect communities in networks do not require a precise definition of community. The problem can be attacked from many angles. For instance, one can remove the edges separating the clusters from each other, that can be identified via some partic-

ular feature (Girvan and Newman, 2002; Radicchi *et al.*, 2004). But defining clusters beforehand is a useful starting point, that allows one to check the reliability of the final results.

III. VALIDATION

In this section we will discuss the crucial issue of validation of clustering algorithms. Validation usually means checking how precisely algorithms can recover the communities in benchmark networks, whose community structure is known. Benchmarks can be computer-generated, according to some model, or actual networks, whose group structure is supposed to be known via non-topological features (metadata). The lack of a universal definition of communities makes the search for benchmarks rather arbitrary, in principle. Nevertheless, the best known artificial benchmarks are based on the modern definition of clusters presented in Section II.C.

We shall present some popular artificial benchmarks and show that partition similarity measures have to be handled with care. We will see under which conditions communities are detectable by methods, and expose the interplay between topological information and metadata. We will conclude by presenting some recent results on signatures of community structure extracted from real networks.

A. Artificial benchmarks

The principle underneath stochastic block models (Section II.C) has inspired many popular benchmark graphs with group structure. Community structure is recovered in the case in which the probability for two vertices to be joined is larger for vertices of the same group than for vertices of different groups (Fig. 8a). For simplicity, let us suppose that there are only two values of the edge probability, p_{in} and $p_{out} < p_{in}$, for edges within and between communities, respectively. Furthermore, we assume that all communities have identical size n_c , so $qn_c = n$, where q is the number of communities. In this version, the model coincides with the *planted l -partition model*, introduced in the context of graph partitioning¹² (Bui *et al.*, 1987; Condon and Karp, 2001; Dyer and Frieze, 1989). The expected internal and external degrees of a vertex are $\langle k_{in} \rangle = p_{in}n_c$ and $\langle k_{out} \rangle = p_{out}n_c(q - 1)$,

¹¹ Since edges are usually placed independently of each other in SBMs, higher order structures like triangles are usually under-represented in the model graphs with respect to the actual graph at study.

¹² Graph partitioning means dividing a graph in subgraphs, such to minimise the number of edges joining the subgraphs to each other. It is related to community detection, as it aims at finding the minimum separation between the parts. However, it usually does not consider how cohesive the parts are (number or density of internal edges), except when special measures are used, like conductance [Eq. (3)].

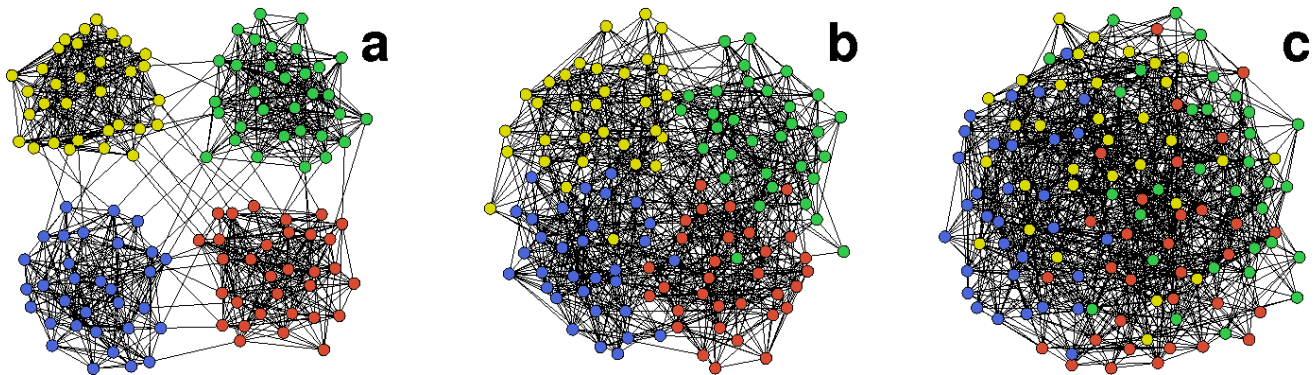


FIG. 9 Benchmark of Girvan and Newman. The three networks correspond to realisations of the model for $\langle k_{out} \rangle = 1$ (a), $\langle k_{out} \rangle = 5$ (b) and $\langle k_{out} \rangle = 8$ (c). In (c) the four groups are hardly distinguishable by eye and methods fail to assign many vertices to their groups. Reprinted figure with permission from Ref. (Guimerà and Amaral, 2005). © 2005, by the Nature Publishing Group.

respectively, yielding an expected (total) vertex degree $\langle k \rangle = \langle k_{in} \rangle + \langle k_{out} \rangle = p_{in}n_c + p_{out}n_c(q - 1)$.

Girvan and Newman (Girvan and Newman, 2002) set $q = 4$, $n_c = 32$ (for a total number of vertices $n = 128$) and fixed the average total degree $\langle k \rangle$ to 16. This implies that $p_{in} + 3p_{out} = 1/2$ and p_{in} and p_{out} are not independent parameters. The benchmark by Girvan and Newman is still the most popular in the literature (Fig. 9).

Performance plots of clustering algorithms typically have, on the horizontal axis, the expected external degree $\langle k_{out} \rangle$. For low values of $\langle k_{out} \rangle$ communities are well separated¹³ and most algorithms do a good job at detecting them. By increasing $\langle k_{out} \rangle$, the performance declines. Still, one expects to do better than by assigning memberships to the vertices at random, as long as $p_{in} > p_{out}$, which means for $\langle k_{out} \rangle < 12$. In Section III.C we will see that the actual threshold is lower, due to random fluctuations.

The benchmark by Girvan and Newman, however, is not a good proxy of real networks with community structure. For one thing, all vertices have equal degree, whereas the degree distribution of real networks is usually highly heterogeneous (Albert *et al.*, 1999). In addition, most clustering techniques find skewed distributions of community sizes (Clauset *et al.*, 2004; Danon *et al.*, 2007; Lancichinetti *et al.*, 2010; Newman, 2004a; Palla *et al.*, 2005; Radicchi *et al.*, 2004). For this reason, Lancichinetti, Fortunato and Radicchi proposed the *LFR benchmark*, having power-law distributions of degree and community size (Lancichinetti *et al.*, 2008) (Fig. 10).

The mixing parameters μ_i of the vertices (Section II.A)

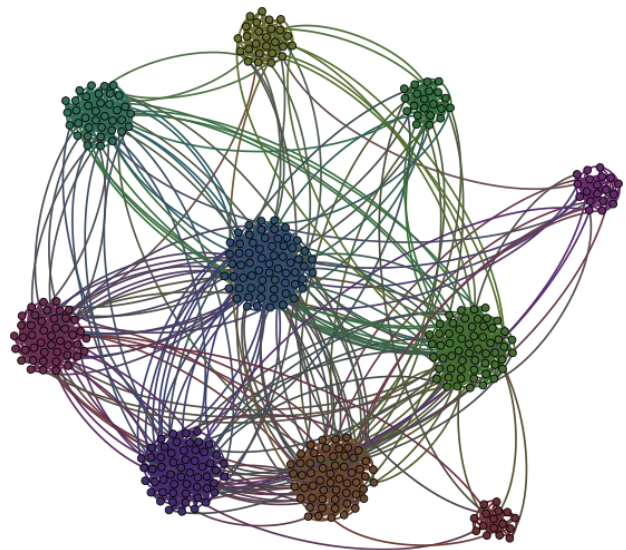


FIG. 10 LFR benchmark. Vertex degree and community size are power-law distributed, to account for the heterogeneity observed in real networks with community structure.

are set equal to a constant μ , which estimates the quality of the partition¹⁴. LFR benchmark networks are built

¹³ They are also more cohesive internally, since $\langle k_{in} \rangle$ is higher, to keep the total degree constant.

¹⁴ The parameter μ is actually only the average of the mixing parameter over all vertices. In fact, since degrees are integer, it is impossible to tune them such to have exactly the same value of μ for each vertex, and keep the constraint on the degree distribution at the same time.

by joining stubs at random, once one has established which stubs are internal and which ones are external with respect to the community of the vertex attached to the stubs. In this respect, it is basically a configuration model (Bollobás, 1980; Molloy and Reed, 1995) with built-in communities.

Clearly, when μ is low, clusters are better separated from each other, and easier to detect. When μ grows, performance starts to decline. But for which range of μ can we expect a performance better than random guessing? Let us suppose that the group structure is detectable for $\mu \in [0, \mu_c]$. The upper limit μ_c should be such that the network is random for $\mu = \mu_c$. The network is random when stubs are combined at random, without distinguishing between internal and external stubs, which yields the standard configuration model. There the expected number of edges between two vertices with degrees k_i and k_j is $k_i k_j / (2m)$, m being the total number of network edges. Let us focus on a generic vertex i , belonging to community C . We denote with K_C and \tilde{K}_C the sum of the degrees of the vertices inside and outside C , respectively. Clearly $K_C + \tilde{K}_C = 2m$. In a random graph built with the configuration model, vertex i would have an expected internal degree¹⁵ $k_i^{int-rand} = k_i(K_C - k_i)/(2m) \approx k_i K_C / (2m)$ and an expected external degree $k_i^{ext-rand} = k_i \tilde{K}_C / (2m)$. Since, by construction, $k_i^{int} = (1 - \mu)k_i$ and $k_i^{ext} = \mu k_i$, the community C is not real when $k_i^{ext} = k_i^{ext-rand}$ and $k_i^{int} = k_i^{int-rand}$, which implies $\mu = \mu_c = \tilde{K}_C / (2m) = 1 - K_C / (2m)$. We see that K_C depends on the community C : the larger the community, the lower the threshold is. Therefore, not all clusters are detectable at the same time, in general. For this to happen, μ must be lower than the minimum of μ_c over all communities: $\mu \leq \mu_c = \min_C \mu_c$. If communities are all much smaller than the network as a whole, $K_C / (2m) \approx 0$ and μ_c could get very close to the upper limit 1 of the variable μ . However, it is possible that the actual threshold is lower than μ_c , due to the perturbations of the group structure induced by random fluctuations (Section III.C). Anyway, in most cases the threshold is going to be quite a bit higher than 1/2, the value which is mistakenly considered as the threshold by some scholars.

The LFR benchmark turns out to be a special version of the recently introduced degree-corrected stochastic block model (Karrer and Newman, 2011), with the degree and the block size distributed according to truncated power laws¹⁶.

The LFR benchmark has been extended to directed

and weighted networks with overlapping communities (Lancichinetti and Fortunato, 2009). The extensions to directed and weighted graphs are rather straightforward. Overlaps are obtained by assigning each vertex to a number of clusters and distributing its internal edges equally among them¹⁷. Recently, another benchmark with overlapping communities has been introduced by Ball, Karrer and Newman (Ball et al., 2011). It consists of two clusters A and B , with overlap C . Vertices in the non-overlapping subsets $A - C$ and $B - C$ set edges only between each other, while vertices in C are connected to vertices of both A and B . The expected degree of all vertices is set equal to $\langle k \rangle$. The authors considered various settings, by tuning $\langle k \rangle$, the size of the overlap and the sizes of A and B , which may be uneven. However, the fact that all vertices have equal degree (on average) makes the model less realistic and flexible than the LFR benchmark.

Following the increasing availability of evolving time-stamped network data sets, the analysis and modelling of temporal networks have received a lot of attention lately (Holme and Saramäki, 2012). In particular, scholars have started to deal with the problem of detecting evolving communities (Section IV.H). A benchmark designed to model dynamic communities was proposed by Granell et al. (Granell et al., 2015). It is based on the planted l -partition model, just like the benchmark of Girvan and Newman, where p_{in} and $p_{out} < p_{in}$ are the edge probabilities within communities and between communities, respectively. Communities may grow and shrink (Fig. 11a), they may merge with each other or split into smaller clusters (Fig. 11b), or do all of the above (Fig. 11c). The dynamics unfold such that at each time the subgraphs are proper communities in the probabilistic sense discussed in Section II.C. In the merge-split dynamics, clusters actually merge before the inter-community edge probability p_{out} reaches the value p_{in} of the intra-community edge probability, due to random fluctuations (Section III.C).

In Section II.C we have shown why random graphs cannot have a meaningful group structure¹⁸. That means that they can be employed as *null benchmarks*, to test whether algorithms are capable to recognise the absence of groups. Many methods find non-trivial communities in such random networks, so they fail the test. We strongly encourage doing this type of exam on new algorithms (Lancichinetti and Fortunato, 2009).

¹⁵ The approximation is justified when the community is large enough that $K_C \gg k_i$.

¹⁶ In fact, the correspondence is exact for a slightly different parametrisation of the benchmark, introduced in (Peixoto, 2014). In this version of the model, instead of the mixing parameter μ , which is local, a global parameter c is used, estimating how strong the community structure is.

¹⁷ A better way to do it would be taking into account the size of the communities the vertex is assigned to, and divide the edges proportionally to the (total) degrees of the communities.

¹⁸ Here we refer to random graphs where the edge probabilities do not depend on their membership in groups. Examples are Erdős and Rényi random graphs, the configuration model, etc..

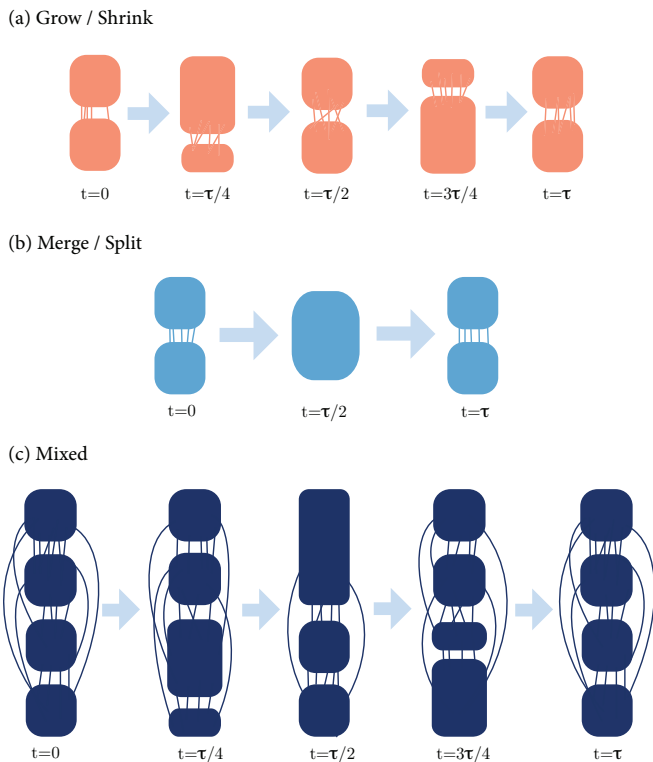


FIG. 11 Dynamic benchmark. (a) Grow-Shrink benchmark. Starting from two communities of equal size, vertices move from one cluster to the other and back. (b) Merge-Split benchmark. It starts with two communities, edges are added until there is one community with uniform link density (merge), then the process is reversed, leading to a fragmentation into two equal-sized clusters. (c) Mixed benchmark. There are four communities: the upper pair undergoes the grow-shrink dynamics of (a), the lower pair the merge-split dynamics of (b). All processes are periodic with period τ . Reprinted figure with permission from (Granell *et al.*, 2015). © 2015, by the American Physical Society.

B. Partition similarity measures

The accuracy of clustering techniques depends on their ability to detect the clusters of networks, whose community structure is known. That means that the partition detected by the method(s) has to match closely the planted partition of the network. How can the similarity of partitions be computed? This is an important problem, with no unique solution. In this section we discuss some issues about partition similarity measures. More information can be found in (Meilä, 2007), (Fortunato, 2010) and (Traud *et al.*, 2011).

Let us consider two partitions $\mathcal{X} = (X_1, X_2, \dots, X_{q_X})$ and $\mathcal{Y} = (Y_1, Y_2, \dots, Y_{q_Y})$ of a network G , with q_X and q_Y clusters, respectively. Let n be the total number of vertices, n_i^X and n_j^Y the number of vertices in clusters X_i and Y_j and n_{ij} the number of vertices shared by clusters X_i and Y_j : $n_{ij} = |X_i \cap Y_j|$. The $q_X \times q_Y$ matrix $N_{\mathcal{X}\mathcal{Y}}$ whose entries are the overlaps n_{ij} is called *confusion ma-*

trix, association matrix or contingency table.

Most similarity measures can be divided in three categories: measures based on *pair counting*, *cluster matching* and *information theory*.

Pair counting means computing the number of pairs of vertices which are classified in the same (different) clusters in the two partitions. Let a_{11} indicate the number of pairs of vertices which are in the same community in both partitions, a_{01} (a_{10}) the number of pairs of elements which are in the same community in \mathcal{X} (\mathcal{Y}) and in different communities in \mathcal{Y} (\mathcal{X}) and a_{00} the number of pairs of vertices that are in different communities in both partitions. Several measures can be defined by combining the above numbers in various ways. A famous example is the *Rand index* (Rand, 1971)

$$R(\mathcal{X}, \mathcal{Y}) = \frac{a_{11} + a_{00}}{a_{11} + a_{01} + a_{10} + a_{00}}, \quad (4)$$

which is the ratio of the number of vertex pairs correctly classified in both partitions (i. e. either in the same or in different clusters), by the total number of pairs. Another notable option is the *Jaccard index* (Ben-Hur *et al.*, 2001),

$$J(\mathcal{X}, \mathcal{Y}) = \frac{a_{11}}{a_{11} + a_{01} + a_{10}}, \quad (5)$$

which is the ratio of the number of vertex pairs classified in the same cluster in both partitions, by the number of vertex pairs classified in the same cluster in at least one partition. The Jaccard index varies over a broader range than the Rand index, due to the dominance of a_{00} in $R(\mathcal{X}, \mathcal{Y})$, which typically confines the Rand index to a small interval slightly below 1. Both measures lie between 0 and 1.

If we denote with \mathcal{X}_C and \mathcal{Y}_C the sets of vertex pairs with are members of the same community in partitions \mathcal{X} and \mathcal{Y} , respectively, the Jaccard index is just the ratio between the intersection and the union of \mathcal{X}_C and \mathcal{Y}_C . Such concept can be used as well to determine the similarity between two clusters A and B

$$J_{AB} = \frac{|A \cap B|}{|A \cup B|}. \quad (6)$$

The score J_{AB} is also called Jaccard index and is the most general definition of the score, for any two sets A and B (Jaccard, 1901). Measuring the similarity between communities is very important to determine, given different partitions, which cluster of a partition corresponds to which cluster(s) of the other(s). For instance, the cluster Y_j of \mathcal{Y} corresponding to cluster X_i of \mathcal{X} is the one maximising the similarity between X_i and Y_j , e. g., $J_{X_i Y_j}$. This strategy is also used to track down the evolution of communities in temporal networks (Lancichinetti and Fortunato, 2012; Palla *et al.*, 2007).

The Rand and the Jaccard indices, as defined in Eqs. (5) and (6), have the disturbing feature that they do not take values in the entire range $[0, 1]$. For this reason,

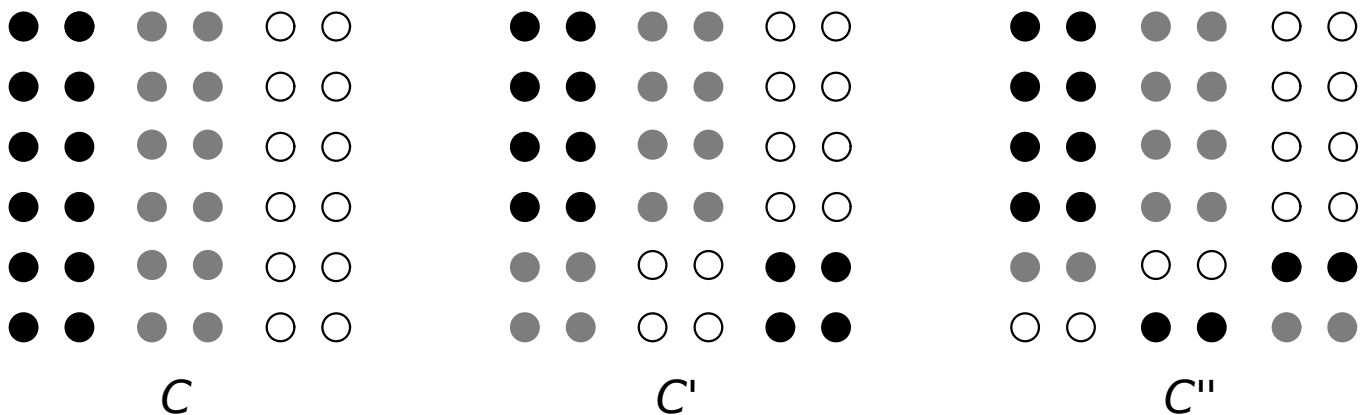


FIG. 12 Partition similarity measures based on cluster matching. There are three partitions in three clusters: \mathcal{C} , \mathcal{C}' and \mathcal{C}'' . The clusters include all elements of columns 1–2, 3–4 and 5–6, which for \mathcal{C} are labelled in black, grey and white, respectively. Partition \mathcal{C}' is obtained from \mathcal{C} by reassigning the same fraction of elements from one cluster to the next, while \mathcal{C}'' is derived from \mathcal{C} by reassigning the same fraction of elements from each cluster equally between the other clusters. From cluster matching scores one concludes that \mathcal{C}' and \mathcal{C}'' are equally similar to \mathcal{C} , while intuition suggests that \mathcal{C}' is closer to \mathcal{C} than \mathcal{C}'' . Adapted figure with permission from (Meilă, 2007). © 2007, by Elsevier.

adjusted versions of both indices exist, in that a baseline is introduced, yielding the expected values of the score for all pairs of partitions $\tilde{\mathcal{X}}$ and $\tilde{\mathcal{Y}}$ obtained by randomly assigning vertices to clusters such that $\tilde{\mathcal{X}}$ and $\tilde{\mathcal{Y}}$ have the same number of clusters and the same size for all clusters of \mathcal{X} and \mathcal{Y} , respectively (Hubert and Arabie, 1985). The baseline is subtracted from the unadjusted version, and the result is divided by the range of this difference, yielding 1 for identical partitions and 0 as expected value for independent partitions. But there are problems with these definitions as well. The null model used to compute the baseline relies on the assumption that the communities of the independent partitions have the same number of vertices as in the partitions whose similarity is to be compared. But such assumption usually does not hold, in practical instances, as algorithms sometimes need the number of communities as input, but they never impose any constraint on the cluster sizes. Adjusted indices have also the disadvantage of nonlocality (Meilă, 2005): the similarity between partitions differing only in one region of the network depends on how the remainder of the network is subdivided. Moreover, the adjusted scores can take negative values, when the unadjusted similarity lies below the baseline.

A better option is to use *standardised indices* (Brennan and Light, 1974): for a given score S_i the value of the null model term μ_i is computed along with its standard deviation σ_i over many different randomisations of the partitions \mathcal{X} and \mathcal{Y} . By computing the z -score

$$z_i = \frac{S_i - \mu_i}{\sigma_i}, \quad (7)$$

we can see how non-random the measured similarity score is, and assess its significance. It can be shown that the z -scores for the Jaccard, Rand and Adjusted Rand indices coincide (Traud *et al.*, 2011), so the measures are sta-

tistically equivalent. Since the actual values S_i of these indices differ for the same pair of partitions, in general, we conclude that the magnitudes of the scores may give a wrong perception about the effective similarity.

Cluster matching aims at establishing a correspondence between pairs of clusters of different partitions based on the size of their overlap. A popular measure is the *fraction of correctly detected vertices*, introduced by Girvan and Newman (Girvan and Newman, 2002). A vertex is correctly classified if it is in the same cluster as at least half of the other vertices in its cluster in the planted partition. If the detected partition has clusters given by the merger of two or more groups of the planted partition, all vertices of those clusters are considered incorrectly classified. The number of correctly classified vertices is then divided by the number n of vertices of the graph, yielding a number between 0 and 1. The recipe to label vertices as correctly or incorrectly classified is somewhat arbitrary. The fraction of correctly detected vertices is similar to

$$H(\mathcal{X}, \mathcal{Y}) = \frac{1}{n} \sum_{k'=\text{match}(k)} n_{kk'}, \quad (8)$$

where k' is the index of the best match $Y_{k'}$ of cluster X_k (Meilă and Heckerman, 2001). A common problem of this type of measures is that partitions whose clusters have the same overlap would have the same similarity, regardless of what happens to the parts of the communities which are unmatched. The situation is illustrated schematically in Fig. 12. Partitions \mathcal{C}' and \mathcal{C}'' are obtained from \mathcal{C} by reassigning the same fraction of their elements to the other clusters. Their overlaps with \mathcal{C} are identical and so are the corresponding similarity scores. However, in partition \mathcal{C}'' the unmatched parts of the clusters are more scrambled than in \mathcal{C}' , which should be re-

flected in a lower similarity score.

Similarity can be also estimated by computing, given a partition, the additional amount of information that one needs to have to infer the other partition. If partitions are similar, little information is needed to go from one to the other. Such extra information can be used as a measure of dissimilarity. To evaluate the Shannon information content (Mackay, 2003) of a partition, we start from the community assignments $\{x_i\}$ and $\{y_i\}$, where x_i and y_i indicate the cluster labels of vertex i in partition \mathcal{X} and \mathcal{Y} , respectively. The labels x and y are the values of two random variables X and Y , with joint distribution $P(x, y) = P(X = x, Y = y) = n_{xy}/n$, so that $P(x) = P(X = x) = n_x^X/n$ and $P(y) = P(Y = y) = n_y^Y/n$. The mutual information $I(X, Y)$ of two random variables is $I(X, Y) = H(X) - H(X|Y)$, where $H(X) = -\sum_x P(x) \log P(x)$ is the Shannon entropy of X and $H(X|Y) = -\sum_{x,y} P(x, y) \log P(x|y)$ is the conditional entropy of X given Y . The mutual information is not ideal as a similarity measure: for a given partition \mathcal{X} , all partitions derived from \mathcal{X} by splitting (some of) its clusters would all have the same mutual information with \mathcal{X} , even though they could be very different from each other. In this case the mutual information equals the entropy $H(X)$, because the conditional entropy is zero. It is then necessary to introduce an explicit dependence on the other partition, that persists even in those special cases. This has been achieved by introducing the *normalized mutual information* (NMI), obtained by dividing the mutual information by the arithmetic average¹⁹ of the entropies of \mathcal{X} and \mathcal{Y} (Fred and Jain, 2003)

$$I_{norm}(\mathcal{X}, \mathcal{Y}) = \frac{2I(X, Y)}{H(X) + H(Y)}. \quad (9)$$

The NMI equals 1 if and only if the partitions are identical, whereas it has an expected value of 0 if they are independent. Since the first thorough comparative analysis of clustering algorithms (Danon *et al.*, 2005), the NMI has been regularly used to compute the similarity of partitions in the literature. However, the measure is sensitive to the number of clusters q_Y of the detected partition, and may attain larger values the larger q_Y , even though more refined partitions are not necessarily closer to the planted one. This may give wrong perceptions about the relative performance of algorithms (Zhang, 2015).

A more promising measure, proposed by Meilă (Meilă, 2007) is the *variation of information* (VI)

$$V(\mathcal{X}, \mathcal{Y}) = H(X|Y) + H(Y|X). \quad (10)$$

The VI defines a metric in the space of partitions as it has the properties of distance (non-negativity, symmetry

and triangle inequality). It is a local measure: the VI of partitions differing only in a small portion of a graph depends on the differences of the clusters in that region, and not on how the rest of the graph is subdivided. The maximum value of the VI is $\log n$, which implies that the scores of an algorithm on graphs of different sizes cannot be compared with each other, in principle. One could divide $V(\mathcal{X}, \mathcal{Y})$ by $\log n$ (Karrer *et al.*, 2008), to force the score to be in the range $[0, 1]$, but the actual span of values of the measure depends on the number of clusters of the partitions. In fact, if the maximum number of communities is q^* , with $q^* \leq \sqrt{n}$, $V(\mathcal{X}, \mathcal{Y}) \leq 2 \log q^*$. Consequently, in those cases where it is reasonable to set an upper bound on the number of clusters of the partitions, the similarities between planted and detected partitions on different graphs become comparable, and it is possible to assess both the performance of an algorithm and to compare algorithms across different benchmark graphs. We stress, however, that the measure may not be suitable when the partitions to be compared are very dissimilar from each other (Traud *et al.*, 2011) and that it shows un-intuitive behaviour in particular instances (Delling *et al.*, 2006).

So far we discussed of comparing partitions. What about covers? Extensions of the measures we have presented to the case of overlapping communities are usually not straightforward. The *Omega index* (Collins and Dent, 1988) is an extension of the Adjusted Rand index (Hubert and Arabie, 1985). Let \mathcal{X} and \mathcal{Y} be covers of the same graph to be compared. We denote with a_{jj} the number of pairs of vertices occurring together in exactly j communities in both covers. It is a natural generalisation of the variables a_{00} and a_{11} we have seen above, where j can also be larger than 1 since a pair of vertices can now belong simultaneously to multiple communities. The variable

$$o(\mathcal{X}, \mathcal{Y}) = \frac{2}{n(n-1)} \sum_j a_{jj} \quad (11)$$

is the fraction of pairs of vertices belonging to the same number of communities in both covers (including the case $j = 0$, which refers to the pairs not being in any community together). The Omega index is defined as

$$\Omega(\mathcal{X}, \mathcal{Y}) = \frac{o(\mathcal{X}, \mathcal{Y}) - o_e(\mathcal{X}, \mathcal{Y})}{1 - o_e(\mathcal{X}, \mathcal{Y})}, \quad (12)$$

where $o_e(\mathcal{X}, \mathcal{Y})$ is the expected value of $o(\mathcal{X}, \mathcal{Y})$ according to the null model discussed earlier, in which vertex labels are randomly reshuffled such to generate covers with the same number and size of the communities.

The NMI has also been extended to covers by Lancichinetti, Fortunato and Kertész (Lancichinetti *et al.*, 2009). The definition is non-trivial: the community assignments of a cover are expressed by a vectorial random variable, as each vertex may belong to multiple clusters at the same time. The measure overestimates the similarity of two covers, in special situations, where intuition suggests much lower values. The problem can be

¹⁹ Strehl and Ghosh introduced an earlier definition of NMI, where the mutual information is divided by the geometric average of the entropies (Strehl and Ghosh, 2002). Alternatively, one could normalise by the larger of the entropies $H(X)$ and $H(Y)$ (Esquivel and Rosvall, 2012; McDaid *et al.*, 2011).

solved by using an alternative normalisation, as shown in (McDaid *et al.*, 2011). Unfortunately neither the definition by Lancichinetti, Fortunato and Kertész nor the one by McDaid, Greene and Hurley are proper extensions of the NMI, as they do not coincide with the classic definition of Eq. (9) when partitions in non-overlapping clusters are compared. However, the differences are typically small, and one can rely on them in practice. Esquivel and Rosvall have proposed an actual extension (Esquivel and Rosvall, 2012). Following the comparative analysis performed in (Lancichinetti and Fortunato, 2009), the NMI by Lancichinetti, Fortunato and Kertész has been regularly used in the literature, also in the case of regular partitions, without overlapping communities²⁰.

If covers are fuzzy (Section II.B), the similarity measures above cannot be used, as they do not take into account the degree of membership of vertices in the communities they belong to. A suitable option is the *Fuzzy Rand index* (Hüllermeier and Rifqi, 2009), which is an extension of the Adjusted Rand index. Both the Fuzzy Rand index and the Omega index coincide with the Adjusted Rand index when communities do not overlap.

For temporal networks, a naïve approach would be comparing partitions (or covers) corresponding to configurations of the system in the same time window, and to see how this score varies across different time windows. However, this does not tell if the clusters are evolving in the same way, as there would be no connection between clusterings at different times. A sensible approach is comparing sequences of clusterings, by building a confusion matrix that takes into account multiple snapshots. This strategy allows one to define dynamic versions of various indices, like the NMI and the VI (Granell *et al.*, 2015).

In conclusion, while there is no clear-cut criterion to establish which similarity measure is best, we recommend to use measures based on information theory. In particular, the VI seems to have more potential than others, for the reasons we explained, modulo the caveats in Refs. (Delling *et al.*, 2006; Traud *et al.*, 2011). There are currently no extensions of the VI to handle the comparison of covers, but it would not be difficult to engineer one, e. g., by following a similar procedure as in (Lancichinetti *et al.*, 2009; McDaid *et al.*, 2011), though this might cost the sacrifice of some of its nice features.

One should keep in mind that the choice of one similarity index or another is a sensitive one, and warped conclusions may be drawn when different measures are adopted. In Fig. 13 we show the accuracy of two algorithms on the LFR benchmark (Section III.A): *Ganxis*, a method based on label propagation (Xie and Szymanski, 2012) and *LinkCommunities*, a method based on grouping edges instead of vertices (Ahn *et al.*, 2010) (Section IV.D). The accuracy is estimated with the NMI

by Lancichinetti, Fortunato and Kertész (Lancichinetti *et al.*, 2009) (left diagram) and with the Omega index [Eq. (12)] (right diagram). From the left plot one would think that *Ganxis* clearly outperforms *LinkCommunities*, whereas from the right plot *Ganxis* still prevails for μ until about 0.5 (though the curves are closer to each other than in the NMI plot) and *LinkCommunities* is better for larger values of μ .

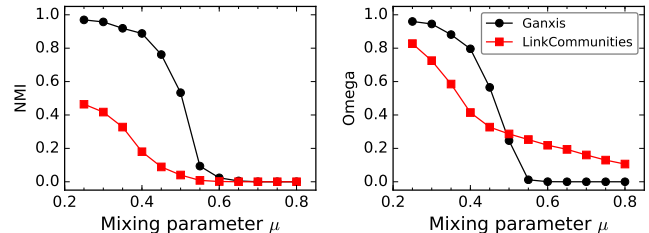


FIG. 13 Importance of choice of partition similarity measures. The plots show the comparison between the planted partition of LFR benchmark graphs and the ones found by two algorithms: *Ganxis* and *LinkCommunities*. In the left diagram similarity was computed with the NMI, in the right one with the Omega index. The performances of the algorithms appear much closer when the Omega index is used. The LFR benchmark graphs used in the analysis have 1 000 vertices, average degree 15, maximum degree 50, exponents 2 and 1 for the degree and community size distributions and range [10, 50] for the community size.

C. Detectability

In validation procedures one assumes that, if the network has clusters, there must be a way to identify them. Therefore, if we do not manage, we have to blame the specific clustering method(s) adopted. But are we certain that clusters are always detectable?

Most networks of interest are *sparse*, i. e., their average degree is much smaller than the number of vertices. This means that the number of edges of the graph is much smaller than the number of possible edges $n(n - 1)/2$. A more precise way to formulate this is by saying that a graph is sparse when, in the limit of infinite size, the average degree of the graph remains finite. A number of analytical calculations can be carried out by using network sparsity. Many algorithms for community detection only work on sparse graphs.

On the other hand, sparsity can also give troubles. Due to the very low density of edges, small amounts of noise could perturb considerably the structure of the system. For instance, random fluctuations in sparse graphs could trick algorithms into finding groups that do not really exist (Section IV.I). Likewise, they could make actual groups undetectable. Let us consider the simplest version of the assortative stochastic block model, which matches the planted partition model (Section III.A). There are q communities of the same size n/q , and only two values for

²⁰ Recently the NMI has been extended to handle the comparison of hierarchical partitions as well (Perotti *et al.*, 2015).

the edge probability: p_{in} for pairs of vertices in the same group and p_{out} for pairs of vertices in different groups. Since the graphs are sparse, p_{in} and p_{out} vanish in the limit of infinite graph size. So we shall use the expected internal and external degrees $\langle k_{in} \rangle = np_{in}/q$ and $\langle k_{out} \rangle = np_{out}(q-1)/q$, which stay constant in that limit. By construction, the groups are communities so long as $p_{in} > p_{out}$ or, equivalently, for $\langle k_{in} \rangle > \langle k_{out} \rangle / (q-1)$. But that does not mean that they are always detectable.

In principle, dealing with the issue of detectability involves examining all conceivable clustering techniques, which is clearly impossible. Fortunately, it is not necessary, because we know what model has generated the communities of the graphs we are considering. The most effective technique to infer the groups is then fitting the stochastic block model on the data (*a posteriori block modelling*). This can be done via the maximum likelihood method (Gelman *et al.*, 2014). In recent work (Decelle *et al.*, 2011), Decelle *et al.* have shown that, in the limit of infinite graph size, the partition obtained this way is correlated with the planted partition whenever

$$\langle k_{in} \rangle - \frac{\langle k_{out} \rangle}{q-1} > \sqrt{\langle k_{in} \rangle + \langle k_{out} \rangle}, \quad (13)$$

which implies

$$\langle k_{in} \rangle > \frac{\langle k_{out} \rangle}{q-1} + \frac{1}{2} \left(1 + \sqrt{1 + \frac{4q\langle k_{out} \rangle}{q-1}} \right). \quad (14)$$

So, given a value of $\langle k_{out} \rangle$, when $\langle k_{in} \rangle$ is in the range $\left[\frac{\langle k_{out} \rangle}{q-1}, \frac{\langle k_{out} \rangle}{q-1} + \frac{1}{2} \left(1 + \sqrt{1 + \frac{4q\langle k_{out} \rangle}{q-1}} \right) \right]$ the probability p_c of classifying a vertex correctly is not larger than the probability $1/q$ of assigning the vertex to a randomly chosen group, although the groups are communities, according to the model. We stress that this result only holds when the graphs are sparse: if p_{in} and p_{out} remain non-zero in the large- n limit (dense graph), the classic detectability threshold $p_{in} > p_{out}$ is correct.

A fortiori, no clustering technique can detect the clusters better than random assignment when the inference of the model parameters fails to do so. If communities are searched via the spectral optimisation of Newman-Girvan’s modularity (Newman, 2006), one obtains the same threshold of Eq. (14) (Nadakuditi and Newman, 2012), provided the network is not too sparse.

For the benchmark of Girvan and Newman (Section III.A) (Girvan and Newman, 2002) it has long been unclear where the actual detectability limit sits. Girvan-Newman benchmark graphs are not infinite, their size being set to 128, so there is no proper detectability transition, but rather a smooth crossover from a regime in which clusters are frequently detectable to a regime where they are frequently undetectable. For this reason there cannot be a sharp threshold separating the two regimes. Still it is useful to have an idea of where the pattern changes. In the following we shall still use the

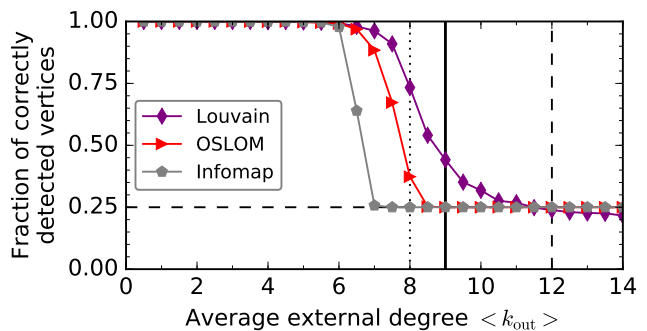


FIG. 14 Detectability of communities. Performances of three popular algorithms on the benchmark by Girvan and Newman. The dotted vertical line at $\langle k_{out} \rangle = 8$ indicates the threshold corresponding to the concept of strong community à la Radicchi *et al.*, the dashed line at $\langle k_{out} \rangle = 12$ the threshold according to the probability-based definition of strong community we have given in Section II.C. The baseline of random assignment is $1/4$ (horizontal dashed line). All algorithms do not do better than random assignment already before $\langle k_{out} \rangle = 12$. The theoretical detectability limit is at $\langle k_{out} \rangle = 9$, in the limit of groups of infinite size.

term threshold to refer to the crossover point. In the beginning, scholars thought that clusters are detectable as long as they satisfy the definition of strong community by Radicchi *et al.* (Radicchi *et al.*, 2004) (Section II.B), i. e., as long as the expected internal degree exceeds the expected external degree, yielding a threshold $\langle k_{in} \rangle = \langle k_{out} \rangle$ (Girvan and Newman, 2002). Since the expected total degree of a vertex is set to 16, communities are detectable as long as $\langle k_{out} \rangle < k_d^{strong} = 8$. It soon became obvious that the actual threshold should be the one of the “modern” definition of community we have presented in Section II.C, according to which the condition²¹ is $p_{in} > p_{out}$, that is $\langle k_{out} \rangle < k_d^{standard} = 12$. However, numerical calculations reveal that algorithms tend to fail long before that limit. From Eq. (14) we see that for the case of four infinite clusters and total expected degree $\langle k_{tot} \rangle = 16$, the theoretical detectability limit is $k_d^{theor} = 9$. In Fig. 14 we see the performance on the benchmark of three well-known algorithms: Louvain (Blondel *et al.*, 2008), a greedy optimisation technique of Newman-Girvan modularity (Newman and Girvan, 2004) (Section IV.F); Infomap, which is based on random walk dynamics (Rosvall and Bergstrom, 2008) (Section IV.G); OSLOM, that searches for clusters via a local optimisation of a significance score (Lancichinetti *et al.*, 2011). The accuracy is estimated via the fraction of correctly detected vertices (Section III.B). The

²¹ In the setting of the Girvan-Newman benchmark, where edge probabilities are identical for all vertices, the strong and weak definitions we presented in Section II.C coincide.

three thresholds k_d^{strong} , $k_d^{standard}$ and k_d^{theor} are represented by vertical lines. The performance of all methods becomes comparable with random assignment well before $k_d^{standard}$. The theoretical limit k_d^{theor} appears to be compatible with the performance curves.

Graph sparsity is a necessary condition for clusters to become undetectable, but it is not sufficient. The symmetry of the model we have considered plays a major role too. Clusters have equal size and vertices have equal degree. This helps to “confuse” algorithms. If communities have unequal sizes and the degree of vertices are correlated with the size of their communities, so that vertices have larger degree, the bigger their clusters, community detection becomes easier, as the degrees can be used as proxy for group membership. In this case, the non-trivial detectability limit disappears when there are four clusters or fewer, while it persists up to a given extent of group size inequality when there are more than four clusters (Zhang *et al.*, 2016). Other types of block structure, like core-periphery, do not suffer from detectability issues (Zhang *et al.*, 2015).

LFR benchmark graphs are more complex models than the one studied in (Zhang *et al.*, 2016) and it is not clear whether there is a non-trivial detectability limit, though it is unlikely, due to the big heterogeneity in the distribution of vertex degree and community size.

D. Structure versus metadata

Another standard way to test clustering techniques is using real networks with known community structure. Knowledge about the memberships of the vertices typically comes from *metadata*, i. e., non-structural information. If vertices are annotated communities are assumed to be groups of vertices with identical tags. Examples are user groups in social networks like LiveJournal and product categories for co-purchasing networks of products of online retailers such as Amazon.

In Fig. 15 we show the most popular of such benchmark graphs, Zachary karate club network (Zachary, 1977). It consists of 34 vertices, the members of a karate club in the United States, who were observed over a period of three years. Edges connect individuals interacting outside the activities of the club. Eventually a conflict between the club president (vertex 34) and the instructor (vertex 1) led to the fission of the club in two separate groups, whose members supported the instructor and the president, respectively (indicated by the colours). Indeed, the groups make sense topologically: vertices 1 and 34 are hubs, and most members are directly connected to either of them.

Most algorithms of community detection have been tested on this network, as well as others, e. g., the American college football network (Evans, 2010; Girvan and Newman, 2002) or Lusseau’s network of bottlenose dolphins (Lusseau, 2003). The idea is that the method doing the best job at recovering groups with identical annotations would also be the most reliable in applications.

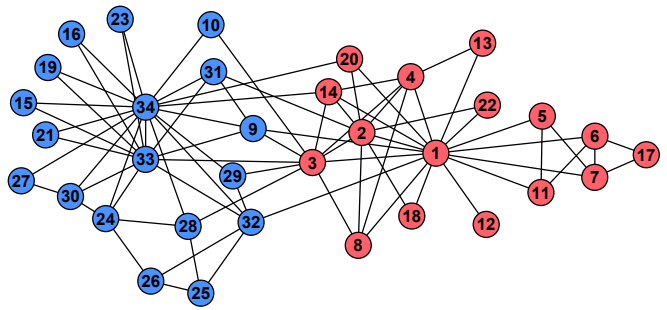


FIG. 15 Zachary karate club network. Symbols of different colours indicate the two groups generated by the fission of the network, following the disagreement between the club’s instructor (vertex 1) and its president (34).

Such idea, however, is based on a questionable principle, i. e., that the groups corresponding to the metadata are also communities in the topological sense we have discussed in Section II. Communities exist because their vertices are supposed to be similar to each other, in some way. The similarity among the vertices is then revealed topologically through the higher edge probability among pairs of members of the same group than between pairs of members of different groups, whose similarity is lower. Hence, when one is provided with annotations or other sources of information that allows to classify vertices based on their similarity, one expects that such similarity-based classes are also the best communities that structure-based algorithms may detect.

Indeed, for some small networks like Zachary’s karate club this seems to be the case. But for quite some time scholars could not test this hypothesis, due to the limited number of suitable data sets. Over the past few years this has finally become possible, due to the availability of several large network data sets with annotated vertices (Hric *et al.*, 2014; Yang and Leskovec, 2012a, 2013, 2014). It turns out that the alignment between the communities found by standard clustering algorithms and the annotated groups is not good, in general. In Fig. 16 we show the similarity between the topological partitions found by different methods and the annotated partitions, for several social, information and technological networks (Hric *et al.*, 2014). The heights of the vertical bars are the values of the normalised mutual information (NMI) (Lancichinetti *et al.*, 2009). Groups of contiguous bars represent the scores for a given data set. To the left of the vertical dashed line we see the results for classic benchmarks, like LFR graphs (Section III.A) (Lancichinetti *et al.*, 2008), Zachary karate club, etc., and the scores are generally good. But for the large data sets to the right of the line the scores are rather low, signalling a significant mismatch between topological and annotated communities. For Amazon co-purchasing network (Yang and Leskovec, 2012b), in which vertices are products and edges are set between products often purchased by the same customer(s), the similarity is quite a

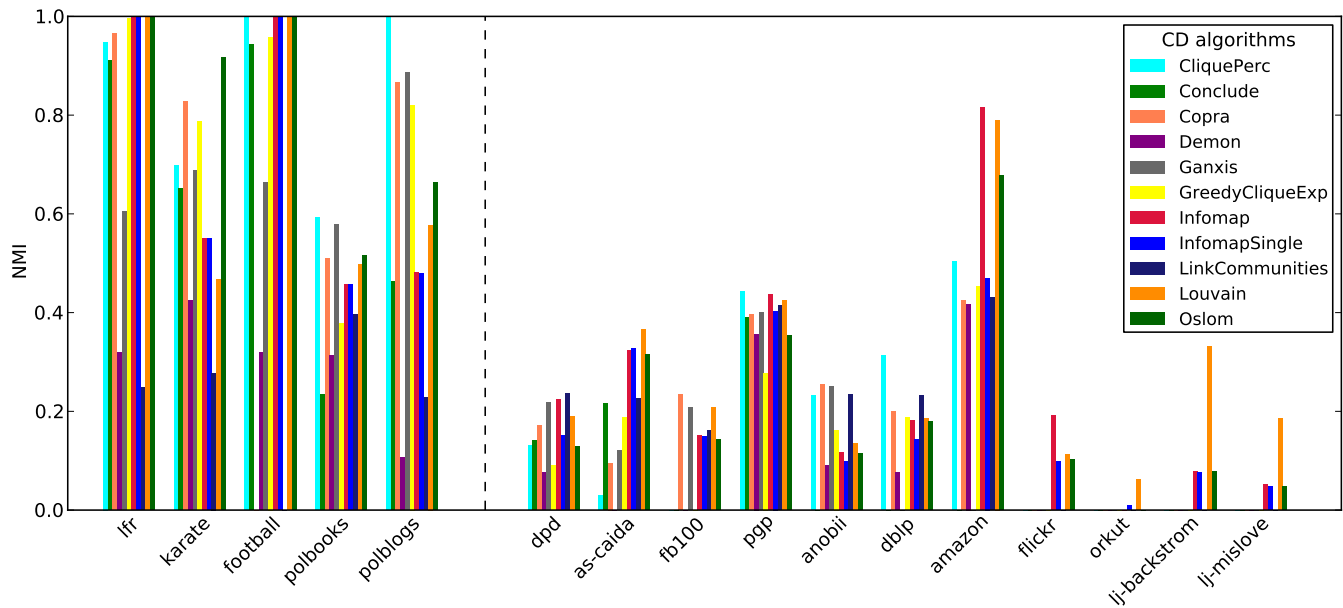


FIG. 16 Mismatch between structural communities and metadata groups. The vertical axis reports the similarity between communities detected via several clustering methods and groups of vertices with identical attributes for several networks, estimated via the NMI. Scores are grouped by data sets on the horizontal axis. The vertical dashed line separates small classic data sets from large ones, recently compiled. The low scores obtained for the latter indicate that the correspondence between structural and annotated communities is poor. Reprinted figure with permission from (Hric *et al.*, 2014). © 2014, by the American Physical Society.

bit higher than for the other networks. This is because the classification of Amazon products is hierarchical (e.g., *Books/Fiction/Fantasy*), so there are different levels of annotated communities, and the reported scores refer to the one which is most similar to the structural ones detected by the algorithms, while the other levels would give lower similarity scores. Low similarity at the partition level does not rule out that some communities of the structural partition significantly overlap with their annotated counterparts, but precision and recall scores show that this is not the case. Results depend more on the network than on the specific method adopted, none of which appears to be particularly good on any (large) data set.

So the hypothesis that structural and annotated clusters are aligned is not warranted, in general. There can be multiple reasons for that. The attributes could be too general or too specific, yielding communities which are too large or too small to be interesting. Moreover, while the best partition of the network delivered by an algorithm can be poorly correlated with the metadata, there may be alternative topological divisions that also belong to a set of valid solutions, according to the algorithm²², but happen to be better correlated with the

annotations (Newman and Clauset, 2016).

The fact that structural and annotated communities may not be strongly correlated has important consequences. Scholars have been regularly testing their algorithms on small annotated graphs, like Zachary’s karate club, by tuning parameters such to obtain the best possible performance on them. This is not justified, in general, as it makes sense only when there is a strong correspondence, which is a priori unknown. Also, forcing an alignment with annotations on one data set does not guarantee that there is going to be a good alignment with the annotations of a different network. Besides, one of the reasons why people use clustering algorithms is to provide an improved classification of the vertices, by using structure. If one obtained the same thing, why bother?

The right thing to do is using structure *along with* the annotations, instead of insisting on matching them. This way the information coming from structure and metadata can be combined and we can obtain more accurate partitions, if there is any correspondence between them. Recent approaches explicitly assume that the metadata (or a portion thereof) are either exactly or approximately correlated with the best topological partition (Bothorel

²² For instance, for clustering methods based on optimisation, there are many partitions corresponding to values of the quality func-

tion very close to the searched optimum (Good *et al.*, 2010). The algorithm will return one (or some) of them, but the others are comparably good solutions.

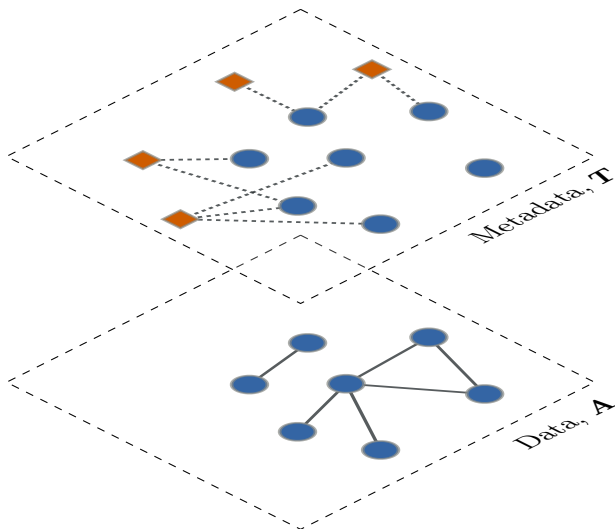


FIG. 17 Data-metadata stochastic block model by Hric et al.. One layer consists of the network itself, with its vertices and edges. The other layer is composed of the graph vertices and vertices representing the annotations, the edges indicating which vertices are associated to which tag. The presence of network vertices on both layers induces a coupling between them. Reprinted figure with permission from (Hric et al., 2016). © 2016, by the American Physical Society.

et al., 2015; Leng et al., 2013; Moore et al., 2011; Peel, 2015; Yang et al., 2013). A better approach is not assuming a priori that the metadata correlate with the structural communities. The goal is quantifying the relationship between metadata and community and use it to improve the results. If there is no correlation, the metadata would be ignored, leaving us with the partition derived from structure alone.

Methods along these lines have been developed, using stochastic block models. Newman and Clauset (Newman and Clauset, 2016) have proposed a model in which vertices are initially assigned to clusters based on metadata, and then edges are placed between vertices according to the degree-corrected stochastic block model (Karrer and Newman, 2011). Hric et al. have designed a similar model (Hric et al., 2016), in which the interplay between structure and metadata is represented by a multilayer network (Fig. 17). The generative model is an extension of the hierarchical stochastic block model (SBM) (Peixoto, 2014) with degree-correction for the case with edge layers (Peixoto, 2015a). Here the metadata is not supposed to correspond simply to a partition of the vertices. The majority of data sets contain rich metadata, with vertices being annotated multiple times, and often few vertices possess the exact same annotations and can be thus associated to the same group. In addition, while the number of communities is required as input by the method of Newman and Clauset, here it is inferred from the data. Finally, it is also possible to assess the metadata in its power to predict the network structure, not only their correlation with latent parti-

tions. This way it is possible to predict *missing vertices* of the network, i. e., to infer the connections of a vertex from its annotations only. We stress that neither method requires that all vertices are annotated.

Applications of the method by Hric et al. (Hric et al., 2016) reveal that in many data sets there are statistically significant correlations between the annotations and the network structure, while in some cases the metadata seems to be largely uncorrelated with structural clusters. We conclude that network metadata should not be used indiscriminately as ground truth for community detection methods. Even when the metadata is strongly predictive of the network structure, the agreement between the annotations and the network division tends to be complex, and very different from the one-to-one mapping that is more commonly assumed. Moreover, data sets usually contain considerable noise in their annotations, and some metadata tags are essentially random, with no relationship to structure.

E. Community structure in real networks

Artificial benchmark graphs are certainly very useful to assess the performance of clustering algorithms. However, one could always question whether the model of community structure they propose is reliable. How can we assess this? In order to characterise “real” communities we have to find them first. But that can only be done via some algorithm, and different algorithms search for different types of objects, in general. Still, one may hope that general properties of communities can be consistently uncovered across different methods and data sets, while other features are more closely tied to the specific method(s) used to detect the clusters and (or) the specific data set at study (or classes thereof).

A seemingly robust feature of communities in real networks is the heterogeneity of their size distribution. Most clustering techniques find skewed distributions of cluster sizes in many networks. So, there appears to be no characteristic size for a community: small communities usually coexist with large ones. This feature is rather independent of the type of network (Fig. 18). It may signal a hierarchy among communities, with small clusters included in large ones. Methods unable to distinguish between hierarchical levels might find “blended” partitions, consisting of communities of different levels and hence of very different sizes. The LFR benchmark was the first graph model to take explicitly into account the heterogeneity of community sizes (Section III.A).

Another interesting question is how the quality of communities depends on their size. Leskovec et al. (Leskovec et al., 2009) carried out a systematic analysis of clusters in many large networks, including traditional and on-line social networks, technological, information networks and web graphs. Instead of considering partitions, they focused on individual communities, which are derived by optimising conductance (Section II.A) around seed ver-

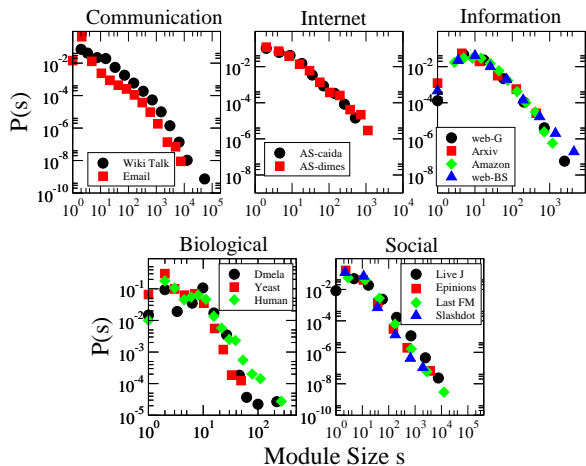


FIG. 18 Distribution of community sizes in real networks. The clusters were detected with Infomap (Rosvall and Bergstrom, 2008), but other methods yield qualitatively similar results. Various classes of networks are considered. All distributions are broad, spanning several orders of magnitude. Reprinted figure with permission from (Lancichinetti *et al.*, 2010).

tices. We remind that the conductance of a cluster is the ratio between the number of external edges and the total degree of the cluster. Minimising conductance effectively combines the two main community demands, i. e., good separation from the rest of the graph (low numerator) and large number of internal edges (high denominator). The measure is also relatively insensitive to the size of the clusters, as both the numerator and the denominator are typically proportional to the number of vertices of the community²³. Therefore one could use it to compare the quality of clusters of different sizes. For any given size k Leskovec *et al.* identified the subgraph with k vertices with the lowest conductance. This way, for each network one can draw the *network community profile* (NCP), showing the minimum conductance as a function of community size. The NCPs of all networks studied by Leskovec *et al.* have a characteristic shape: they go downwards till $k \sim 100$ vertices, and then they rise monotonically for larger subgraphs [Fig. 19 (left)]. Alternative shapes have been recently found for other data sets (Jeub *et al.*, 2015).

For networks characterised by NCPs like the one in Fig. 19 (left) the most pronounced communities are fairly small in size. Such small clusters are weakly connected to the rest of the network, often by a single edge (in this case they are called *whiskers*), and form the *periphery*

of the graph. Large clusters have comparatively lower quality and melt into a big *core*. Large communities can often be split in parts with lower conductance, so they can be considered conglomerates of smaller communities. A schematic picture of the resulting network structure is shown in Fig. 19 (right). The shape of the NCP is fairly independent of the specific technique adopted to identify the subgraphs with minimum conductance. The different shapes of the NCPs encountered in data suggest that core-periphery is not the only model of group structure of real networks (Jeub *et al.*, 2015).

The NCP is a signature that can be used to select generative mechanisms of community structure. Indeed, many standard models typically yield NCP sloping steadily downwards, at odds with the ones encountered in many social and information networks. Stochastic block models (Section II.C) are sufficiently versatile that they can reproduce the NCP shape of Fig. 19 (left), by suitably tuning the parameters. In the standard LFR benchmark (Section III.A) the mixing parameters are tightly concentrated about a value μ by construction, hence all clusters have approximately conductance μ , yielding a roughly flat NCP²⁴ (Jeub *et al.*, 2015). However, the model can be easily modified by making μ community-dependent and a large variety of NCPs are attainable, including the one of Fig. 19 (left).

The main problem of working with NCPs is that they are based on extreme statistics, as one systematically reports the minimum conductance for a given cluster size. How representative is this extremal subgraph of the population of subgraphs with the same size? There may be just a few clusters of a given size with low conductance. It may happen that many subgraphs have conductance near the minimum corresponding to their size(s), which would then be representative. Alternatively most subgraphs might have much larger conductance than the minimum but low enough that they can be still considered communities. In this case one should conclude that communities of that size are not of very high quality, on average. The above scenarios might lead to different conclusions about the actual community structure of the system. In general, even if one could produce a version of the NCP where the trend refers to representative samples of communities of equal size (whatever that means), the actual values of the conductance are as important as the shape of the curve. If conductance is sufficiently low for all cluster sizes, it means that there are good communities of any size. The fact that small clusters could be of higher quality does not undermine the role of large clusters. The observation that large clusters consist of smaller clusters of higher quality may just be evidence of hierarchical structure in the network, which is a trade-

²³ This is exactly true when the ratio between the external and the total degree (mixing parameter) is the same for all community vertices.

²⁴ If all vertices of a subgraph have mixing parameter equal to μ , it can be easily shown that the conductance of the subgraph is exactly equal to μ .

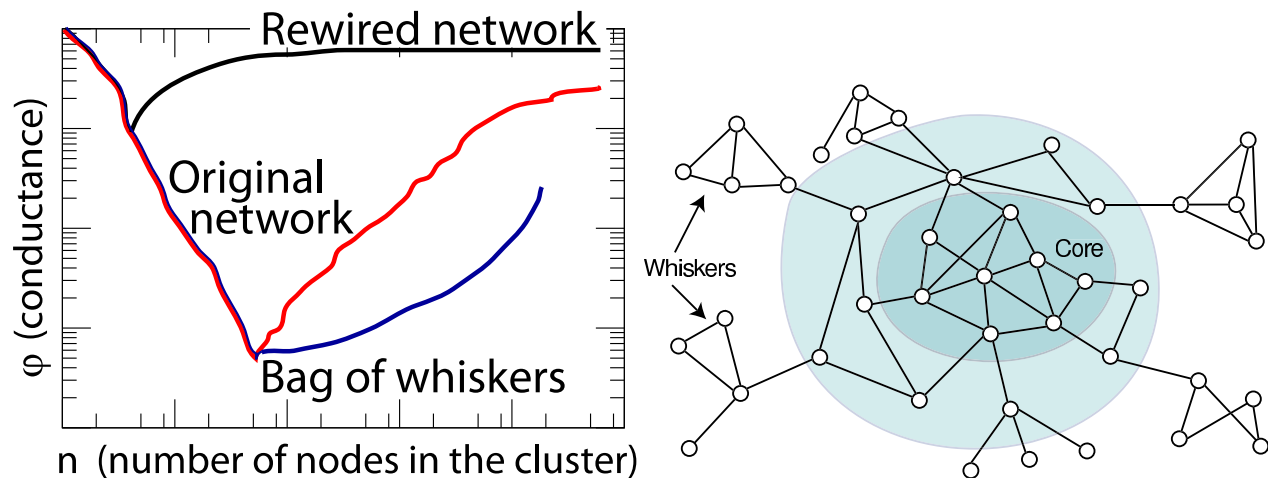


FIG. 19 Core-periphery structure of real networks. (Left) Schematic shape of the network community profile (NCP), showing how the minimum conductance of subgraphs of size k varies with k . This pattern is very common in large social and information networks. The “best” communities in terms of conductance have a size of about 100 vertices (minimum of the curve), whereas communities of larger sizes have lower quality. The curve labeled *Rewired network* is the NCP of a randomised version of the network, where edges are randomly rewired by keeping the degree distribution; the one labeled *Bag of whiskers* gives the minimum conductance scores of communities composed of disconnected pieces. (Right) Scheme of the core-periphery structure in large social and information networks associated to the NCP above. Most vertices are in a central core, where large communities are blended together, whereas the best communities, which are rather small, are weakly connected to the core. Reprinted figure with permission from Ref. (Leskovec *et al.*, 2009). © 2009, by Taylor and Francis.

mark of many complex systems (Simon, 1962). In that case high levels of the hierarchy are not less important than low ones, a priori. In fact, the actual relative importance of communities should not only come from the sheer value of specific metrics, like conductance, but also from their statistical significance (Section IV.I).

That notwithstanding, we strongly encourage analyses like the one by Leskovec *et al.*, as they provide a statistical characterisation of community structure, in a way that is only weakly algorithm-dependent. One has to define operationally what a cluster is, but in a simple intuitive way that allows us to draw conclusions about the structure of the graph. In principle one could do the same by analysing the clusters delivered by any algorithm, but there would be two important drawbacks. First, the clusters may not be easy to interpret, as most clustering algorithms usually do not require a clear-cut definition of community. Second, one would have to handle a partition of the network in communities, instead of probing locally the group structure of the network. Therefore, for a given vertex one would have only one cluster (or a handful, if communities overlap), while a local exploration allows to analyse a whole population of candidate subgraphs, which gives more information. The local subgraphs recovered this way do not need to be strongly matching the clusters delivered by any algorithm, but they provide useful signatures that allow to restrict the set of possible model explanations for the network’s group structure. Such investigation can be replicated on any model graph to check whether the results match (e. g., whether the NCPs coincide).

Another approach to infer properties of clusters of real networks is using annotations. While we have shown that annotated clusters do not necessarily coincide with structural ones (Section III.D), general features can be still derived, provided they are consistently found across different data sets and annotations. A recent analysis by Yang and Leskovec has questioned the common picture of networks with overlapping communities (Yang and Leskovec, 2014). Scholars usually assume that clusters overlap at their boundaries, hence edge density should be larger in the non-overlapping parts (Fig. 5). Instead, by analysing the overlaps of annotated clusters in large social and information networks, Yang and Leskovec found that the probability that two vertices are connected is larger in the overlaps, and grows with the number of communities sharing that pair of vertices. In addition, *connector vertices*, i. e., vertices with the largest number of neighbours within a community, are more likely to be found in the overlaps. These findings suggest that the overlaps may play an important role in the community structure of networks. In Fig. 20 we compare the conventional view with the one resulting from the analysis. The *Community-Affiliation Graph Model* (AGM) (Yang and Leskovec, 2014) and the *Cluster Affiliation Model for Big Networks* (BIGCLAM) (Yang and Leskovec, 2013) are clustering techniques based on generative models of networks featuring communities with dense overlaps. The models are based on the principle that vertices are more likely to be neighbours the more the communities sharing them, in line with the empirical finding of (Yang and Leskovec, 2014).

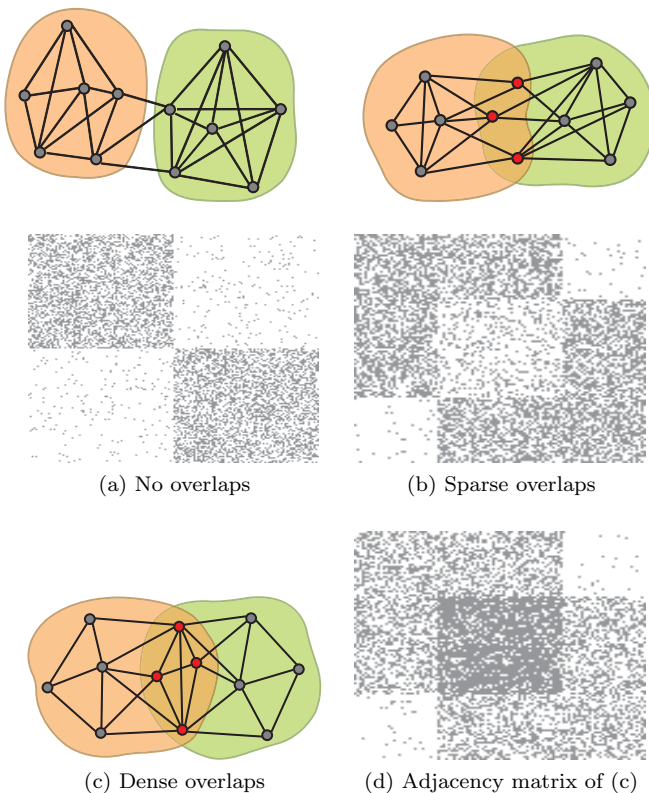


FIG. 20 Stylised views of community structure. In (a) and (b) we show the conventional pictures of non-overlapping and overlapping clusters, respectively. Under the network diagrams we see the corresponding adjacency matrices. The overlaps have a lower edge density than the rest of the communities. The analysis by Yang and Leskovec suggests that a more realistic model could be the one shown in (c, d), where the overlaps are denser than the non-overlapping parts. Reprinted figure with permission from (Yang and Leskovec, 2014). © 2014, by the Association for Computing Machinery, Inc.

Actual overlapping communities exist in many contexts. However, it is unclear whether soft clustering is statistically founded. A recent analysis aiming at identifying suitable stochastic block models to describe real network data indicate that in many cases hard partitions ought to be preferred, as they give simpler descriptions of the group structure of the data than soft partitions (Peixoto, 2015b). This could be due to the fact that the underlying models are based on placing edges independently of each other, neglecting higher order structures between vertices, like motifs. By adopting approaches that take into account higher-order structures things may change and community overlaps might become a statistically robust feature. The pervasive overlaps found by Yang and Leskovec in annotated data can be found if higher order effects are considered (Persson *et al.*, 2016; Rosvall *et al.*, 2014), without ad hoc hypotheses.

IV. METHODS

There are many algorithms to detect communities in graphs. They can be grouped in categories, based on different criteria, like the actual operational method (Fortunato, 2010), or the underlying concept of community (Coscia *et al.*, 2011). In most applications, however, just a few popular algorithms are employed. In this section we present a critical analysis of these methods. We show the advantages of knowing the number of clusters before-hand and how it is possible to derive robust solutions from partitions delivered by stochastic clustering techniques. We discuss approaches to the problem of detecting communities in evolving networks and how to assess the significance of the detected clustering. We conclude by suggesting the methods that currently appear to be most promising.

A. How many clusters?

In general, the only preliminary information available to any algorithm is the structure of the network, i. e., which pairs of vertices are connected to each other and which are not (possibly including weights). Any insight about community structure is supposed to be given as output of the procedure. Naturally, it would be valuable to have some information on the unknown division of the network beforehand, as one could reduce considerably the huge space of possible solutions, and increase the chance of successfully identifying the communities.

Among all the possible pre-detection inputs, the number q of clusters plays a prominent role. Many popular classes of algorithms require the specification of q before they run, like methods imported from data clustering or parametric statistical inference approaches (Section IV.E). Other methods are capable to infer q as they can choose among partitions into different numbers of communities. But even such methods could benefit from a preliminary knowledge of q (Darst *et al.*, 2014). In Fig. 21 we report standard accuracy plots of two algorithms on the planted partition model (Section III.A) with two clusters of equal size. The algorithms are modularity optimisation via simulated annealing (Guimerà and Amaral, 2005) and the Absolute Potts Model (APM) (Ronhovde and Nussinov, 2010) (Section IV.G). There are two performance curves for each method: one comes from the standard application of the method, without constraints; the other is obtained by forcing the method to explore only the subset of partitions with the correct number of clusters $q = 2$.

We see that the accuracy improves considerably when q is known. This is particularly striking in the case of modularity optimisation, which is known to have a limited resolution, preventing the method from identifying the correct scale of the communities, even when the latter are very pronounced (Fortunato and Barthélemy, 2007; Good *et al.*, 2010) (Section IV.F). Knowing q and con-

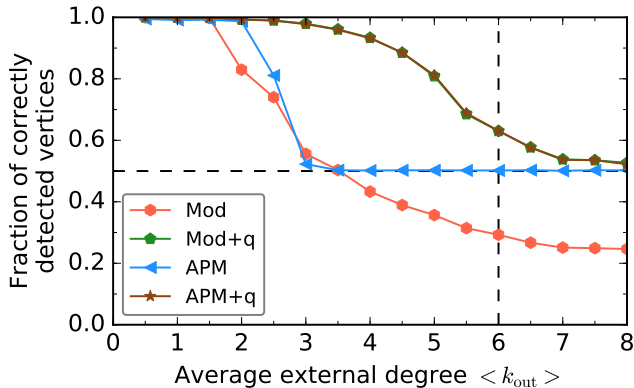


FIG. 21 Knowing the number of clusters beforehand improves community detection. The diagram shows the performance on the planted partition model of two methods: modularity optimisation via simulated annealing (Guimerà and Amaral, 2005) and the Absolute Potts Model (APM) (Ronhovde and Nussinov, 2010). Networks have 400 vertices, which are grouped in two equal-sized communities. The accuracy is measured via the fraction of correctly detected vertices (Section III.B). The horizontal line indicates the accuracy of random guessing, the dashed vertical line the theoretical detectability limit (Section III.C). For each algorithm we show two curves, referring to the results of the method in the absence of any information on the number of clusters, and when such information is fed into the model as initial input. In both cases, knowing the number of clusters beforehand leads to a much better performance.

straining the optimisation of the measure to partitions with fixed q , the problem can be alleviated (Nadakuditi and Newman, 2012).

But how do we know how many clusters there are? Here we briefly discuss some heuristic techniques, for statistically principled methods we defer the reader to Section IV.E. It has been recently shown that in the planted partition model q can be correctly inferred all the way up to the detectability limit from the spectra of two matrices: the *non-backtracking matrix* \mathbf{B} (Krzakala et al., 2013) and the *flow matrix* \mathbf{F} (Newman, 2013). They are $2m \times 2m$ matrices, where m is the number of edges of the graph. Each edge is considered in both directions, yielding $2m$ directed edges and indicated with the notation $i \rightarrow j$, meaning that the edge goes from vertex i to vertex j . Their elements read

$$B_{i \rightarrow j, r \rightarrow s} = \delta_{is}(1 - \delta_{jr}) \quad (15)$$

and

$$F_{i \rightarrow j, r \rightarrow s} = \frac{\delta_{is}(1 - \delta_{jr})}{k_i - 1}. \quad (16)$$

In Eq. (16) k_i is the degree of vertex i . So the elements of \mathbf{F} are basically the elements of \mathbf{B} , normalised by vertex degrees. This is done to account for the heterogeneous degree distributions observed in most real networks. Both matrices have non-zero elements only for

each pair of edges forming a directed path from the first vertex of one edge to the second of the other edge. To do that, edges have to be incident at one vertex. As a matter of fact, the non-backtracking matrix \mathbf{B} is just the adjacency matrix of the (directed) edges of the graph.

The name of the matrix \mathbf{B} is due to a connection with the properties of non-backtracking walks. A *non-backtracking walk* (Angel et al., 2015) is a path across the edges of a graph that is allowed to return to a vertex visited previously only after at least two other vertices have been visited; immediate returns like $1 \rightarrow 2 \rightarrow 1$ are forbidden. The elements of the k -th power of \mathbf{B} yield the number of non-backtracking walks of length k from a (directed) edge of the graph to another and the trace of the power matrix the number of closed non-backtracking walks of length k starting from any given (directed) edge.

A remarkable property of both matrices is that on networks with homogeneous groups (i. e., of similar size and internal edge density) most eigenvalues, which are generally complex, are enclosed by a circle centred at the origin, and that the number of eigenvalues lying outside of the circle is a good proxy of the number of communities of the network (Krzakala et al., 2013; Newman, 2013). For \mathbf{B} the circle's radius is given by the square root \sqrt{c} of the leading eigenvalue c , which may diverge for networks with heterogeneous degree distributions (e. g., power laws); for \mathbf{F} it equals $\sqrt{\langle k/(k-1) \rangle / \langle k \rangle}$, which is never greater than 1.

Unfortunately, computing the eigenvalues of the non-backtracking or the flow matrix is lengthy. Both are $2m \times 2m$ matrices. The adjacency matrix \mathbf{A} has $n \times n$ elements, so \mathbf{B} and \mathbf{F} are larger by a factor of $\langle k \rangle^2$, where $\langle k \rangle$ is the average degree of the network. An approximate but reliable computation of the spectra requires a time which scales superlinearly (approximately quadratic) with the network size n . So the problem is intractable for graphs with number of edges of the order of millions or higher. Also, if communities have diverse sizes and edge densities, as it happens in most networks encountered in applications, the bulk of eigenvalues may not have a circular shape, and it may become problematic to identify eigenvalues falling outside of the bulk.

Besides, non-backtracking walks must contain cycles, hence trees²⁵ dangling off the graph do not affect the spectrum of \mathbf{B} , which remains unchanged if all dangling trees are removed. This is a disturbing feature, as tree-like regions of the graph may play a role in the network's community structure, and most methods would find different partitions if trees are kept or removed²⁶. The spectrum of the flow matrix, instead, changes when dangling trees are kept or removed (Newman, 2013). In

²⁵ We remind that trees are connected acyclic graphs.

²⁶ Singh and Humphries showed that the problem can be solved via *reluctant backtracking walks*, in which the walker has a small but non-zero probability of returning to the vertex immediately (Singh and Humphries, 2015).

the limiting case in which the network itself is a tree, all eigenvalues of \mathbf{B} and \mathbf{F} are zero and even if there were a community structure one gets no relevant information.

The number of clusters can also be deduced by studying how the eigenvectors of graph matrices rotate when the adjacency matrix of the graph is subjected to random perturbations (Sarkar *et al.*, 2016). On stochastic block models this approach infers the correct value of q up to a threshold preceding the detectability limit. The method is also computationally expensive.

In general, if one can identify a set (range) of promising q -values, from preliminary information or via calculations like the ones described above or in Section IV.E, it is better to run constrained versions of clustering methods, searching for solutions only among partitions with those numbers of communities, than letting the methods discover q by themselves, which may lead to solutions of lower quality.

B. Consensus clustering

Many clustering techniques are stochastic in character and do not deliver a unique answer. A common scenario is when the desired solution corresponds to extrema of a cost function, that can only be found via approximation techniques, with results depending on random seeds and on the choice of initial conditions. Techniques not based on optimisation sometimes have the same feature, when tie-break rules are adopted in order to choose among multiple equivalent options encountered along the calculation.

What to do with all these partitions? Sometimes there are objective criteria to sort out a specific partition and discard all others. For instance, in algorithms based on optimisation, one could pick the solution yielding the largest (smallest) value of the function to optimise. For other techniques there is no clear-cut criterion.

A promising approach is combining the information of the different outputs into a new partition. Consensus clustering (Goder and Filkov, 2008; Strehl and Ghosh, 2002; Topchy *et al.*, 2005) is based on this idea. The goal is searching for a *consensus partition*, that is better fitting than the input partitions. Consensus clustering is a difficult combinatorial optimisation problem. An alternative greedy strategy (Strehl and Ghosh, 2002) relies on the *consensus matrix*, which is a matrix based on the co-occurrence of vertices in communities of the input partitions (Fig. 22). The consensus matrix is used as an input for the graph clustering technique adopted, leading to a new set of partitions, which produce a new consensus matrix, etc., until a unique partition is finally reached, which is not changed by further iterations. The steps of the procedure are listed below. The starting point is a network G with n vertices and a clustering algorithm \mathbf{A} .

1. Apply \mathbf{A} on G n_P times, yielding n_P partitions.
2. Compute the consensus matrix \mathbf{D} : D_{ij} is the num-

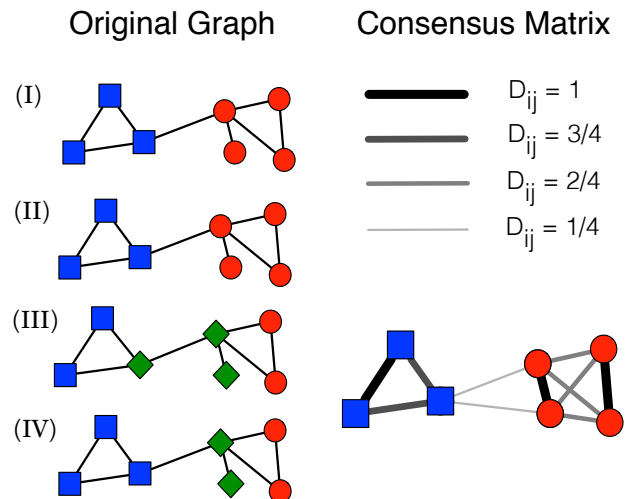


FIG. 22 Consensus clustering in networks. A simple graph has a natural partition in two communities [squares and circles on diagrams (I) and (II)]. The combination of (I), (II), (III) and (IV) yields the weighted consensus matrix illustrated on the right. The thickness of each edge is proportional to its weight. In the consensus matrix the community structure of the original network is more visible: the two communities have become cliques, with “heavy” edges, whereas inter-community edges are rather weak. This improvement is obtained despite the presence of two inaccurate partitions in three clusters (III and IV). Reprinted figure with permission from (Lancichinetti and Fortunato, 2012). © 2012, by the Nature Publishing Group.

ber of partitions in which vertices i and j of G are assigned to the same community, divided by n_P .

3. All entries of \mathbf{D} below a chosen threshold τ are set to zero²⁷.
4. Apply \mathbf{A} on \mathbf{D} n_P times, yielding n_P partitions.
5. If the partitions are all equal, stop²⁸. Otherwise go back to 2.

Since the consensus matrix is in general weighted, the algorithm \mathbf{A} must be able to handle weighted networks, even if the graph at study is binary. Fortunately many popular algorithms have natural extensions to the weighted case.

The integration of consensus clustering with popular existing techniques leads to more accurate partitions

²⁷ Without thresholding the consensus matrix would quickly turn into a dense matrix, rendering the application of clustering algorithms computationally expensive. However, the method does not strictly require thresholding, and if the network is not too large one can skip step 3 and use the full matrix all along (Bruno *et al.*, 2015).

²⁸ The consensus matrix is block-diagonal in this case.

than those delivered by the methods alone on LFR benchmark graphs (Lancichinetti and Fortunato, 2012). Interestingly, this holds even for methods whose direct application gives poor results on the same graphs, like modularity optimisation (Section IV.F). The variability of the partitions, rather than being a problem, becomes a factor of performance enhancement. The outcome of the procedure depends on the choice of the threshold parameter τ and the number of input partitions n_P , which can be selected by testing the performance on benchmark networks (Lancichinetti and Fortunato, 2012). Consensus clustering is also a promising technique to detect communities in evolving networks (Section IV.H).

C. Spectral methods

Spectral graph clustering is an approach to detect clusters using spectral properties of the graph (Fortunato, 2010; von Luxburg, 2006). The eigenvalue spectrum of several graph matrices (e. g., the adjacency matrix, the Laplacian, etc.) typically consists of a dense bulk of closely spaced eigenvalues, plus some outlying eigenvalues separated from the bulk by a significant gap. The eigenvectors corresponding to these outliers contain information about the large-scale structure of the network, like community structure²⁹. Spectral clustering consists in generating a projection of the graph vertices in a metric space, by using the entries of those eigenvectors as coordinates. The i -th entries of the eigenvectors are the coordinates of vertex i in a k -dimensional Euclidean space, where k is the number of eigenvectors used. The resulting points can be grouped in clusters by using standard partitioning techniques like k -means clustering (MacQueen, 1967).

Spectral clustering is not always reliable, however. When the network is very sparse (Section II.C) the separation between the eigenvalues of the community-related eigenvectors and the bulk is not sharp. Eigenvectors corresponding to eigenvalues outside of the bulk may be correlated to high-degree vertices (hubs), instead of group structure. Likewise, community-related eigenvectors can be associated to eigenvalues ending up inside the bulk. In these situations, selecting eigenvectors based on whether their associated eigenvalues are inside or outside the bulk yields a heterogeneous set, containing information both on communities and on other features (e. g., hubs). Using those eigenvectors for the spectral clustering procedure renders community detection more difficult, sometimes impossible. Unfortunately, many of the networks encountered in practical studies are very sparse and can lead to this type of problems.

²⁹ Typically each such eigenvector is *localised*, in that its entries are markedly different from zero in correspondence of the vertices of a community, while the other entries are close to zero.

Indeed on sparse networks constructed with the planted partition model spectral methods relying on standard matrices [adjacency matrix, Laplacian, modularity matrix (Newman, 2006), etc.] fail before the theoretical detectability limit (Section III.C) (Krzakala *et al.*, 2013). The non-backtracking matrix \mathbf{B} of Eq. (15) was introduced to address this problem (Krzakala *et al.*, 2013). On the planted partition model the associated eigenvalues of the community-related eigenvectors of \mathbf{B} are separated from the bulk until the theoretical detectability limit, so spectral methods using the top eigenvectors of \mathbf{B} are capable to find communities as long as they are detectable, modulo the caveats we expressed in Section IV.A.

D. Overlapping communities: Vertex or Edge clustering?

Soft clustering, where communities may overlap, is an even harder problem than hard clustering, where there is no community overlap. The possibility of having multiple memberships for the vertices introduces additional degrees of freedom in the problem, causing a huge expansion of the space of possible solutions. It has been pointed out that overlapping communities, especially in social networks, reflect different types of associations between people (Ahn *et al.*, 2010; Evans and Lambiotte, 2009). Two actors could be co-workers, friends, relatives, sport mates, etc.. Actor A could be a work colleague of B and a friend of C , so she would sit in the overlap between the community of colleagues of B and the community of friends of C . For this reason, it has been suggested that an effective way to recover overlapping clusters is to group edges, rather than vertices. In the example above, the edges connecting A with B and A with C would be placed in different groups, and since they both have A as endpoint, the latter turns out to be an overlapping vertex.

Moreover, edge clustering is claimed to have the additional advantage of reconciling soft clustering with hierarchical community structure (Ahn *et al.*, 2010). If there is hierarchy, communities are nested within each other as many times as there are hierarchical levels. Hierarchical structure is often represented via *dendrograms*³⁰, with the network being divided in clusters, which are in turn divided in clusters, and so on until one ends up with singleton clusters, consisting of one vertex each. But this can be done only if communities do not share vertices.

³⁰ A dendrogram, or *hierarchical tree*, is a tree diagram used to represent hierarchical partitions. At the bottom there are as many nodes as there are vertices in the graph, representing the singleton clusters. At the top there is one node (root), standing for the partition grouping all vertices in a single cluster. Horizontal lines indicate mergers of a pair of clusters or, equivalently, splits of one cluster. Each vertex of the tree identifies one cluster, whose elements can be read by following all bifurcations starting from the vertex all the way down to the leaves of the tree.

Overlapping vertices should be assigned to multiple clusters of lower hierarchical levels, yielding multiple copies of them in the dendrogram. Instead, one could build a dendrogram displaying edge communities, where each edge is assigned to a single cluster, but clusters can still overlap because edges in different clusters may share one endpoint (Ahn *et al.*, 2010).

Some remarks are in order. First, there may still be overlapping communities even if there were a single type of association between the vertices. For instance, if we keep only the friendship relationships within a given population of actors, there are many social circles and there could be active actors with multiple ties within two circles, or more. Second, in the traditional picture of networks with community structure (Fig. 4), the edges connecting two different groups may be assigned to one of the communities they join or they could be put together in a separate group. Either way, they would signal an overlap between the communities, which is artificial. This happens even in the extreme case of a single edge connecting vertices A and B of two groups, as that edge will have to be assigned to a group, which inevitably forces A and B into a common cluster. Third, if we rely on the picture emerging from the analysis by Yang and Leskovec (Yang and Leskovec, 2014) (Section III.E) overlaps between clusters could be much denser than we expect, hence not only vertices but also edges may be shared among different groups, and edge dendrograms would have the same problem as classic vertex dendrograms³¹. Fourth, the computational complexity of the calculation can rise substantially, as in networks of interest there are typically many more edges than vertices. Finally, there is nothing revealing that there is a conceptual or algorithmic advantage in grouping edges versus vertices, other than works showing that a specific edge clustering technique outperforms some vertex clustering techniques on a specific set of networks.

To shed some light on the situation, we performed the following test. We took some network data sets with annotated vertices, giving an indication about what the communities of those networks could be³². For each network G we derived the corresponding *line graph* $L(G)$, which is the graph whose vertices are the edges of G , while edges are set between pairs of vertices of $L(G)$ whose corresponding edges in G are adjacent at one of their endpoints. Vertex communities of $L(G)$ are then edge communities of the original network G . The question is whether by working on $L(G)$ the detection improves or not. We searched for overlapping communities

with OSLOM (Lancichinetti *et al.*, 2011). We applied OSLOM on the original graphs and on their line graphs. The covers found on the line graphs were turned into covers of the vertices of G , by replacing each vertex of $L(G)$ with the pair of vertices of the corresponding edge of G .

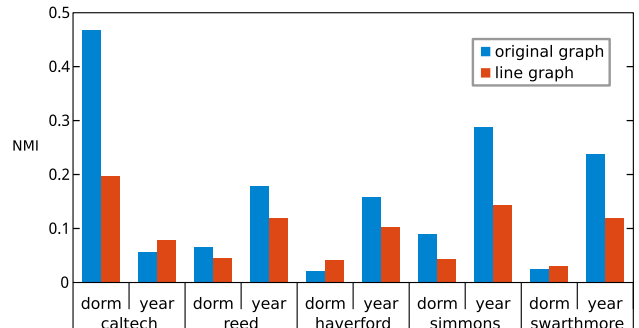


FIG. 23 Comparison between edge communities and vertex communities. The diagram shows the similarity between the covers of annotated vertices of five social networks and the topological covers found by OSLOM on them (left bar of each pair) and on their line graphs (right bar). The networks represent FaceBook friendships between students of US universities (Traud *et al.*, 2012). There are several annotations for each student, we selected those which are more closely related to topological groups: year of study and dormitory. The similarity was computed by using the normalised mutual information (NMI), in the version for covers proposed by Lancichinetti, Fortunato and Kertész (Lancichinetti *et al.*, 2009). Vertex communities detected in the original graphs are overall better correlated with the annotated clusters than edge communities.

The results can be seen in Fig. 23, showing how similar the covers found on the original networks and on the line graphs are with respect to the covers of annotated vertices. Neither approach is very accurate, as expected (see Section III.D and Fig. 16), but vertex communities show a greater association to the annotated clusters than edge communities, except in a few instances where the similarity is very low. Analyses carried out on LFR benchmark graphs (not shown) lead to the same conclusion. We stress that traditional line graphs have the problem that edges adjacent to a hub vertex in the original graph turn into vertices who are all connected to each other, forming giant cliques, which might dominate the structure of the line graph, misleading clustering techniques. The procedure can be refined by introducing weights for the edges of the line graphs, that can be computed in various ways, e. g., based on the similarity of the neighbourhoods of adjacent edges in the original network (Ahn *et al.*, 2010).

Still we believe that our tests provide some evidence that edge clustering is no better than vertex clustering, in general. The superiority of algorithms based on either approach should be assessed a posteriori, case by case, and the answer may depend on the specific data sets under investigation.

³¹ In this case, if we used edge clustering, each edge would be placed in one cluster only. However, when one turns edge communities into vertex communities, multiple relationships can be still recovered (Ahn *et al.*, 2010).

³² We have seen in Section III.D that metadata are not necessarily correlated with topological clusters. We used data sets for which there is some correlation.

E. Methods based on statistical inference

Statistical inference provides a powerful set of tools to tackle the problem of community detection. The standard approach is to fit a generative network model on the data (Ball *et al.*, 2011; Guimerà and Sales-Pardo, 2009; Hastings, 2006; Karrer and Newman, 2011; Newman and Leicht, 2007; Peixoto, 2014). The stochastic block model (SBM) is by far the most used generative model of graphs with communities (see Section II.C and references therein). We have seen that it can describe other types of group structure, like disassortative and core-periphery structure (Fig. 8). The unnormalised maximum log-likelihood that a given partition g in q groups of the network G is reproduced by the standard SBM reads (Karrer and Newman, 2011)

$$\mathcal{L}_S(G|g) = \sum_{r,s=1}^q e_{rs} \log \left(\frac{e_{rs}}{n_r n_s} \right), \quad (17)$$

where e_{rs} is the number of edges running from group r to group s , n_r (n_s) the number of vertices in r (s) and the sum runs over all pairs of groups (including when $r = s$). This version of the model, however, does not account for the degree heterogeneity of most real networks, so it does a poor job at describing the group structure of many of them. Therefore, Karrer and Newman proposed the *degree-corrected stochastic block model* (DCSBM) (Karrer and Newman, 2011), in which the degrees of the vertices are kept constant, on average, via the introduction of additional suitable parameters³³. The unnormalised maximum log-likelihood for the DCSBM is

$$\mathcal{L}_{DC}(G|g) = \sum_{r,s=1}^q e_{rs} \log \left(\frac{e_{rs}}{e_r e_s} \right), \quad (18)$$

where e_r (e_s) is the sum of the degrees of the vertices in r (s).

The most important drawback of this type of approach is the need to specify the number q of groups beforehand, which is usually unknown for real networks. This is because a straight maximisation of the likelihoods of Eqs. (17) and (18) over the whole set of possible solutions yields the trivial partition in which each vertex is a cluster (*overfitting*). In Section IV.A we have seen ways to extract q from spectral properties of the graph. But it would be better to have statistically principled methods, to be consistent with the approach used to perform the inference.

A possibility is *model selection*, for instance by choosing the model that best compresses the data (Grünwald

et al., 2005; Rissanen, 1978). The extent of the compression can be estimated via the total amount of information necessary to describe the data, which includes not only the fitted model, but also the information necessary to describe the model itself, which is a growing function of the number of blocks q (Peixoto, 2013). This quantity, that we indicate with Σ , is called the *description length*. Minimising the description length naturally avoids overfitting. Partitions with large q are associated to “heavy” models in terms of their information content, and do not represent the best compression. On the other hand, partitions with low q have high information content, even if the model itself is not loaded with parameters. Hence the minimum description length corresponds to a non-trivial number of groups and it makes sense to minimise Σ to infer the block structure of the graph.

It turns out that this approach has a limited resolution on the standard SBM: the maximum number of blocks that can be resolved scales as \sqrt{n} for a fixed average degree $\langle k \rangle$, where n is the number of vertices of the network. This means that the minimum size of detectable blocks scales as \sqrt{n} , just as it happens for modularity maximisation (Section IV.F). A more refined method of model selection, consisting in a nested hierarchy of stochastic block models, where an upper level of the hierarchy serves as prior information to a lower level, brings the resolution limit down to $\log n$, enabling the detection of much smaller blocks (Peixoto, 2014).

Other techniques to extract the number of groups have been proposed (Côme and Latouche, 2015; Daudin *et al.*, 2008; Handcock *et al.*, 2007; Latouche *et al.*, 2012; Newman and Reinert, 2016).

F. Methods based on optimisation

Optimisation techniques have received the greatest attention in the literature. The goal is finding an extremum, usually the maximum, of a function indicating the quality of a clustering, over the space of all possible clusterings. Quality functions can express the goodness of a partition or of single clusters.

The most popular quality function is the *modularity* by Newman and Girvan (Newman and Girvan, 2004). It estimates the quality of a partition of the network in communities. The general expression of modularity is

$$Q = \frac{1}{2m} \sum_{ij} (A_{ij} - P_{ij}) \delta(C_i, C_j), \quad (19)$$

where m is the number of edges of the network, the sum runs over all pairs of vertices i and j , A_{ij} is the element of the adjacency matrix, P_{ij} is the *null model term* and in the Kronecker delta at the end C_i and C_j indicate the communities of i and j . The term P_{ij} indicates the average adjacency matrix of an ensemble of networks, derived by randomising the original graph, such to preserve some of its features. Therefore, modularity measures how different the original graph is from such randomisations.

³³ The authors were inspired by modularity maximisation, which gives far better results when the null model consists of rewiring edges by preserving the degree sequence of the network (on average), than by preserving only the total number of edges.

The concept was inspired by the idea that by randomising the network structure communities are destroyed, so the comparison between the actual structure and its randomisation reveals how non-random the group structure is. A standard choice is $P_{ij} = k_i k_j / 2m$, k_i and k_j being the degrees of i and j , and corresponds to the expected number of edges joining vertices i and j if the edges of the network were rewired such to preserve the degree of all vertices, on average. This yields the classic form of modularity

$$Q = \frac{1}{2m} \sum_{ij} \left(A_{ij} - \frac{k_i k_j}{2m} \right) \delta(C_i, C_j). \quad (20)$$

Other choices of the null model term allow us to incorporate specific features of network structure, like bipartiteness (Barber, 2007), correlations (MacMahon and Garlaschelli, 2015), signed edges (Traag and Bruggeman, 2009), space embeddedness (Expert *et al.*, 2011), etc.. The extension of Eq. (20) and of its variants to the case of weighted networks is straightforward (Newman, 2004). For simplicity we focus on unweighted graphs here, but the issues we discuss are general.

Because of the delta, the only contributions to the sum come from vertex pairs belonging to the same cluster, so we can group these contributions together and rewrite the sum over the vertex pairs as a sum over the clusters³⁴

$$Q = \sum_C \left[\frac{l_C}{m} - \left(\frac{k_C}{2m} \right)^2 \right]. \quad (21)$$

Here l_C the total number of edges joining vertices of community C and k_C the sum of the degrees of the vertices of C (Section II.A). The first term of each summand in Eq. (21) is the fraction of edges of the graph falling within community C , whereas the second term is the expected fraction of edges that would fall inside C if the graph were taken from the ensemble of random graphs preserving the degree of each vertex of the original network, on average. The difference in the summand would then indicate how “non-random” subgraph C is. The larger the difference the more confident we can be that the placement of edges within C is not random (Fig. 24). Large values of Q are then supposed to indicate partitions with high quality.

Modularity maximisation is NP-hard (Brandes *et al.*, 2008). Therefore one can realistically hope to find only decent approximations of the modularity maximum and a wide variety of approaches has been proposed. Due to its simplicity, the prestige of its inventors and early results on the benchmark of Girvan and Newman (Section III.A) and on small real benchmark networks, like Zachary karate club network (Fig. 15), modularity has

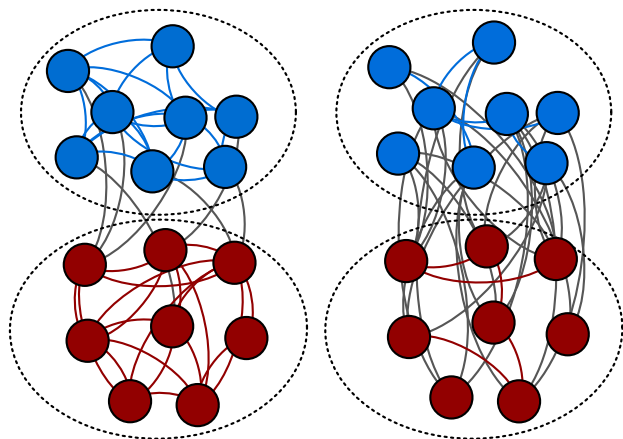


FIG. 24 Modularity by Newman and Girvan. The network on the left has a visible community structure, with two clusters, whose vertices are highlighted in blue and red, respectively. Modularity measures how different the clusters of the partition are from the corresponding clusters of the ensemble of random graphs obtained by randomly joining the vertices, such to preserve their degrees, on average. The picture on the right shows the result of one such randomisation. The internal edges are coloured in blue and red. They are just a handful compared to the number of edges joining the same groups of vertices in the original network (blue and red lines in the left picture), while there are now many more edges running between the subgroups (black lines): the randomisation has destroyed the community structure of the graph, as expected. The value of modularity for the bipartition on the left is expected to be large.

become the best known and most studied object in network clustering. In fact, soon after its introduction, it seemed to represent the essence of the problem, and the key to its solution.

However, it became quickly clear that the measure is not as good as it looks. For one thing, there are high-modularity partitions even in random graphs without groups (Guimerà *et al.*, 2004). This seems counterintuitive, given that modularity has been designed to capture the difference between random and non-random structure. Modularity is a sort of distance between the actual network and *an average* over random networks, ignoring altogether the distribution of the relevant community variables, like the fractions of edges within the clusters, over all realisations generated by the configuration model. If the distribution is not strongly peaked, the values of the community variables measured on the original graph may be found in a large number of randomised networks, even though the averages look far away from them. In other words, we should pay more attention to the *significance* of the maximum modularity value Q_{max} , than to the value itself. How can we estimate the significance of Q_{max} ? A natural way is maximising Q over all partitions of every randomised graph. One then computes the average $\langle Q_{rand} \rangle$ and the standard deviation σ_Q^{rand} of the resulting values. The statistical significance of Q_{max}

³⁴ A partition quality function that can be formulated as a sum over the clusters is called *additive*.

is indicated by the distance of Q_{max} from the null model average $\langle Q_{rand} \rangle$ in units of the standard deviation σ_Q^{rand} , i. e., by the z -score

$$z = \frac{Q_{max} - \langle Q_{rand} \rangle}{\sigma_Q^{rand}}. \quad (22)$$

If $z \gg 1$, Q_{max} indicates strong community structure. This approach has problems, though. The main drawback is that the distribution of Q_{rand} over the ensemble of null model random graphs, though peaked, is not Gaussian. Therefore, one cannot attribute to the values of the z -score the significance corresponding to a Gaussian distribution, and one ought to compute the statistical significance for the correct distribution. Also, the z -score depends on the network size, so the same values may indicate different levels of significance for networks differing considerably in size.

Next, it is not true that the modularity maximum always corresponds to the most pronounced community structure of a network. In Fig. 25 we show the well-known example of the ring of cliques (Fortunato and Barthélemy, 2007). The network consists of 16 cliques with four vertices each. Every clique has two neighbouring cliques, connected to it via a single edge. Intuition suggests that the graph has a natural community structure, with 16 communities, each corresponding to one clique. Indeed, the Q -value of this partition is $Q_1 = 89/112 \approx 0.79464\dots$, pretty close to 1, which is the upper bound of modularity. However, there are partitions with larger values, like the partition in 8 clusters indicated by the dashed contours, whose modularity is $Q_2 = 90/112 \approx 0.80357 > Q_1$.

This is due to the fact that Q has a preferential scale for the communities, deriving from the underlying null model and revealed by its explicit dependence on the number of edges m of the network [Eq. (21)]. According to the configuration model, the expected number l_{AB} of edges running between two subgraphs A and B with total degree k_A and k_B , respectively, is approximately $k_A k_B / 2m$. Consequently, if k_A and k_B are of the order of \sqrt{m} or smaller, l_{AB} could become smaller than 1. This means that in many randomisations of the original graph G , subgraphs A and B are disconnected and even a single edge joining them in G signals a non-random association. In these cases, modularity is larger when A and B are put together than when they are treated as distinct communities, as in the example of Fig. 25. The modularity scale depends only on the number of edges m , and it may have nothing to do with the size of the actual communities of the network. The resolution limit questions the usefulness of modularity in practical applications (Fortunato and Barthélemy, 2007).

Many attempts have been made to mitigate the consequences of this disturbing feature. One approach consists in introducing a resolution parameter γ into modularity's formula (Arenas *et al.*, 2008b; Reichardt and Bornholdt, 2006). By tuning γ it is possible to arbitrarily vary the resolution scale of the method, going from very large to

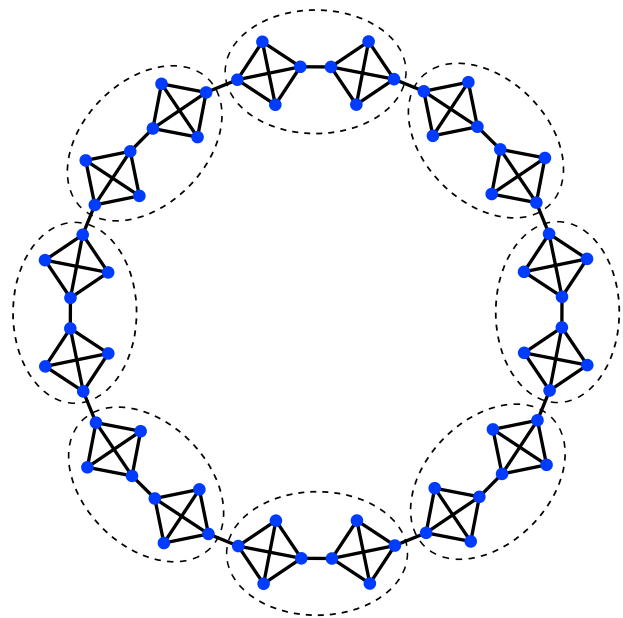


FIG. 25 Resolution limit of modularity optimisation. The network in the figure is made of cliques of four vertices, arranged such to form a ring-like structure, with each clique joined to two other cliques by a single edge. The naïve expectation is that modularity would reach its maximum for the partition whose communities are the cliques, which appears to be the natural partition of the network. However, it turns out that there are partitions with higher modularity, whose clusters are combinations of cliques, like the partition indicated by the dashed contours.

very small communities. We shall discuss such multi-resolution approaches in Section IV.G. Here we emphasize that multi-resolution versions of modularity do not provide a reliable solution to the problem. This is because modularity maximisation has an additional bias: large subgraphs are usually split in smaller pieces (Lancichinetti and Fortunato, 2011). This problem has the same source as the resolution limit, namely the choice of the null model. Since modularity has a preferential scale for the communities, when a subgraph is too large it is convenient to break it down, to increase the modularity of the partition. So, when there is no characteristic scale for the communities, like when there is a broad cluster size distribution, large communities are likely to be broken, and small communities are likely to be merged. Since multi-resolution versions of modularity can only shift the resolution scale of the measure back and forth, they are unable to correct both effects at the same time³⁵ (Lan-

³⁵ More promising results can be obtained with hierarchical multi-level methods, in which multi-resolution modularity is applied iteratively on every cluster with independent resolution param-

cichinetti and Fortunato, 2011). In addition, tuning the resolution parameter in the search for good partitions is usually computationally very demanding, as in many cases the optimisation procedure has to be repeated over and over for all γ -values one desires to investigate.

We stress that the resolution limit is a feature of modularity itself, not of the specific way adopted to maximise it. Therefore, there is no magic heuristic that can circumvent this issue. The Louvain method (Blondel *et al.*, 2008) has been held as one such magic heuristic. The method performs a greedy optimisation of Q in a hierarchical manner, by assigning each vertex to the community of their neighbours yielding the largest Q , and creating a smaller weighted super-network whose vertices are the clusters found previously. Partitions found on this super-network hence consist of clusters including the ones found earlier, and represent a higher hierarchical level of clustering. The procedure is repeated until one reaches the level with largest modularity. In the comparative analysis of clustering algorithms performed by Lancichinetti and Fortunato on the LFR benchmark (Lancichinetti and Fortunato, 2009), the Louvain algorithm was the second best-performing method, after Infomap (Rosvall and Bergstrom, 2008). This has given the impression that the peculiar strategy of the method solves the resolution problems above, which is not true. The reason why the performance is so good is that Lancichinetti and Fortunato adopted the lowest partition of the hierarchy, the one with the smallest clusters (Lancichinetti and Fortunato, 2014). By using the partition with highest modularity performance degrades considerably (Fig. 26), as expected. As suggested by the developers of the algorithm themselves, using the lowest level helps avoiding unnatural community mergers; as an example, they showed that the natural partition of the ring of cliques (Fig. 25) can be recovered this way. However, the bottom level has lower modularity than the top level, so we face a sort of contradiction, in that users are encouraged to use sub-optimal partitions, even though one assumes that the best clustering corresponds to the highest value of the quality function, which is what the method is supposed to find. There is no guarantee that the bottom level yields the most meaningful solution. On the other hand, users have the option of choosing among a few partitions and a slightly higher chance to find what they search for.

Moreover, the modularity landscape is characterised by a larger than exponential³⁶ number of distinct partitions, whose modularity values are very close to the global maximum (Good *et al.*, 2010). This explains why many heuristic methods of modularity maximisation are able to come very close to the global maximum of Q ,

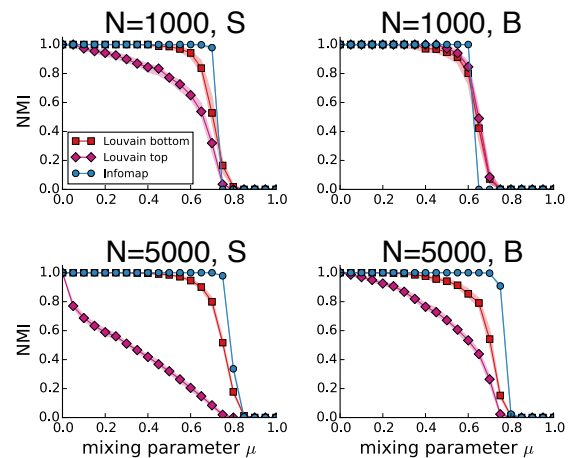


FIG. 26 Performance of the Louvain method. The panels indicate the accuracy of the algorithm to detect the planted partition of the LFR benchmark as a function of the mixing parameter, for different choices of the network size (1000 and 5000 vertices) and of the range of community sizes (label S indicates that communities have between 10 and 50 vertices, label B that they have between 20 and 100 vertices). Accuracy is calculated via the normalised mutual information (NMI), in the version by Lancichinetti, Fortunato and Kertész (Lancichinetti *et al.*, 2009). Results are heavily depending on the hierarchical level one chooses at the end of the procedure. When one picks the top level (diamonds), which is the one with largest modularity, the accuracy is poor, as expected, especially when communities are smaller. When one goes for the bottom level (squares), which has lower modularity and smaller clusters than the top level partition, there is a far better agreement with the planted partition and the performance gets closer to that of Infomap (circles). The squares follow the performance curves used in the comparative analysis by Lancichinetti and Fortunato (Lancichinetti and Fortunato, 2009). Courtesy from Andrea Lancichinetti.

but it also implies that the global maximum is basically impossible to find. In addition, high- Q partitions are not necessarily similar to each other, despite the proximity of their modularity scores. The optimal structural partition, which may not correspond to the modularity maximum due to problems exposed above, may however have a large Q -value. Therefore the optimal partition is basically indistinguishable from a huge number of high-modularity partitions, which are in general structurally dissimilar from it. The large structural diversity of high-modularity partitions implies that one cannot rely on any of them, at least in principle. Reliable solutions could be singled out when the domain user imposes some constraints on the clustering of the system, or when she expects it to have specific features. In the absence of additional information or expectations, consensus clustering could be used to derive more robust partitions. Indeed, it has been shown that the consensus of many high-modularity partitions, combined with a hierarchical

eters, so that a coexistence of very diverse scales is permitted (Granell *et al.*, 2012). Such approaches, however, deviate from the original idea of modularity maximisation, which is based on a global null model valid for the network as a whole.

³⁶ Exponential in the number n of graph vertices.

approach, could help to solve resolution problems and to avoid to find communities in random graphs without groups (Zhang and Moore, 2014).

As of today, modularity optimisation is still the most used clustering technique in applications. This may appear odd, given the serious issues of the method and the fact that nowadays more powerful techniques are available, like a posteriori stochastic block modelling (Section IV.J). Indeed Newman has proven that optimising modularity is equivalent to maximising the likelihood that the planted partition model reproduces the network (Newman, 2016). But the planted partition model is a very specific case of the general stochastic block model, in that the intra-group edge probabilities are all equal to the same value p_{in} and the inter-group edge probabilities are all equal to the same value p_{out} . There is no reason to limit the inference to this specific case, when one could use the full model.

Optimising partition quality functions may lead to resolution problems, just like it happens for modularity³⁷. Instead, one could try to optimise *cluster quality functions*. One starts with some function $q(C)$ expressing how “community-like” a subgraph is and with a seed vertex s . The goal is to build a cluster C_s including s such that $q(C_s)$ is maximum³⁸. This is usually done by exploring the neighbours of the temporary subgraph C_s , starting from the neighbours of s when C_s includes only s . The neighbouring vertex whose inclusion yields the largest increase of q is added to the subgraph. When a new vertex is included, the structure of the subgraph is altered and the other vertices can be examined again, as it might be advantageous to knock some of them out. The process stops when the quality $q(C_s)$ cannot be increased anymore via the inclusion or the exclusion of vertices.

The optimisation of cluster quality functions offers a number of advantages over the optimisation of partition quality functions. First, it is consistent with the idea that communities are local structures, which are sensitive to what happens in their neighbourhood, but are fairly unaffected by the rest of the network: the structure of a social circle in Europe is hardly influenced by the dynamics of social circles in Australia, though they are parts of the same global social network of humans. Consequently, if a network undergoes structural changes in one region, community structure is altered and is to

be recovered only in that region, while the clustering of the rest of the network remains the same. By optimising partition quality functions, instead, any little change may have an effect on every community of the graph. Second, since cluster quality functions do not embody any global scale, severe resolution problems are usually avoided³⁹. Moreover, one can investigate only parts of the network, which is particularly valuable when the graph is large and a global analysis would be out of reach, computationally. The local exploration of the graph allows to reach vertices already assigned to clusters, so overlaps can be naturally detected. In the last years several algorithms based on the optimisation of cluster quality functions have been designed (Baumes *et al.*, 2005; Clauset, 2005; Huang *et al.*, 2011; Lancichinetti *et al.*, 2009, 2011).

G. Methods based on dynamics

Communities can also be identified by running dynamical processes on the network, like diffusion (Jeub *et al.*, 2015; Pons and Latapy, 2005; Rosvall and Bergstrom, 2008; Van Dongen, 2000; Zhou, 2003a,b; Zhou and Lipowsky, 2004), spin dynamics (Raghavan *et al.*, 2007; Reichardt and Bornholdt, 2006; Ronhovde and Nussinov, 2010; Traag *et al.*, 2011), synchronisation (Arenas *et al.*, 2006; Boccaletti *et al.*, 2007), etc.. In this section we focus on diffusion and spin dynamics, that inform most approaches.

Random walk dynamics is by far the most exploited in community detection. If communities have high internal edge density and are well-separated from each other, random walkers would be trapped in each cluster for quite some time, before finding a way out and migrating to another cluster. We briefly discuss two broad classes of algorithms: methods based on vertex similarity and methods based on the map equation.

The first class of techniques consists in using random walk dynamics to estimate the similarity between pairs of vertices. For instance, in the popular method *Walktrap* the similarity between vertices i and j is given by the probability that a random walker moves from i to j in a fixed number of steps t (Pons and Latapy, 2005). The parameter t has to be large enough, to allow for the exploration of a significant portion of the graph, but not too big, as otherwise one would approach the stationary limit in which transition probabilities trivially depend on the degrees of the vertices. If there is a pronounced community structure, pairs of vertices in the same cluster are much more easily reachable by a random walk than pairs of vertices in different clusters, so the vertex similarity is expected to be considerably higher within groups than between groups⁴⁰. In that case, clusters can be readily

³⁷ Traag and Van Dooren have shown that one can design additive quality functions such that the best partition of the network induces the optimal partition for any subgraph S , i. e., the partition found when the detection is performed only on S (Traag *et al.*, 2011). This is possible when the coefficients of the summand corresponding to each community does not depend on global properties of the graph. Even those functions have their own preferential community scale, though.

³⁸ For some functions the optimum corresponds to their minimum, not the maximum. This occurs when they are related to variables that are supposed to be small when communities are good, like the density of edges between clusters.

³⁹ If one defines the quality of the cluster with respect to the rest of the network, global scales may still slip into the function.

⁴⁰ A related method is the *Markov Cluster Algorithm*

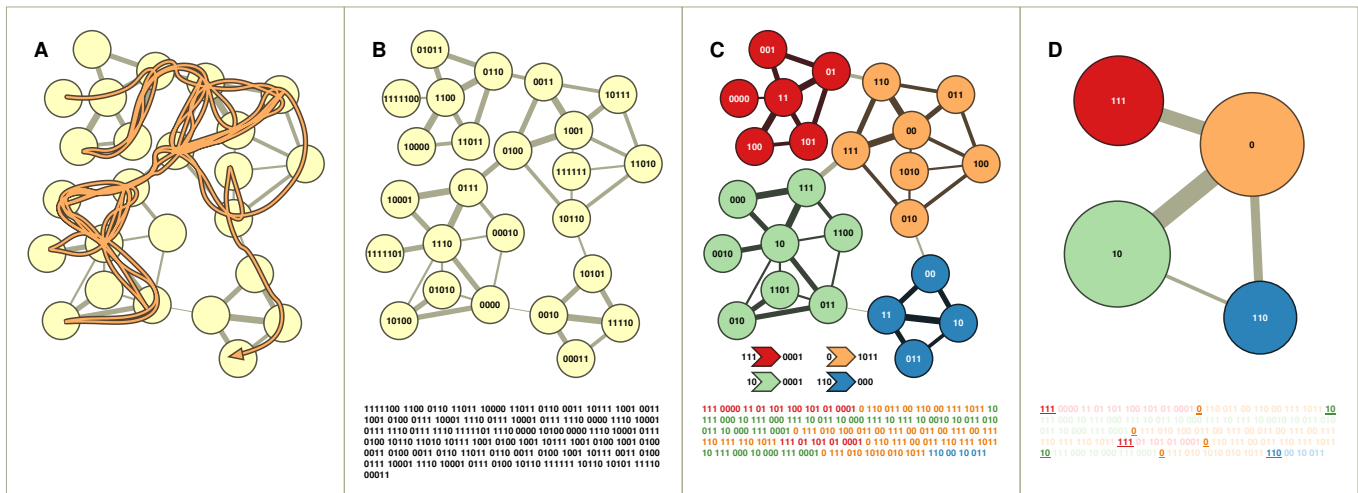


FIG. 27 Infomap. The random walk in (A) can be described as a sequence of the vertices, each labeled with unique codewords (B), or by dividing the graph in regions and using unique codewords only for the vertices of the same region (C). This way the same codeword can be used for multiple vertices, at the cost of indicating when the random walker leaves a region to enter a new one, as in that case one has to specify the codeword of the new region, to unambiguously locate the walker. The network has four communities [indicated by the colours in (C)], and in this case the map-like description of (C) is more parsimonious than the one in (B). This is shown by looking at the actual code needed in either case (bottom of the figures), which is clearly shorter for (C). In (D) the transitions between the clusters are highlighted. Reprinted figure with permission from (Rosvall and Bergstrom, 2008). © 2008, by the National Academy of Sciences, USA.

identified via standard hierarchical or partitional clustering techniques (Jain *et al.*, 1999; Xu and Wunsch, 2008). This class of methods have a high computational complexity, higher than quadratic in the number n of vertices (on sparse graphs), so they cannot be used on large networks. Besides, they are often parameter-dependent.

The map equation stems from a seminal paper by Rosvall and Bergstrom (Rosvall and Bergstrom, 2008), who asked what is the most parsimonious way to describe an infinitely long random walk taking place on the graph. The information content of any description is given by the total number of bits required to indicate the various stages of the process. The simplest description is obtained by listing sequentially all vertices reached by the random walker, each vertex being described by a unique codeword. However, if the network has a community structure, there may be a more compact description, which follows the principle of geographic maps,

where there are multiple cities and streets with the same name across regions. Vertex codewords could be recycled among different communities, which play the role of regions/states, and vertices with identical name are distinguished by specifying the community they belong to. If clusters are well separated from each other, transitions between clusters are infrequent, so it is advantageous to use the map, with the communities as regions, because in the description of the random walk the codewords of the clusters will not be repeated many times, while there is a considerable saving in the description due to the limited length of the codewords used to denote the vertices (Fig. 27). The map equation yields the description length of an infinite random walk consists of two terms, expressing the Shannon entropy of the walk within and between clusters. The best partition is the one yielding the minimum description length.

This method, called Infomap, can be applied to weighted networks, both undirected and directed. In the latter case, random walk dynamics is modified by introducing a teleportation probability, as in the PageRank process (Brin and Page, 1998), to ensure that a non-trivial stationary state is reached. It has been successfully extended to the detection of hierarchical community structure (Rosvall and Bergstrom, 2011) and of overlapping clusters (Viamontes Esquivel and Rosvall, 2011). In classic random walks the probability of reaching a vertex only depends on where the walker stands, not on where it is coming from. The map equation has also been extended to random walks whose transition probabilities depend on earlier steps too (higher-order Markov

(MCL) (Van Dongen, 2000), which consists of iterating two operations: raising to a power the *transfer matrix* \mathbf{T} of the graph, whose element T_{ij} equals the probability that a random walker, sitting at j , moves to i ; raising the elements of the resulting matrix to a power, such that the larger values are enhanced with respect to the smaller ones, many of which are set to zero to lighten the calculations, while the remaining ones are normalised by dividing them by the sum of elements of their column, yielding a new transfer matrix. The process eventually reaches a stationary state, corresponding to the matrix of a disconnected graph, whose connected components are the sought clusters.

dynamics) (Persson *et al.*, 2016; Rosvall *et al.*, 2014), retaining memory of the (recent) past. Applications show that in this way one can recover overlapping communities more easily than by using standard first-order random walk dynamics, especially pervasive overlaps, which are usually out of reach for most clustering algorithms (Section III.E).

Infomap and its variants usually return different partitions than structure-based methods (e. g., modularity optimisation). This is because they are based on flows running across the system, as opposed to structural variables like number of edges, vertex degrees, etc.. The difference is particularly striking on directed graphs (Rosvall and Bergstrom, 2008), where edge directions heavily constrain the possible flows. Structural features obviously play a major role on the dynamics of processes running on graphs, but dynamics cannot be generally reduced to an interplay of structural elements, at least not simple ones like, e. g., vertex degrees. Sometimes structural and dynamic approaches are equivalent, though. For instance, Newman-Girvan’s modularity is a special case of a general quality function, called *stability*, expressing the persistence of a random walk within communities (Delvenne *et al.*, 2010; Lambiotte *et al.*, 2008).

The methods we have discussed so far are global, in that they aim at finding the whole community structure of the system. However, random walks along with other dynamical processes can be used as well to explore the network locally, starting from seed vertices (Jeub *et al.*, 2015). Good communities correspond to bottlenecks of the dynamics and depend on the choice of the seed vertices, the time scale of the dynamics, etc.. Such local perspective enables to identify community overlaps in a natural way, due to the possibility of reaching vertices multiple times, even if they are already classified.

Spin dynamics (Baxter, 2007) are also regularly used in network clustering. The first step is to define a spin model on the network, consisting of a set of spin variables $\{s_i, i = 1, 2, \dots, n\}$, assigned to the vertices and a Hamiltonian $\mathcal{H}(\{s\})$, expressing the energy of the spin configuration $\{s\}$. For community detection, spins are usually integers: $s = 1, 2, \dots, q$. Contributions to the energy are usually given by spin-spin interactions. The coupling of a spin-spin interaction can be *ferromagnetic* (negative) or *antiferromagnetic* (positive), if the energy is lower when the spins are equal or not, respectively. The goal is to find those spin configurations that minimise the Hamiltonian $\mathcal{H}(\{s\})$. If couplings are all ferromagnetic, the minimum energy would be trivially obtained for the configurations where all vertices have identical spin values. Instead, one would like to have identical spins for vertices of the same cluster, and different spins for vertices in different clusters, to identify the community structure. Therefore, Hamiltonians feature both ferromagnetic and anti-ferromagnetic interactions [*spin glass dynamics* (Mezard *et al.*, 1987)]. A popular model consists in rewarding edges between vertices in the same cluster, as well as non-edges between vertices in different clusters, and pe-

nalising edges between vertices of different clusters, along with non-edges between vertices in the same cluster. This way, if the edge density within communities is appreciably larger than the edge density between communities, as it often happens, having equal spin values for vertices in the same cluster would considerably lower the energy of the configuration. On the other hand, to bring the energy further down the spins of vertices in different clusters should be different, as many such vertices would be disjoint from each other, and such non-edges would increase the energy of the system if the corresponding spin variables were equal. A general expression for the Hamiltonian along these lines is (Reichardt and Bornholdt, 2006)

$$\mathcal{H}(\{s\}) = - \sum_{ij} [a_{ij}A_{ij} - b_{ij}(1 - A_{ij})]\delta(s_i, s_j), \quad (23)$$

where A_{ij} is the element of the adjacency matrix, $a_{ij}, b_{ij} \geq 0$ are arbitrary coefficients, and the Kronecker delta selects only the pairs of vertices with the same spin value.

A popular model is obtained by setting $a_{ij} = 1 - b_{ij}$ and $b_{ij} = \gamma P_{ij}$, where γ is a tunable parameter and P_{ij} a null model term, expressing the expected number of edges running between vertices i and j under a suitable randomisation of the graph structure. The resulting Hamiltonian is (Reichardt and Bornholdt, 2006)

$$\mathcal{H}_{RB}(\{s\}) = - \sum_{ij} (A_{ij} - \gamma P_{ij})\delta(s_i, s_j). \quad (24)$$

If $\gamma = 1$ and $P_{ij} = k_i k_j / 2m$, k_i (k_j) being the degree of i (j) and m the total number of graph edges, the Hamiltonian of Eq. (24) coincides with the modularity by Newman and Girvan [Eq. (20)], up to an irrelevant multiplicative constant. Consequently, modularity can be interpreted as the Hamiltonian of a spin glass as well.

By setting $a_{ij} = 1$ and $b_{ij} = \gamma$ we obtain the *Absolute Potts Model* (APM) (Ronhovde and Nussinov, 2010), whose Hamiltonian reads

$$\mathcal{H}_{APM}(\{s\}) = - \sum_{ij} [A_{ij} - \gamma(1 - A_{ij})]\delta(s_i, s_j). \quad (25)$$

Here, there is no null model term. The models of Eqs. (24) and (25) can be trivially extended to weighted graphs (Traag *et al.*, 2011). They allow to explore the network at different resolutions, by suitably tuning the parameter γ . However, there usually is no information about the community sizes, so it is not possible to decide *a priori* the proper value(s) of γ for a specific graph. A common heuristic is to estimate the *stability* of partitions as a function of γ . It is plausible that partitions recovered for a given γ -value will not be disrupted if γ is varied a little. So, the whole range of γ can be split into intervals, each interval corresponding to the most frequent partition detected in it. Good candidates for the unknown community structure of the system could

be the partitions found in the widest intervals of γ , as they are likely to be more stable (or robust) than the other partitions⁴¹. However, the results of the algorithm do not usually have a linear relationship with γ , hence the width of the intervals is not necessarily correlated with stability, as intervals of the same width but centred at different values of γ may have rather different importance.

A good operational definition of stability is based on the stochastic character of optimisation methods, which typically deliver different results for the same system and set of parameters, by changing initial conditions and/or random seeds. If a partition is robust in a given range of γ -values, most partitions delivered by the algorithm will be very similar. On the other hand, if one explores a γ -region in between two strong partitions, the algorithm will deliver the one or the other partition and the individual replicas will be, on average, not so similar to each other. So, by calculating the similarity $S(\gamma)$ of partitions found by the method at a given resolution parameter γ (for different choices of initial conditions and random seeds), stable communities are revealed by peaks of $S(\gamma)$ (Ronhovde and Nussinov, 2009). Since clustering in large graphs can be very noisy, peaks may not be well resolved. Noise can be reduced by working with consensus partitions of the individual partitions returned by the method for a given γ (Section IV.B). These manipulations are computationally costly, though. Besides, multi-resolution techniques may miss relevant cluster sizes, as it happens for multi-resolution modularity (Lancichinetti *et al.*, 2011) (Section IV.F).

H. Dynamic clustering

Due to the increasing availability of time-stamped network data, there is currently a lot of activity on the development of methods to analyse temporal networks (Holme and Saramäki, 2012). In particular, the problem of detecting dynamic communities has received a lot of attention (Fortunato, 2010; Spiliopoulou, 2011).

Clustering algorithms used for static graphs can be (and often are) used for dynamic networks as well. What needs to be established is how to handle the evolution. Typically one can describe it as a succession of *snapshots* G_1, G_2, \dots, G_l , where each snapshot G_t corresponds to the configuration of the graph in a given time window⁴². There are two possible strategies.

The simplest approach is to detect the community structure for each individual snapshot, which is a static graph (Asur *et al.*, 2007; Hopcroft *et al.*, 2004; Palla *et al.*, 2007). Next, pairs of communities of consecutive windows are associated. A standard procedure is finding the cluster C_t^i in window t that is most similar to cluster C_{t+1}^j in window $t+1$, for instance by using Jaccard similarity score [Eq. (6)] (Palla *et al.*, 2007). This way every community has an image in each phase of the network evolution and one can track its dynamics. Various scenarios are possible. Communities may disappear at some point and new communities may appear, following the exclusion or the introduction of vertices and edges, respectively. Furthermore, a cluster may fragment into smaller ones or merge with others. However, since snapshots are handled separately, this strategy often produces significant variations between partitions close in time, especially when the data sets are noisy, as it usually happens in applications.

It would be preferable to have a unified framework, in which communities are inferred both from the current structure of the graph and from the knowledge of the community structure at previous times. An interesting implementation of this strategy is *evolutionary clustering* (Chakrabarti *et al.*, 2006). The goal of the approach is finding a partition that is both faithful to the system configuration at snapshot t and close to the partition derived for the previous snapshot $t-1$. A cost function is introduced, whose optimisation yields a tradeoff between such two constraints. There is ample flexibility on how this can be done, in practice. Many known clustering techniques normally used for static graphs can be reformulated within this evolutionary framework. Some interesting algorithms based on evolutionary clustering have been proposed (Chi *et al.*, 2007; Lin *et al.*, 2008). Mucha *et al.* have also presented a method that couples the system's configurations of different snapshots, within a modularity-based framework (Mucha *et al.*, 2010). In the resulting quality function (*multislice modularity*), all configurations are simultaneously taken into account and the coupling between them is expressed by a tunable parameter. The approach can handle general multilayer networks (Boccaletti *et al.*, 2014; Kivelä *et al.*, 2014), where layers are either networks whose vertices are connected by a specific edge type (e. g., friendship, work relationships, etc., in social networks), or networks whose vertices have connections (interactions, dependencies) with the vertices of other networks/layers. On the other hand, since the approach is based on modularity optimisation, it has the drawbacks exposed in Section IV.F.

Consensus clustering (Section IV.B) is a natural approach to find stable dynamic clusterings by combining multiple snapshots. Let us suppose we have a time range going from t_0 to t_m , that we want to divide into w windows of size Δt . For the sake of stability, one should consider sliding windows, i. e., overlapping time intervals. This way consecutive partitions will be based on system configurations sharing a lot of vertices and edges, and

⁴¹ We stress, however, that the persistence of partitions in intervals is not necessarily related to clustering robustness (Lewis *et al.*, 2010; Onnela *et al.*, 2012).

⁴² A graph configuration consists of the sets of vertices and edges that are active within the given time frame, along with the intensity of their interactions in that frame (weights) and possibly other aspects of the dynamics, like burstiness (Barabási, 2010), duration of the interactions, etc..

change is (typically) smooth. In order to have exactly w frames, each of them has to be shifted by an interval $\delta t = (t_m - t_0)/w$ with respect to the previous one. So we obtain the windows $[t_0, t_0 + \Delta t]$, $[t_0 + \delta t, t_0 + \Delta t + \delta t]$, $[t_0 + 2\delta t, t_0 + \Delta t + 2\delta t]$, ..., $[t_m - \Delta t, t_m]$. The community structure of each snapshot can be found via any reliable static clustering technique. Next, the consensus partition from the clusterings of r consecutive snapshots, with r suitably chosen, is derived (Lancichinetti and Fortunato, 2012). Again, one could consider sliding windows: for instance, the first window could consist of the first r snapshots, the second one by those from 2 to $r + 1$, and so on until the interval spanned by the last r snapshots. In Fig. 28 we show an application of this procedure on the citation network of papers published in journals of the American Physical Society (APS).

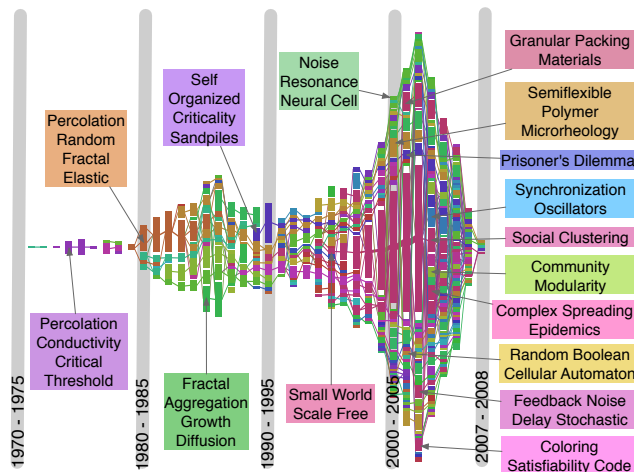


FIG. 28 Consensus clustering on dynamic networks. Time evolution of clusters of the citation network of papers published in journals of the American Physical Society (APS). The clusters with the keyword *Network(s)* among the top 15 most frequent words appearing in the title of the papers were selected. Communities were detected with Infomap (Rosvall and Bergstrom, 2008) on snapshots spanning each a window of 5 years, except at the right end of each diagram: since there is no data after 2008, the last windows must have 2008 as upper limit, so their size shrinks (2004 – 2008, 2005 – 2008, 2006 – 2008, 2007 – 2008). Each vertical bar represents a consensus partition combining pairs of consecutive snapshots. A color uniquely identifies a community, the width of the links between clusters is proportional to the number of papers they have in common. The rapid growth of the field *Complex Networks* is clearly visible, as well as its later split into a number of smaller subtopics, like *Community Structure*, *Epidemic Spreading*, *Robustness*, etc.. Reprinted figure with permission from (Lancichinetti and Fortunato, 2012). © 2012, by the Nature Publishing Group.

An alternative way to uncover the evolution of communities by accounting for the correlation between configurations of neighbouring time intervals is to use probabilistic models (Peixoto, 2015a; Peixoto and Rosvall, 2015;

Sarkar and Moore, 2005; Yang *et al.*, 2009).

If the system is large and its structure is updated in a stream fashion, instead of working on snapshots one could detect the clustering *online*, every time the configuration of the system varies due to new information, like the addition of a new vertex or edge (Aggarwal and Philip, 2005; Zanghi *et al.*, 2008). An advantage of this approach is that change is due to the effect that the small variation in the network structure has on the system, and it can be tracked by simply adjusting the partition of the previous configuration, which can be usually done rather quickly.

I. Significance

Let us suppose that we have identified the communities, somehow. Are we done? Unfortunately, things are not that simple.

In Fig. 29 (top left) we show the adjacency matrix of the random graph á la Erdős-Rényi illustrated in Fig. 8d. The graph has 5000 vertices, so the matrix is 5000×5000 . Black dots indicate the existence of an edge between the corresponding vertices, while missing edges are represented in white. By construction, there is no group structure. However, we can rearrange the elements of the matrix, by reordering the vertex labels. In Fig. 29 (top right) we see that, by doing that, one can generate a group structure, of the assortative type, with two blocks of equal size. If we increase the number of blocks to three Fig. 29 (bottom left) and ten Fig. 29 (bottom right) we can make the matrix look more and more modular. This is why many clustering techniques detect communities in random networks as well, though they should not. Where do the groups come from? Since they cannot be real by construction, they must be generated by random fluctuations in the network construction process. Random fluctuations are particularly relevant on sparse graphs (Section III.C).

The lesson we learn from this example is that it is not sufficient to identify groups in the network, but one should also ask *how significant*, or non-random, they are. Unfortunately, most clustering algorithms are not able to assess the significance of their results. If the groups are compatible with random fluctuations, they are not proper groups and should be disregarded. The lower the chance that they are generated by randomness, the more confident we can be that the blocks reflect some actual group structure. Naturally, this can be done only if one has a reliable *null model*, describing how the structure of the network at study can be randomised and allowing us to estimate how likely it is that the candidate group structure is generated this way. The configuration model (Bollobás, 1980; Molloy and Reed, 1995) is a popular null model in the literature. It generates all possible configurations preserving the number of vertices and edges of the network at study, and the degrees of its vertices. One may compute some variables of the origi-

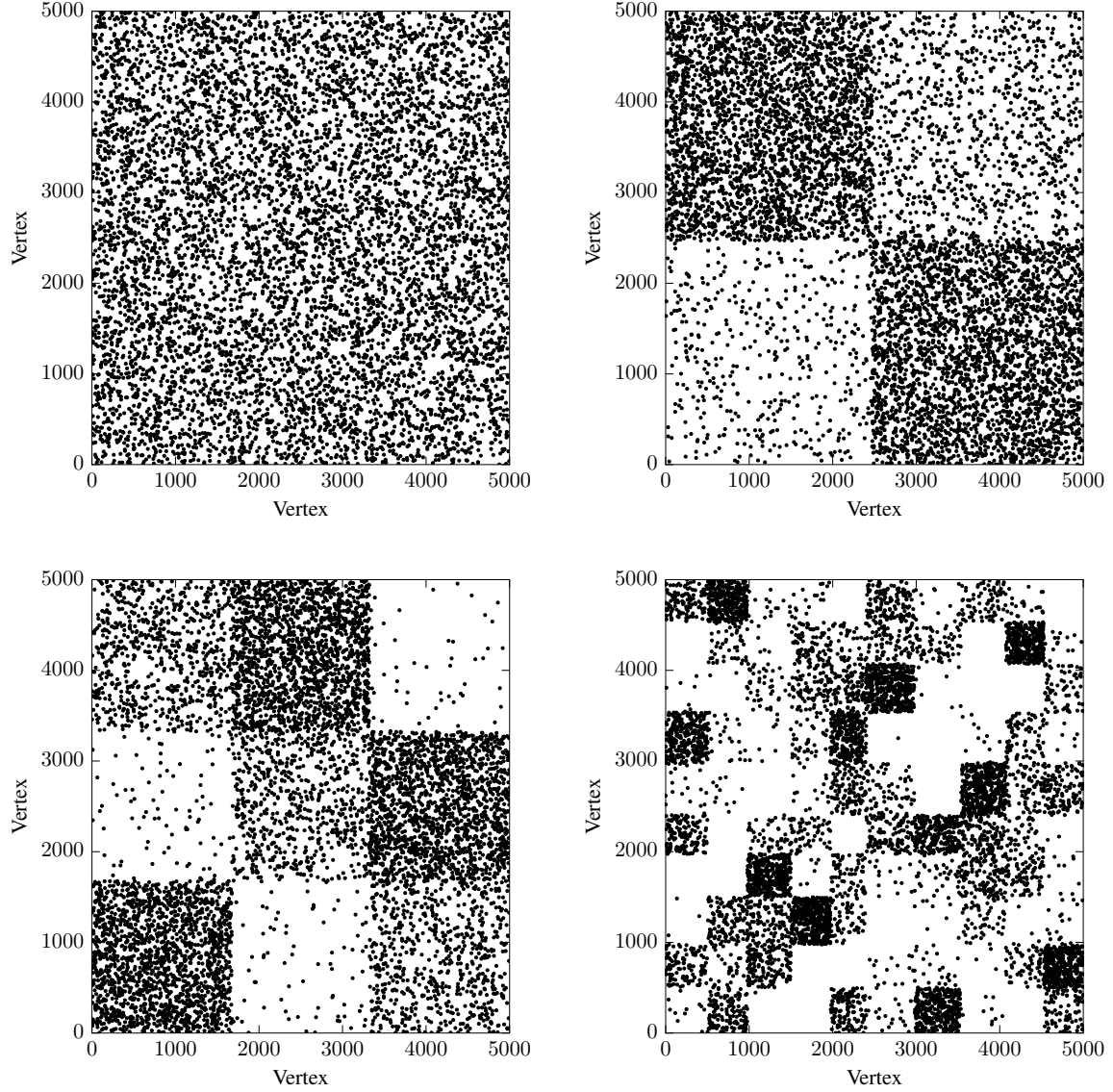


FIG. 29 Artificial groups in random networks. The elements of the adjacency matrix of an Erdős-Rényi random graph (top left) can be rearranged, by suitably reshuffling the list of vertices. This procedure may produce a block structure, with the blocks becoming increasingly more visible the smaller their size. Such groups are not real, though, but they are generated by random fluctuations in the edge patterns among the vertices. The construction principle of the network does not give any special role to groups of vertices, since all pairs of vertices have identical probability to be joined. Courtesy by Tiago P. Peixoto.

nal network, and estimate the probability that the model reproduces them, or *p-value*, i. e., the fraction of model configurations yielding values of the variables compatible with those measured on the original graph. If the *p-value* is sufficiently low (5% is a standard threshold), one concludes that the property at study cannot be generated by randomness only. For community structure, one can compute various properties of the clusters, e. g., their internal density, and compare them with the model values. Some clustering algorithms, like OSLOM (Lancichinetti *et al.*, 2011) are based on this principle. Along the same lines, *z-scores* can be used as well [see the example of Eq. (22)]. Degree-corrected stochastic block models (Karrer and Newman, 2011) (Section IV.E) also include the configuration model, which corresponds to the case without group structure⁴³. In this case significance can be estimated by doing model selection between the versions with and without blocks (Section IV.E).

A concept very related to significance is that of *robustness*. If clusters are significant it means that they are resilient if the network structure is perturbed, to some extent. One way to quantitatively assess this is introducing into the system a controlled amount of noise, and checking how much noise it takes to disrupt the group structure. The greater the required perturbation, the more robust the communities. For instance, a perturbation could be rewiring a fraction of randomly chosen edges (Karrer *et al.*, 2008). After the network is perturbed, the community structure is derived and compared to the one of the original network⁴⁴. The trend of the partition similarity shows how the group structure responds to perturbations.

A similar approach consists in sampling network configurations from a population which the original network is supposed to belong to (*bootstrapping*), and comparing the clusterings found in those configurations, to check how frequently subsets of vertices are clustered together in different samples, which is an index of the robustness (significance) of their clusters (Rosvall and Bergstrom, 2010).

J. Which method then?

At the end of the day, what most people want to know is: which method shall I use on my data? Since the clustering problem is ill-defined, there is no clear-cut answer to it.

Popular techniques are based on similar ideas of com-

munities, like the ones we reviewed in Sections II.B and II.C. What makes the difference is the way clusters are sought. The specific procedure affects the reliability of the results (e. g., because of resolution problems) and the time complexity of the calculation, determining the scope of the method and constraining its applicability.

Most methods propose a universal recipe, that is supposed to hold on every data set. In so doing, one neglects the peculiarities of the network at study, which is valuable information that could orient the method towards more reliable solutions. But algorithms are usually not so flexible to account for specific network features. For instance, in some cases, there is no straightforward extension capable to handle high-level features like edge direction or overlapping communities⁴⁵.

Validation of algorithms, like the comparative analysis of (Lancichinetti and Fortunato, 2009), have allowed to identify a set of methods that perform well on artificial benchmarks. There are two important issues, though. First, we do not know how well real networks are described by currently used benchmark models. Therefore, there is no guarantee that methods performing well on benchmarks also give reliable results on real data sets. Structural analyses like the ones discussed in Section III.E might allow to identify more promising benchmark models. Second, if we rely so much on current benchmarks, which are versions of the stochastic block model (SBM), we already know what the best method is: a posteriori block modelling, i. e., fitting a SBM on the data. Indeed, there are several advantages to this approach. It is more general, it does not only discover communities but several types of group structures, like disassortative groups (Fig. 8b) and core-periphery structure (Fig. 8c). It can also capture the existence of hierarchies among the clusters. Moreover, it yields much richer results than standard clustering algorithms, as it delivers the entire set of parameters of the most likely SBM, with which one can construct the whole network, instead of just grouping vertices. SBMs are very versatile as well. They can be extended to a variety of contexts, e. g., directed networks (Peixoto, 2014), networks with weighted edges (Aicher *et al.*, 2014), with overlapping communities (Airoldi *et al.*, 2008), with multiple layers (Peixoto, 2015a), with annotations (Hric *et al.*, 2016; Newman and Clauset, 2016). Besides, the procedure can be applied to any network model with group structure, not necessarily SBMs. The choice between alternative models can be done via model selection. A posteriori block modelling is not among the fastest techniques available. Networks

⁴³ Actually it would be a variant of the configuration model, as the degree sequence of the vertices would be preserved only on average, not exactly. It is the same null model used in the standard formulation of modularity (Section IV.F).

⁴⁴ For reliable results multiple configurations have to be generated, for a given amount of noise, and the similarity scores have to be averaged.

⁴⁵ Especially extensions of clustering algorithms to the case of directed graphs are not straightforward and often impossible. Spectral methods may not work because spectra of directed graphs may be rather involved (for instance the eigenvalues of the adjacency matrix are typically not real). Likewise, some processes on directed graphs may not reach a stationary state, like simple random walks.

with millions of vertices and edges could be investigated this way, but very large networks remain out of reach. Fortunately, many networks of interest can be attacked. The biggest problem of this class of methods, i. e., the determination of the number of clusters, seems to be solvable (Section IV.E). We recommend to exploit the power of this approach in applications.

Algorithms based on the optimisation of cluster quality functions should be considered as well (Section IV.F), because they may avoid resolution problems and explore the network locally, which is often the only option when the system is too large to be studied as a whole.

Algorithms based on the optimisation of partition quality functions, like modularity maximisation, are plagued by the problems we discussed in Section IV.F. Nevertheless, if one knows, or discovers, the correct number of clusters q , and the optimisation is constrained on the subset of partitions having q clusters, such algorithms become competitive (Darst *et al.*, 2014; Nadakuditi and Newman, 2012).

We also encourage to use approaches based on dynamics (Section IV.G). In principle, the resulting clustering depends on the specific dynamics adopted. In practice, there often is a substantial overlap between the clusters found with different dynamics. An important question is whether dynamics may uncover groups that are not recoverable from network structure alone. Differences in the clusterings found via dynamical versus structural approaches could be due to the fact that dynamical processes are sensitive to more complex structural elements than edges (e. g., paths, motifs) (Arenas *et al.*, 2008a; Benson *et al.*, 2016; Serrouz *et al.*, 2011) (Section II.C). However, even if that were true, dynamical approaches could be more natural ways to handle such higher-order structures, and to make sense of the resulting community structure.

In general, however, the final word on the reliability of a clustering algorithm is to be given by the user, and any output is to be taken with care. Intuition and domain knowledge are indispensable elements to support or disregard solutions.

V. SOFTWARE

In this section we provide a number of links where one can find the code of clustering algorithms and related techniques and models.

- *Artificial benchmarks.* Code to generate LFR benchmark graphs (Section III.A) can be found here <https://sites.google.com/site/andrealancichinetti/files>. The code for the dynamic benchmark by Granell *et al.* (Granell *et al.*, 2015) is available at <https://github.com/rkdarst/dynbench>.
- *Partition similarity measures.* Many partition similarity measures have their own function in R,

Python and MatLab and are easy to find. The variant of the NMI for covers proposed by Lancichinetti *et al.* (Lancichinetti *et al.*, 2009) can be found at <https://sites.google.com/site/andrealancichinetti/mutual>, the one by Esquivel and Rosvall (Esquivel and Rosvall, 2012) at <https://bitbucket.org/dsign/gecmi/wiki/Home>.

- *Consensus clustering.* The technique proposed by Lancichinetti and Fortunato (Lancichinetti and Fortunato, 2012) to derive consensus partitions from multiple outputs of stochastic clustering algorithms can be downloaded from <https://sites.google.com/site/andrealancichinetti/software>.
- *Spectral methods.* The spectral clustering method by Krzakala *et al.* (Krzakala *et al.*, 2013), based on the non-backtracking matrix (Sections IV.A and IV.C), can be downloaded here: <http://lib.itp.ac.cn/html/panzhang/dea/dea.tar.gz>.
- *Edge clustering.* The code for the edge clustering technique by Ahn *et al.* (Ahn *et al.*, 2010) can be found here: <http://barabasilab.neu.edu/projects/linkcommunities/>. The link to the stochastic block model based on edge clustering by Ball *et al.* (Ball *et al.*, 2011) is provided below.
- *Methods based on statistical inference.* The code to perform the inference of the degree-corrected stochastic block model⁴⁶ by Karrer and Newman is available at <http://www-personal.umich.edu/~mejn/dcbm/>. The weighted stochastic block model by Aicher *et al.* (Aicher *et al.*, 2014) can be found at <http://tuvalu.santafe.edu/~aaronc/wsbm/>. The code for the overlapping stochastic block model based on edge clustering by Ball *et al.* (Ball *et al.*, 2011) is at <http://www-personal.umich.edu/~mejn/OverlappingLinkCommunities.zip>. The model combining structure and metadata by Newman and Clauset (Newman and Clauset, 2016) is coded at http://www-personal.umich.edu/~mejn/Newman_Clauset_code.zip. The program to infer the bipartite stochastic block model by Larremore *et al.* (Larremore *et al.*, 2014) can be found at <http://danlarremore.com/bipartiteSBM/>.

The algorithms for the inference of community structure developed by Tiago Peixoto are implemented within the Python module `graph-tool` and can be found at <https://graph-tool.skewed>.

⁴⁶ We stress that the method is parametric, in that the number of clusters has to be provided as input. In Section IV.E we have pointed to techniques to infer the number of clusters beforehand.

[de/static/doc/dev/community.html](#). They allow us to perform model selection of various kinds of stochastic block models: degree-corrected (Karrer and Newman, 2011), with overlapping groups (Peixoto, 2015b), and for networks with layers, with valued edges and evolving in time (Peixoto, 2015a). The hierarchical block model of (Peixoto, 2014), that searches for clusters at high resolution, is also available. All such variants can be combined at ease by selecting a suitable set of options.

The algorithms for the inference of overlapping communities via the Community-Affiliation Graph Model (AGM) (Yang and Leskovec, 2012a) and the Cluster Affiliation Model for Big Networks (BIG-CLAM) (Yang and Leskovec, 2013) (Section III.E) can be found in the package <http://infolab.stanford.edu/~crucis/code/agm-package.zip>.

- *Methods based on optimisation.* There is a lot of free software for modularity optimisation. In the `igraph` library (<http://igraph.org>) there are several functions, both in the *R* and in the Python package: `cluster_fast_greedy` (*R*) and `community_fastgreedy` (Python), implementing the fast greedy optimisation by Clauset et al. (Clauset et al., 2004); `cluster_leading_eigen` (*R*) and `community_leading_eigenvector` (Python) for the optimisation based on the leading eigenvector of the modularity matrix (Newman, 2006); `cluster_louvain` (*R*) and `community_multilevel` (Python) are the implementations of the Louvain method (Blondel et al., 2008); `cluster_optimal` (*R*) and `community_optimal_modularity` turn the task into an integer programming problem (Brandes et al., 2008); `cluster_spinglass` (*R*) and `community_spinglass` (Python) optimise the multi-resolution modularity proposed by Reichardt and Bornholdt (Reichardt and Bornholdt, 2006).

Some methods based on the optimisation of cluster quality functions are also available. The code for the optimisation of the local modularity by Clauset (Clauset, 2005) can be found at http://tuvalu.santafe.edu/~aaronc/shared/LocalCommunity2005_GPL.zip. The code for OSLOM is downloadable from the dedicated website <http://www.oslom.org>.

- *Methods based on dynamics.* Infomap (Rosvall and Bergstrom, 2008) is currently a very popular algorithm and its code can be found in various places. It has a dedicated website <http://www.mapequation.org>, where several extensions can be downloaded, including hierarchical community structure (Rosvall and Bergstrom, 2011), overlapping clusters (Viamontes Esquivel and Rosvall, 2011) and memory (Rosvall et al.,

2014). Infomap has also its own functions on `igraph`, both in the *R* and in the Python package (`cluster_infomap` and `community_infomap`, respectively). *Walktrap* (Pons and Latapy, 2005), another popular method based on random walk dynamics, is available on `igraph`, via the functions `cluster_walktrap` (*R*) and `community_walktrap` (Python). The local community detection algorithms proposed in (Jeub et al., 2015) can be downloaded from <http://people.maths.ox.ac.uk/jeub/code.html>.

- *Dynamic clustering.* The code to optimise the multislice modularity by Mucha et al. (Mucha et al., 2010) is available at <http://netwiki.amath.unc.edu/GenLouvain/GenLouvain>. Detection of dynamic communities can be performed as well with consensus clustering (Section IV.B) and via stochastic block models (Section IV.E). Links to the related code have been provided above.

VI. OUTLOOK

As long as there will be networks, there will be people looking for communities in them. So it is of uttermost importance to have a set of reliable concepts and principles guiding scholars towards promising solutions for network clustering. We have presented established views of the main aspects of the problem, and exposed the strengths as well as the limits of popular notions and approaches.

What's next? We believe that there will be a trend towards the development of domain-dependent algorithms, exploiting as much as possible information and peculiarities of network data sets. Generalist methods could still be used to get first indications about community structure and orient the investigation in promising directions. Some existing approaches are sufficiently flexible to accommodate various features of networks and community structure (Section IV.J).

At the same time, we believe that it is necessary to find accurate models of networks with community structure, both for the purpose of designing realistic benchmark graphs for validation, and for a more precise inference of the groups and of their features. Investigations of real networks at the level of subgraphs, along the lines of those discussed in Section III.E, are instrumental to the definition of such models.

While benchmark graphs can be improved, there is one test that one can rely on to assess the performance of clustering algorithms: applying methods on random graphs without group structure. We know that many popular techniques find groups in such graphs as well, failing the test. On a related note, it is critical to determine how non-random the clusters detected on real networks are, i. e., to estimate their significance (Section IV.I).

We stress that this exposition is by no means complete. The emphasis is on the fundamental aspects of network clustering and on main stream approaches. We discussed

works and listed references which are of more immediate relevance to the topics discussed. A number of topics have not been dealt with. Still we hope that this work will help practitioners to design more and more reliable methods and domain users to extract useful information from their data.

Acknowledgments

We thank Alex Arenas, Florian Kimm, Tiago Peixoto, Mason Porter and Martin Rosvall for a careful reading of the manuscript and many valuable comments. We gratefully acknowledge MULTIPLEX, grant No. 317532 of the European Commission.

References

- Aggarwal, C. C., and S. Y. Philip, 2005, in *Proc. of SIAM Int. Conf. on Data Mining (SDM)* (SIAM), pp. 56–67.
- Ahn, Y.-Y., J. P. Bagrow, and S. Lehmann, 2010, *Nature* **466**(7307), 761.
- Aicher, C., A. Z. Jacobs, and A. Clauset, 2014, *J. Complex Netw.* **3**(2), 221.
- Airoldi, E. M., D. M. Blei, S. E. Fienberg, and E. P. Xing, 2008, *J. Mach. Learn. Res.* **9**, 1981.
- Alba, R. D., 1973, *J. Math. Sociol.* **3**, 113.
- Albert, R., H. Jeong, and A.-L. Barabási, 1999, *Nature* **401**, 130.
- Angel, O., J. Friedman, and S. Hoory, 2015, *Trans. Am. Math. Soc.* **367**(6), 4287.
- Arenas, A., A. Díaz-Guilera, and C. J. Pérez-Vicente, 2006, *Phys. Rev. Lett.* **96**(11), 114102.
- Arenas, A., A. Fernández, S. Fortunato, and S. Gómez, 2008a, *J. Phys. A* **41**(22), 224001.
- Arenas, A., A. Fernández, and S. Gómez, 2008b, *New J. Phys.* **10**(5), 053039.
- Asur, S., S. Parthasarathy, and D. Ucar, 2007, in *KDD '07: Proceedings of the 13th ACM SIGKDD International Conference on Knowledge Discovery and Data Mining* (ACM, New York, NY, USA), pp. 913–921.
- Ball, B., B. Karrer, and M. E. J. Newman, 2011, *Phys. Rev. E* **84**, 036103.
- Barabási, A.-L., 2010, *Bursts: the hidden patterns behind everything we do, from your e-mail to bloody crusades* (Penguin).
- Barber, M. J., 2007, *Phys. Rev. E* **76**(6), 066102.
- Barrat, A., M. Barthélemy, and A. Vespignani, 2008, *Dynamical processes on complex networks* (Cambridge University Press, Cambridge, UK).
- Baumes, J., M. K. Goldberg, M. S. Krishnamoorthy, M. M. Ismail, and N. Preston, 2005, in *IADIS AC*, edited by N. Guimaraes and P. T. Isaias (IADIS), pp. 97–104.
- Baxter, R. J., 2007, *Exactly solved models in statistical mechanics* (Courier Corporation).
- Ben-Hur, A., A. Elisseeff, and I. Guyon, 2001, in *Pacific Symposium on Biocomputing*, volume 7, pp. 6–17.
- Benson, A. R., D. F. Gleich, and J. Leskovec, 2016, *Science* **353**(6295), 163.
- Blondel, V. D., J.-L. Guillaume, R. Lambiotte, and E. Lefebvre, 2008, *J. Stat. Mech.* **P10008**.
- Boccaletti, S., G. Bianconi, R. Criado, C. del Genio, J. G.-nes, M. Romance, I. Sendiña-Nadal, Z. Wang, and M. Zanin, 2014, *Phys. Rep.* **544**(1), 1.
- Boccaletti, S., M. Ivanchenko, V. Latora, A. Pluchino, and A. Rapisarda, 2007, *Phys. Rev. E* **75**(4), 045102.
- Bollobás, B., 1980, *Eur. J. Combin.* **1**(4), 311.
- Bomze, I. M., M. Budinich, P. M. Pardalos, and M. Pelillo, 1999, in *Handbook of Combinatorial Optimization*, edited by D.-Z. Du and P. Pardalos (Kluwer Academic Publishers, Norwell, USA), pp. 1–74.
- Bothorel, C., J. D. Cruz, M. Magnani, and B. Micenkova, 2015, *Netw. Sci.* **3**(03), 408.
- Brandes, U., D. Delling, M. Gaertler, R. Görke, M. Hoefler, Z. Nikoloski, and D. Wagner, 2008, *IEEE Trans. Knowl. Data Eng.* **20**(2), 172.
- Brennan, R. L., and R. J. Light, 1974, *Br. J. Math. Stat. Psychol.* **27**(2), 154.
- Brin, S., and L. E. Page, 1998, *Comput. Netw. ISDN* **30**, 107.
- Bron, C., and J. Kerbosch, 1973, *Commun. ACM* **16**, 575.
- Bruno, A. M., W. N. Frost, and M. D. Humphries, 2015, *Neuron* **86**(1), 304.
- Bui, T. N., S. Chaudhuri, F. T. Leighton, and M. Sipser, 1987, *Combinatorica* **7**(2), 171.
- Caldarelli, G., 2007, *Scale-free networks* (Oxford University Press, Oxford, UK).
- Chakrabarti, D., R. Kumar, and A. Tomkins, 2006, in *KDD '06: Proceedings of the 12th ACM SIGKDD International Conference on Knowledge Discovery and Data Mining* (ACM, New York, NY, USA), pp. 554–560.
- Chakraborty, T., A. Dalmia, A. Mukherjee, and N. Ganguly, 2016, preprint arXiv:1604.03512.
- Chi, Y., X. Song, D. Zhou, K. Hino, and B. L. Tseng, 2007, in *KDD '07: Proceedings of the 13th ACM SIGKDD International Conference on Knowledge Discovery and Data Mining* (ACM, New York, NY, USA), pp. 153–162.
- Clauset, A., 2005, *Phys. Rev. E* **72**(2), 026132.
- Clauset, A., M. E. J. Newman, and C. Moore, 2004, *Phys. Rev. E* **70**(6), 066111.
- Cohen, R., and S. Havlin, 2010, *Complex Networks: Structure, Robustness and Function* (Cambridge University Press, Cambridge, UK).
- Collins, L. M., and C. W. Dent, 1988, *Multivar. Behav. Res.* **23**(2), 231.
- Côme, E., and P. Latouche, 2015, *Stat. Modelling* **15**(6), 564.
- Condon, A., and R. M. Karp, 2001, *Random Struct. Algor.* **18**, 116.
- Coscia, M., F. Giannotti, and D. Pedreschi, 2011, *Stat. Anal. Data Min.* **4**(5), 512.
- Danon, L., A. Díaz-Guilera, J. Duch, and A. Arenas, 2005, *J. Stat. Mech.* **P09008**.
- Danon, L., J. Duch, A. Arenas, and A. Díaz-Guilera, 2007, in *Large Scale Structure and Dynamics of Complex Networks: From Information Technology to Finance and Natural Science*, edited by C. G. and V. A. (World Scientific, Singapore), pp. 93–114.
- Darst, R. K., Z. Nussinov, and S. Fortunato, 2014, *Phys. Rev. E* **89**(3), 032809.
- Daudin, J.-J., F. Picard, and S. Robin, 2008, *Stat. Comput.* **18**(2), 173.
- Decelle, A., F. Krzakala, C. Moore, and L. Zdeborová, 2011, *Phys. Rev. Lett.* **107**, 065701.
- Delling, D., M. Gaertler, R. Görke, and D. Wagner, 2006, *Experiments on comparing graph clusterings*, Technical Report, Universität Karlsruhe, Germany.

- Delvenne, J.-C., S. N. Yaliraki, and M. Barahona, 2010, Proc. Natl. Acad. Sci. USA **107**(29), 12755.
- Dorogovtsev, S. N., and J. F. F. Mendes, 2013, *Evolution of networks: From biological nets to the Internet and WWW* (Oxford University Press).
- Dyer, M. E., and A. M. Frieze, 1989, J. Algorithms **10**(4), 451.
- Erdős, P., and A. Rényi, 1959, Publ. Math. Debrecen **6**, 290.
- Erdős, P., and A. Rényi, 1960, Publ. Math. Inst. Hungar. Acad. Sci **5**, 17.
- Esquivel, A. V., and M. Rosvall, 2012, eprint arXiv:1202.0425.
- Estrada, E., 2011, *The structure of complex networks: theory and applications* (Oxford University Press, UK).
- Estrada, E., and P. A. Knight, 2015, *A First Course in Network Theory* (Oxford University Press, UK).
- Evans, T. S., 2010, J. Stat. Mech. Theor. Exp. **2010**(12), P12037.
- Evans, T. S., and R. Lambiotte, 2009, Phys. Rev. E **80**(1), 016105.
- Expert, P., T. S. Evans, V. D. Blondel, and R. Lambiotte, 2011, Proc. Natl. Acad. Sci. USA **108**(19), 7663.
- Fienberg, S. E., and S. Wasserman, 1981, Sociol. Methodol. **12**, 156.
- Fortunato, S., 2010, Phys. Rep. **486**, 75.
- Fortunato, S., and M. Barthélemy, 2007, Proc. Natl. Acad. Sci. USA **104**, 36.
- Fred, A., and A. K. Jain, 2003, in *Computer Vision and Pattern Recognition, 2003. Proceedings. 2003 IEEE Computer Society Conference on* (IEEE), volume 2, pp. II–128.
- Gelman, A., J. B. Carlin, H. S. Stern, and D. B. Rubin, 2014, *Bayesian Data Analysis*, volume 2 (Taylor & Francis).
- Girvan, M., and M. E. Newman, 2002, Proc. Natl. Acad. Sci. USA **99**(12), 7821.
- Goder, A., and V. Filkov, 2008, in *ALLENEX*, pp. 109–117.
- Good, B. H., Y.-A. de Montjoye, and A. Clauset, 2010, Phys. Rev. E **81**(4), 046106.
- Granell, C., R. K. Darst, A. Arenas, S. Fortunato, and S. Gómez, 2015, Phys. Rev. E **92**(1), 012805.
- Granell, C., S. Gómez, and A. Arenas, 2012, Int. J. Bifurcat. Chaos **22**(07), 1250171.
- Grünwald, P. D., I. J. Myung, and M. A. Pitt, 2005, *Advances in Minimum Description Length: Theory and Applications* (MIT Press, Cambridge, USA).
- Guimerà, R., and L. A. N. Amaral, 2005, Nature **433**, 895.
- Guimerà, R., and M. Sales-Pardo, 2009, Proc. Natl. Acad. Sci. USA **106**(52), 22073.
- Guimerà, R., M. Sales-Pardo, and L. A. Amaral, 2004, Phys. Rev. E **70**(2), 025101 (R).
- Handcock, M. S., A. E. Raftery, and J. M. Tantrum, 2007, J. Roy. Stat. Soc. A **170**(46), 1.
- Hastings, M. B., 2006, Phys. Rev. E **74**(3), 035102.
- Holland, P., K. B. Laskey, and S. Leinhardt, 1983, Soc. Netw. **5**, 109.
- Holme, P., and J. Saramäki, 2012, Phys. Rep. **519**(3), 97.
- Hopcroft, J., O. Khan, B. Kulis, and B. Selman, 2004, Proc. Natl. Acad. Sci. USA **101**, 5249.
- Hric, D., R. K. Darst, and S. Fortunato, 2014, Phys. Rev. E **90**, 062805.
- Hric, D., T. P. Peixoto, and S. Fortunato, 2016, Phys. Rev. X **6**, 031038.
- Hu, Y., H. Chen, P. Zhang, M. Li, Z. Di, and Y. Fan, 2008, Phys. Rev. E **78**(2), 026121.
- Huang, J., H. Sun, Y. Liu, Q. Song, and T. Wenginger, 2011, PLoS ONE **6**(8), e23829.
- Hubert, L., and P. Arabie, 1985, J. Classif. **2**(1), 193.
- Hüllermeier, E., and M. Rifqi, 2009, in *Joint 2009 International Fuzzy Systems Association World Congress and 2009 European Society of Fuzzy Logic and Technology Conference, IFSA-EUSFLAT 2009*, pp. 1294–1298.
- Jaccard, P., 1901, Bull. Soc. Vaud. Sci. Nat. **37**, 547.
- Jain, A. K., M. N. Murty, and P. J. Flynn, 1999, ACM Comput. Surv. **31**(3), 264.
- Jeub, L. G., P. Balachandran, M. A. Porter, P. J. Mucha, and M. W. Mahoney, 2015, Phys. Rev. E **91**(1), 012821.
- Karrer, B., E. Levina, and M. E. J. Newman, 2008, Phys. Rev. E **77**(4), 046119.
- Karrer, B., and M. E. J. Newman, 2011, Phys. Rev. E **83**, 016107.
- Kivelä, M., A. Arenas, M. Barthelemy, J. P. Gleeson, Y. Moreno, and M. A. Porter, 2014, J. Complex Netw. **2**(3), 203.
- Krzakala, F., C. Moore, E. Mossel, J. Neeman, A. Sly, L. Zdeborová, and P. Zhang, 2013, Proc. Natl. Acad. Sci. USA **110**(52), 20935.
- Lambiotte, R., J. Delvenne, and M. Barahona, 2008, eprint arXiv:0812.1770.
- Lancichinetti, A., and S. Fortunato, 2009, Phys. Rev. E **80**(1), 016118.
- Lancichinetti, A., and S. Fortunato, 2009, Phys. Rev. E **80**(5), 056117.
- Lancichinetti, A., and S. Fortunato, 2011, Phys. Rev. E **84**, 066122.
- Lancichinetti, A., and S. Fortunato, 2012, Sci. Rep. **2**, 336.
- Lancichinetti, A., and S. Fortunato, 2014, Phys. Rev. E **89**, 049902.
- Lancichinetti, A., S. Fortunato, and J. Kertesz, 2009, New J. Phys. **11**(3), 033015.
- Lancichinetti, A., S. Fortunato, and F. Radicchi, 2008, Phys. Rev. E **78**(4), 046110.
- Lancichinetti, A., M. Kivelä, J. Saramäki, and S. Fortunato, 2010, PLoS ONE **5**(8), e11976.
- Lancichinetti, A., F. Radicchi, J. J. Ramasco, and S. Fortunato, 2011, PLoS ONE **6**(4), e18961.
- Larremore, D. B., A. Clauset, and A. Z. Jacobs, 2014, Phys. Rev. E **90**(1), 012805.
- Latouche, P., E. Birmele, and C. Ambroise, 2012, Stat. Modelling **12**(1), 93.
- Leng, M., Y. Yao, J. Cheng, W. Lv, and X. Chen, 2013, in *Database Systems for Advanced Applications* (Springer), pp. 324–338.
- Leskovec, J., K. J. Lang, A. Dasgupta, and M. W. Mahoney, 2009, Internet Math. **6**(1), 29.
- Lewis, A., N. Jones, M. Porter, and C. Deane, 2010, BMC Syst. Biol. **4**(1), 100.
- Liben-Nowell, D., J. Novak, R. Kumar, P. Raghavan, and A. Tomkins, 2005, Proc. Natl. Acad. Sci. USA **102**(33), 11623.
- Lin, Y.-R., Y. Chi, S. Zhu, H. Sundaram, and B. L. Tseng, 2008, in *WWW '08: Proceeding of the 17th International Conference on World Wide Web* (ACM, New York, NY, USA), pp. 685–694.
- Luccio, F., and M. Sami, 1969, IEEE Trans. Circuit Th. CT **16**, 184.
- Luce, R. D., 1950, Psychometrika **15**(2), 169.
- Luce, R. D., and A. D. Perry, 1949, Psychometrika **14**(2), 95.
- Lusseau, D., 2003, Proc. Royal Soc. London B **270**, S186.
- von Luxburg, U., 2006, *A tutorial on spectral clustering*, Technical Report 149, Max Planck Institute for Biological Cy-

- bernetics.
- Mackay, D. J. C., 2003, *Information Theory, Inference, and Learning Algorithms* (Cambridge University Press, Cambridge, UK).
- MacMahon, M., and D. Garlaschelli, 2015, Phys. Rev. X **5**, 021006.
- MacQueen, J. B., 1967, in *Proc. of the fifth Berkeley Symposium on Mathematical Statistics and Probability*, edited by L. M. L. Cam and J. Neyman (University of California Press, Berkeley, USA), volume 1, pp. 281–297.
- Malliaros, F. D., and M. Vazirgiannis, 2013, Phys. Rep. **533**(4), 95.
- McDaid, A. F., D. Greene, and N. Hurley, 2011, eprint arXiv:1110.2515.
- Meilă, M., 2005, in *Proceedings of the 22nd International Conference on Machine Learning (ACM)*, pp. 577–584.
- Meilă, M., 2007, J. Multivar. Anal. **98**(5), 873.
- Meilă, M., and D. Heckerman, 2001, Mach. Learn. **42**(1), 9.
- Mezard, M., G. Parisi, and M. Virasoro, 1987, *Spin glass theory and beyond* (World Scientific Publishing Company, Singapore).
- Mokken, R. J., 1979, Qual. Quant. **13**(2), 161.
- Molloy, M., and B. Reed, 1995, Random Struct. Algor. **6**, 161.
- Moody, J., and D. R. White, 2003, Am. Sociol. Rev. **68**(1), 103.
- Moore, C., X. Yan, Y. Zhu, J.-B. Rouquier, and T. Lane, 2011, in *Proceedings of the 17th ACM SIGKDD International Conference on Knowledge Discovery and Data Mining (ACM, New York, NY, USA)*, KDD '11, pp. 841–849.
- Mucha, P. J., T. Richardson, K. Macon, M. A. Porter, and J. P. Onnela, 2010, Science **328**(5980), 876.
- Nadakuditi, R. R., and M. E. J. Newman, 2012, Phys. Rev. Lett. **108**, 188701.
- Newman, M., 2010, *Networks: An Introduction* (Oxford University Press, Inc., New York, NY, USA).
- Newman, M., 2013, eprint arXiv:1308.6494.
- Newman, M., 2016, eprint arXiv:1606.02319.
- Newman, M., and A. Clauset, 2016, Nat. Commun. **7**, 11863.
- Newman, M. E. J., 2004, Phys. Rev. E **70**(5), 056131.
- Newman, M. E. J., 2004a, Eur. Phys. J. B **38**, 321.
- Newman, M. E. J., 2004b, Phys. Rev. E **69**(6), 066133.
- Newman, M. E. J., 2006, Proc. Natl. Acad. Sci. USA **103**, 8577.
- Newman, M. E. J., 2012, Nat. Phys. **8**(1), 25.
- Newman, M. E. J., and M. Girvan, 2004, Phys. Rev. E **69**(2), 026113.
- Newman, M. E. J., and E. A. Leicht, 2007, Proc. Natl. Acad. Sci. USA **104**, 9564.
- Newman, M. E. J., and G. Reinert, 2016, Phys. Rev. Lett. **117**, 078301.
- Onnela, J.-P., D. J. Fenn, S. Reid, M. A. Porter, P. J. Mucha, M. D. Fricker, and N. S. Jones, 2012, Phys. Rev. E **86**, 036104.
- Palla, G., A.-L. Barabási, and T. Vicsek, 2007, Nature **446**, 664.
- Palla, G., I. Derényi, I. Farkas, and T. Vicsek, 2005, Nature **435**, 814.
- Parthasarathy, S., Y. Ruan, and V. Satuluri, 2011, in *Social Network Data Analytics* (Springer), pp. 79–113.
- Peel, L., 2015, J. Complex Netw. **3**(3), 431.
- Peixoto, T. P., 2013, Phys. Rev. Lett. **110**, 148701.
- Peixoto, T. P., 2014, Phys. Rev. X **4**, 011047.
- Peixoto, T. P., 2015a, Phys. Rev. E **92**(4), 042807.
- Peixoto, T. P., 2015b, Phys. Rev. X **5**, 011033.
- Peixoto, T. P., and M. Rosvall, 2015, eprint arXiv:1509.04740.
- Perotti, J. I., C. J. Tessone, and G. Caldarelli, 2015, Phys. Rev. E **92**, 062825.
- Persson, C., L. Bohlin, D. Edler, and M. Rosvall, 2016, eprint arXiv:1606.08328.
- Pons, P., and M. Latapy, 2005, in *International Symposium on Computer and Information Sciences* (Springer), pp. 284–293.
- Porter, M. A., J.-P. Onnela, and P. J. Mucha, 2009, Notices Amer. Math. Soc. **56**(9), 1082.
- Radicchi, F., C. Castellano, F. Cecconi, V. Loreto, and D. Parisi, 2004, Proc. Natl. Acad. Sci. USA **101**, 2658.
- Raghavan, U. N., R. Albert, and S. Kumara, 2007, Phys. Rev. E **76**(3), 036106.
- Rand, W. M., 1971, J. Am. Stat. Assoc. **66**(336), 846.
- Reichardt, J., and S. Bornholdt, 2006, Phys. Rev. E **74**(1), 016110.
- Rissanen, J., 1978, Automatica **14**, 465.
- Ronhovde, P., and Z. Nussinov, 2009, Phys. Rev. E **80**(1), 016109.
- Ronhovde, P., and Z. Nussinov, 2010, Phys. Rev. E **81**, 046114.
- Rosvall, M., and C. T. Bergstrom, 2008, Proc. Natl. Acad. Sci. USA **105**, 1118.
- Rosvall, M., and C. T. Bergstrom, 2010, PLoS one **5**(1), e8694.
- Rosvall, M., and C. T. Bergstrom, 2011, PLoS ONE **6**(4), e18209.
- Rosvall, M., A. V. Esquivel, A. Lancichinetti, J. D. West, and R. Lambiotte, 2014, Nat. Commun. **5**.
- Sarkar, P., and A. W. Moore, 2005, ACM SIGKDD Explor. Newsl. **7**(2), 31.
- Sarkar, S., S. Chawla, P. A. Robinson, and S. Fortunato, 2016, Phys. Rev. E **93**, 062312.
- Schaeffer, S. E., 2007, Comput. Sci. Rev. **1**(1), 27.
- Scott, J., 2000, *Social Network Analysis: A Handbook* (SAGE Publications, London, UK).
- Seidman, S. B., and B. L. Foster, 1978, J. Math. Sociol. **6**, 139.
- Serrour, B., A. Arenas, and S. Gómez, 2011, Comput. Commun. **34**(5), 629 .
- Simon, H., 1962, Proc. Am. Phil. Soc. **106**(6), 467.
- Singh, A., and M. D. Humphries, 2015, Scientific reports **5**, 8828.
- Snijders, T., and K. Nowicki, 1997, J. Classif. **14**, 75.
- Spiliopoulou, M., 2011, in *Social Network Data Analytics*, edited by C. C. Aggarwal (Springer US), pp. 149–175.
- Strehl, A., and J. Ghosh, 2002, J. Mach. Learn. Res. **3**, 583, ISSN 1532-4435.
- Topchy, A., A. K. Jain, and W. Punch, 2005, IEEE Trans. Pattern Anal. Mach. Intell. **27**, 1866.
- Traag, V. A., and J. Bruggeman, 2009, Phys. Rev. E **80**(3), 036115.
- Traag, V. A., P. Van Dooren, and Y. Nesterov, 2011, Phys. Rev. E **84**, 016114.
- Traud, A., E. Kelsic, P. Mucha, and M. Porter, 2011, SIAM Review **53**(3), 526.
- Traud, A. L., P. J. Mucha, and M. A. Porter, 2012, Physica A **391**(16), 4165.
- Van Dongen, S., 2000, *Graph Clustering by Flow Simulation*, Ph.D. thesis, Dutch National Research Institute for Mathematics and Computer Science, University of Utrecht, Netherlands.
- Viamontes Esquivel, A., and M. Rosvall, 2011, Phys. Rev. X

- 1, 021025.
- Wasserman, S., and K. Faust, 1994, *Social network analysis* (Cambridge University Press, Cambridge, UK).
- Xie, J., S. Kelley, and B. K. Szymanski, 2013, *ACM Comput. Surv.* **45**(4), 43:1.
- Xie, J., and B. K. Szymanski, 2012, in *Proceedings of the 16th Pacific-Asia Conference on Advances in Knowledge Discovery and Data Mining - Volume Part II* (Springer-Verlag, Berlin, Heidelberg), PAKDD'12, pp. 25–36.
- Xu, R., and D. Wunsch, 2008, *Clustering* (John Wiley & Sons, Piscataway, NJ, USA).
- Yang, J., and J. Leskovec, 2012a, in *Data Mining (ICDM), 2012 IEEE 12th International Conference on* (IEEE), pp. 1170–1175.
- Yang, J., and J. Leskovec, 2012b, in *Proceedings of the ACM SIGKDD Workshop on Mining Data Semantics* (ACM, New York, NY, USA), MDS'12, pp. 3:1–3:8.
- Yang, J., and J. Leskovec, 2013, in *Proceedings of the Sixth ACM International Conference on Web Search and Data Mining* (ACM, New York, NY, USA), WSDM'13, pp. 587–596.
- Yang, J., and J. Leskovec, 2014, *ACM Trans. Intell. Syst. Technol.* **5**(2), 26:1.
- Yang, J., J. McAuley, and J. Leskovec, 2013, in *2013 IEEE 13th International Conference on Data Mining (ICDM)* (IEEE), pp. 1151–1156.
- Yang, T., Y. Chi, S. Zhu, Y. Gong, and R. Jin, 2009, in *SIAM Int. Conf. on Data Mining (SDM)* (SIAM), volume 9, pp. 990–1001.
- Zachary, W. W., 1977, *J. Anthropol. Res.* **33**, 452.
- Zanghi, H., C. Ambroise, and V. Miele, 2008, *Pattern Recogn.* **41**(12), 3592.
- Zhang, P., 2015, *J. Stat. Mech. Theor. Exp.* **P11006**.
- Zhang, P., and C. Moore, 2014, *Proc. Natl. Acad. Sci.* **111**(51), 18144.
- Zhang, P., C. Moore, and M. Newman, 2016, *Phys. Rev. E* **93**(1), 012303.
- Zhang, X., T. Martin, and M. E. Newman, 2015, *Phys. Rev. E* **91**(3), 032803.
- Zhou, H., 2003a, *Phys. Rev. E* **67**(6), 061901.
- Zhou, H., 2003b, *Phys. Rev. E* **67**(4), 041908.
- Zhou, H., and R. Lipowsky, 2004, *Lect. Notes Comp. Sci.* **3038**, 1062.